

The Pennsylvania State University
The Graduate School
Department of Civil and Environmental Engineering

**TEST FRAMEWORK DEVELOPMENT FOR USE OF COAL COMBUSTION
PRODUCTS (CCPS) IN EMBANKMENT CONSTRUCTION AND MINE LAND
RECLAMATION**

A Thesis in
Civil Engineering
by
Nicholas T. Plaks

© 2010 Nicholas T. Plaks

Submitted in Partial Fulfillment
of the Requirements
for the Degree of

Master of Science

August 2010

The thesis of Nicholas T. Plaks was reviewed and approved* by the following:

Angelica Palomino
Assistant Professor of Civil Engineering
Thesis Adviser

Barry E. Scheetz
Professor of Civil Engineering

Shelley Stoffels
Associate Professor of Civil Engineering

Peggy Johnson
Professor of Civil Engineering
Head of the Department of Civil Engineering

*Signatures are on file in the Graduate School.

ABSTRACT

Coal combustion products (CCPs) are by-products created when coal is burned for energy production. In 2007 alone, the United States produced in excess of 125 million tons of CCPs. Despite the fact that approximately 40% of the CCPs were used beneficially, 60% of the CCPs were disposed of via land filling. Reusing CCPs in large volume, civil engineering applications could greatly reduce and potentially outperform the natural materials currently required for these structures, which in many cases is more economical. Recycling CCPs also reduces the carbon footprint associated with mining naturally occurring material. However, CCPs are often perceived as strictly a waste product due to their chemical composition and potentially hazardous leachate even though not all CCPs should be considered environmentally unsound. In fact, their chemical composition can vary widely depending on the source power plant location, the power plant type, and the fuel source. Therefore it is necessary that CCPs be characterized both mechanically and chemically to qualify their utilization in civil engineering structures. The missing component in the current state of practice is a consistent methodology for categorizing CCPs as either environmentally and structurally sound or harmful when used as a construction material, and this methodology should be application-based. This paper describes the development of a detailed testing framework in order to qualify the use of CCPs in large-volume civil engineering applications, in particular embankments and mine land reclamation. The testing framework is then implemented for three types of CCPs with an analysis of results.

TABLE OF CONTENTS

LIST OF TABLES	viii
ACKNOWLEDGEMENTS	ix
Chapter 1: INTRODUCTION.....	1
Motivation	2
Objectives	3
Hypothesis	3
Chapter 2: LITERATURE REVIEW	4
Coal Mining in Pennsylvania.....	4
Coal Fired Power Plants	6
Conventional (Pulverized) Coal Fired Power Plants.....	8
Fluidized Bed Combustion Power Plants	10
Current CCP Applications	12
Chapter 3: PRELIMINARY TESTING FRAMEWORK.....	23
Chapter 4: MATERIALS.....	29
FGD Material.....	29
Fluidized Bed Combustion.	29
Class F Fly Ash.....	30
Chapter 5: TESTING METHODOLOGY	31
Material Characterization	31
Scanning Electron Microscopy.	31
Particle Size Distribution.....	31
BET Specific Surface.	31
Zeta Potential.	32
Moisture/Density Relationships.	32
Specific Gravity.	32
Chemical Analysis	34
Instrumental Neutron Activation Analysis (INAA).	34
Inductively coupled plasma mass spectroscopy (ICP-MS).....	34
Combustion Infrared Detection (IR).	34

Mechanical Tests	35
Unconfined Compression Testing.....	35
Hydraulic Conductivity.	36
Effluent Chemical Analysis.....	37
X-Ray Diffraction.	38
Chapter 6: RESULTS AND DISCUSSION	39
Characterization	39
Mechanical Tests	45
Chapter 7: RECOMMENDED TESTING FRAMEWORK	56
Chapter 8: CONCLUSIONS	58
Chapter 9: RECOMMENDATIONS FOR FUTURE WORK.....	59
REFERENCES.....	60
Appendix A: HYDRAULIC CONDUCTIVITY PROCEDURE.....	63
Appendix B: PROCTOR DATA.....	73
Appendix C: HYDRAULIC CONDUCTIVITY DATA	76
Appendix D: UNCONFINED COMPRESSION TEST DATA.....	80
Appendix E: PARTICLE SIZE DISTRIBUTION DATA.....	145
Appendix F: BASELINE CHEMICAL ANALYSIS	148
Appendix G: EFFLUENT CHEMICAL ANALYSIS	151

LIST OF FIGURES

Figure 1: CCP beneficial use vs. production (after ACAA, 2009)	2
Figure 2: Cross-sections of anthracite vs. bituminous fields (Hornberger et al., 2004)	4
Figure 3: Physiographic provinces of Pennsylvania (Hornberger et al., 2004)	5
Figure 4: Distribution of conventional coal fired power plants in Pennsylvania (Dalberto et al., 20004).....	7
Figure 5: Schematic of coal fired power plant (Powerspan Corp., 2009)	8
Figure 6: Distribution of FBC power Plants in Pennsylvania (Dalberto et al., 2004)	10
Figure 7: Cumulative coal refuse consumption in both anthracite and bituminous fields in Pennsylvania (Dalberto et al., 2004)	11
Figure 8: Variation of unconfined compressive strength values of fly ash (FA) and snow-added fly ash (FI) with time (Baykal et al., 2004).....	18
Figure 9: Variation of splitting tensile strength values of fly ash (FA) and snow-added fly ash (FI) with time (Baykal et al., 2004).....	19
Figure 10: Swell stain vs. time at 100 and 1000kPa (Deschamps, 1998).....	20
Figure 11: Vertical movement of manhole (Deschamps, 1998)	21
Figure 12: Possible Tests for Using CCPs in Embankment Construction.....	25
Figure 13: Hitachi S-3000H SEM.....	33
Figure 14: Standard Proctor mold and hammer	33
Figure 15: Boart Longyear frame Figure 16: Geocomp Load Trac II frame	35
Figure 17: Pressurized permeability cell Figure 18: Sample preparation	37
Figure 19: Hydraulic conductivity test configuration	37
Figure 20: Proctor curves for FGD material, FBC ash, and class F fly ash.....	40
Figure 21: Zeta potential vs. solution pH for FGD material, FBC ash, and class F fly ash	41
Figure 22: Scanning electron micrographs of FGD material (a) 400x, (b) 1500x, (c) 700x, (d) 70x ..	42
Figure 23: Scanning electron micrographs of FBC ash (a) 950x, (b) 3000x, (c) 1400x, (d) 90x	43

Figure 24: Scanning electron micrographs of class F ash (a) 950x, (b) 3500x, (c) 10000x, (d) 120x	44
Figure 25: Peak strength vs. curing time for FGD material, FBC ash, and Class F fly ash	45
Figure 26: Typical shear crack failure mode for FGD material.....	46
Figure 27: Typical spalling failure Figure 28: Typical vertical cracking failure.....	47
Figure 29: Class F fly ash sample after 56 days of curing.....	48
Figure 30: XRD Patterns for FGD material initially mixed at optimum water content. Samples cured for 1-180 Days	49
Figure 31: XRD Patterns for FBC ash initially mixed at optimum water content. Samples cured for 1-180 Days	50
Figure 32: XRD Patterns for class F fly ash initially mixed at optimum water content. Samples cured for 1-90 Days	51
Figure 33: Hydraulic conductivity as a function of time	52
Figure 34: Hydraulic conductivity vs. concentration	55
Figure 35: Test framework for embankment construction and mine land reclamation.....	56

LIST OF TABLES

Table 1. Outline of CCP Application	12
Table 2. Engineering Properties of Fly Ash (Bacon, 1976).....	15
Table 3. Influence of Age on Values of Cohesion and Angle of Internal Friction for Compacted Fly Ash (Joshi et. al., 1976)	16
Table 4. Comparison of the Properties of Compacted Fly Ash and Compacted Fly Ash with Snow (Babykal et al., 2004)	18
Table 5. Optimum Water Content and Maximum Dry Density from Standard Proctor Compaction Test (Deschamps, 1998)	19
Table 6. Hydraulic Conductivity of Uncured Samples using Falling Head Test (Deschamps, 1998).....	20
Table 7. CCP Source Locations	29
Table 8. Zeta Potential and System Stability (ASTM Standard D 4187-82).....	32
Table 9. Hydraulic Conductivity Test Parameters	36
Table 10. Proctor Test Results for FGD Material, FBC Ash, and Class F Fly Ash	40
Table 11. d10, d50, and d90 values for FGD material, FBC ash, and Class F Fly ash	40
Table 12. Specific Gravity (Gs) and Specific Surface (Sa) of the Materials Used in this Study	41
Table 13. Maximum Observed Concentrations and DEP Maximum Acceptable Leachate Concentrations	54

ACKNOWLEDGEMENTS

Dr. Angelica Palomino: The Pennsylvania State University

Dr. Barry E. Scheetz: The Pennsylvania State University

Steve Dixon: Reliant Energy

Larry LaBuz: PPL

Paul Kish: First Energy

Rusty Taylor: Robindale Energy

Randy Lindermuth: Reading Anthracite

Phil Kiser: Piney Creek

John Buck: Civil & Environmental Consultants, Inc.

Anthony M. DiGioia: DiGioia, Gray & Associates, LLC

Jeff Gittleman: Hawk Mountain Labs

John Blasosky: John Blazosky Associates

Robert Hershey: Meisner & Earl, Inc.

Chapter 1: INTRODUCTION

Coal combustion products (CCPs) are by-products created when coal is burned for energy production. These products include fly ash, bottom ash, boiler by-products, flue gas desulfurization (FGD) by-products, and others (ACAA, 2009). In 2007 alone, the United States produced in excess of 125 million tons of CCPs. Despite the fact that approximately 40% of the CCPs were used beneficially, for example using fly ash as a supplemental cementitious material in Portland cement concrete, 60% of the CCPs were disposed of via land filling. Figure 1 outlines the beneficial use of CCPs vs. production from 1966-2007 (ACAA, 2009). This figure clearly illustrates that the amount of CCPs being produced far exceeds the CCPs being recycled. Furthermore, the difference between the two continues to grow.

There are significant advantages to reusing CCPs for large volume civil engineering applications such as mine land reclamation and embankment structures. Currently, CCPs not beneficially used are either stockpiled or disposed of in landfills and slurry ponds. This practice consumes large quantities of land space. Reuse of CCPs, as opposed to disposal, would reserve landfills to be used for residential waste which currently has no other viable disposal methods. Utilizing CCPs in these engineering applications could greatly reduce the amount of natural materials currently required for these structures. The excavation, transportation, and installation of natural materials have an associated cost which could potentially be significantly reduced if CCPs were used from a coal power plant in the vicinity of the construction project (Kumar and Patil, 2006). In some cases CCPs have even out-performed natural materials (Bacon, 1976). Typical intrinsic CCP properties also present various advantages. These advantages include the potential cementitious nature of CCPs (strength gain with time), low unit weight, high factor of safety for slope stability, high shear strength per unit weight ratio, and the immediate availability of large volumes of material (Butalia and Wolfe, 2001) (ACAA, 2009).

Despite their relevant advantages, CCPs are often perceived as strictly a waste product due to their chemical composition and potentially hazardous leachate. However, not all CCPs should be considered environmentally unsound. In fact, their chemical composition can vary widely depending on the source power plant location, the power plant type, and the fuel source. Therefore it is necessary that CCPs be characterized both mechanically and chemically to qualify their utilization in civil engineering structures.

In order to increase the beneficial use of CCPs, the perception of these materials as a waste product needs to be changed. Moreover, there is potential for these materials to be categorized as “green” since CCPs have been successfully utilized in civil engineering structures. The missing component in the current state of practice is a consistent methodology for categorizing CCPs as either environmentally and structurally sound or harmful when used as a construction material, and this methodology should be application-based.

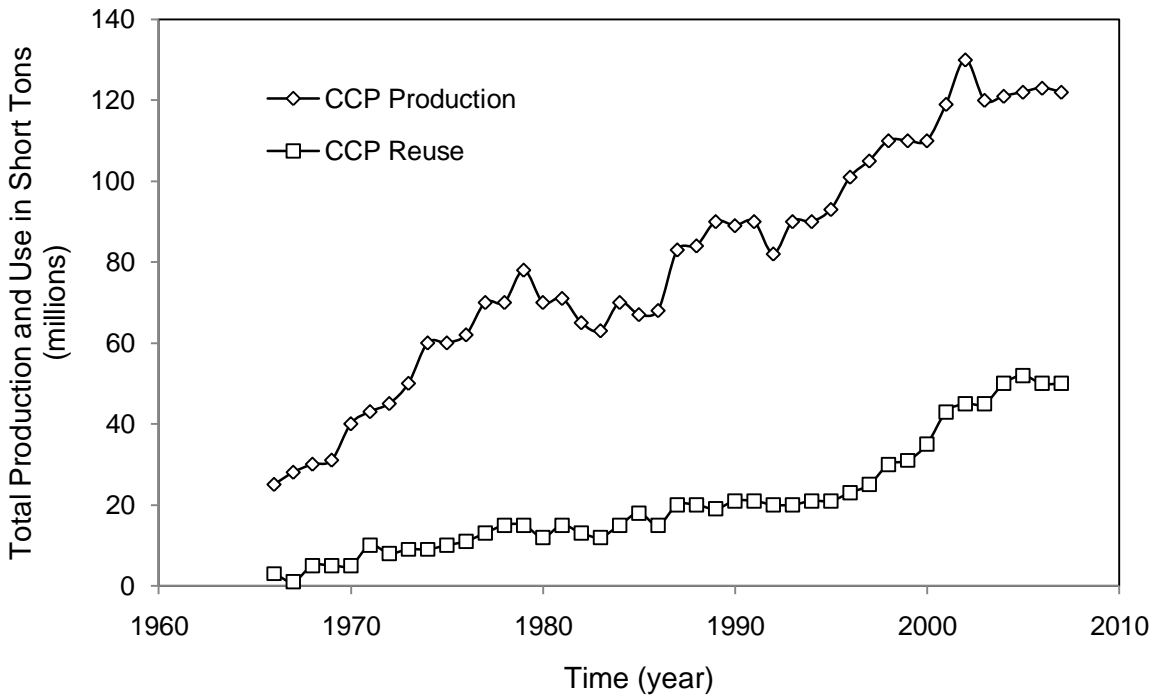


Figure 1: CCP beneficial use vs. production (after ACAA, 2009)

Motivation

The motivation for this study can be summarized as follows:

- Excess quantities of CCPs are produced annually which are not beneficially used
- CCPS are variable depending on the type of power plant and the fuel source and must be properly examined for implementation
- Using CCPs for large-volume, engineering applications is potentially much more economical compared to using naturally occurring materials
- The material properties of CCPs may led to superior performance compared to other naturally occurring materials in certain applications
- No such testing framework currently exists

Objectives

This study will focus on coal combustion products produced in the Commonwealth of Pennsylvania. The objectives of this study are to:

1. Develop a minimal set of practical mechanical and chemical tests that will qualify CCP formulation specific to large-volume civil engineering applications. These parameters should provide appropriate specifications to allow the use of CCPs without negative structural or environmental impact.
2. Apply the test framework to three distinct types of CCPs for a given application as a case study.

Hypothesis

CCPs can be evaluated in a logical, methodical manner to determine whether or not the material is usable as a civil engineering material in large-volume applications via a specific testing framework which includes characterization, chemical, and mechanical property measurements.

The specific questions to be addressed in this study are:

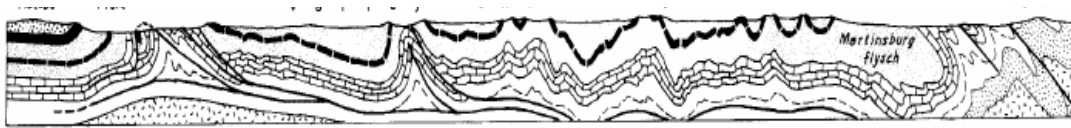
1. What material properties (characterization, chemical, and mechanical) are required for an embankment/mine land reclamation application?
2. Do CCPs meet the minimum requirements for use in embankments/mine land reclamation? Based on the literature review, do CCP properties have to be modified prior to use?
3. Does FGD material, FBC Ash, and Class F fly ash meet the minimal material requirements for the given application?

Chapter 2: LITERATURE REVIEW

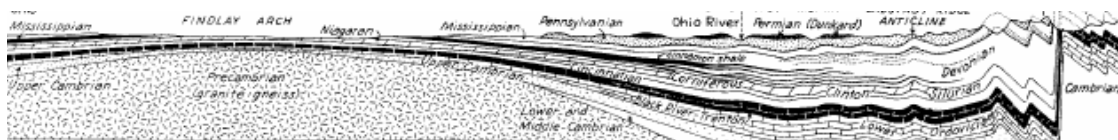
Coal Mining in Pennsylvania

Since the beginning of the commercial coal mining industry in Pennsylvania in the late 1700's, the state has produced in excess of 16.3 billion tons of both Bituminous and Anthracite coal (Dalberto et al., 2004). Anthracite coal, a metamorphic rock, contains a greater amount of carbon compared to bituminous coal which is considered a sedimentary rock.

Metamorphic anthracite coal is created with heat and pressure, therefore it is commonly found where the geologic structure has been faulted and folded from mountain building events. As shown in Figure 2, the complexity of the geologic structure where anthracite is located makes it difficult to map compared to the relative simplicity of the bituminous fields (Hornberger et al., 2004).



Cross-section of the Valley and Ridge Province (Anthracite)



Cross-section of the Allegheny Plateau (Bituminous)

Figure 2: Cross-sections of anthracite vs. bituminous fields (Hornberger et al., 2004)

Pennsylvania's anthracite fields are located in the Valley and Ridge province of the Appalachian Mountains (see Figure 3). The rock strata within this province are, from oldest to youngest, the Pottsville and Llewellyn formations respectively. This province is approximately 1200 miles extending from the Saint Lawrence Lowland to Alabama. The valley ridge province is made up of three sections which include the northern/Hudson-Champlain section, the middle section stretching from the Delaware River to the New River, and the southern section from Virginia to Alabama (Hornberger et al., 2004).

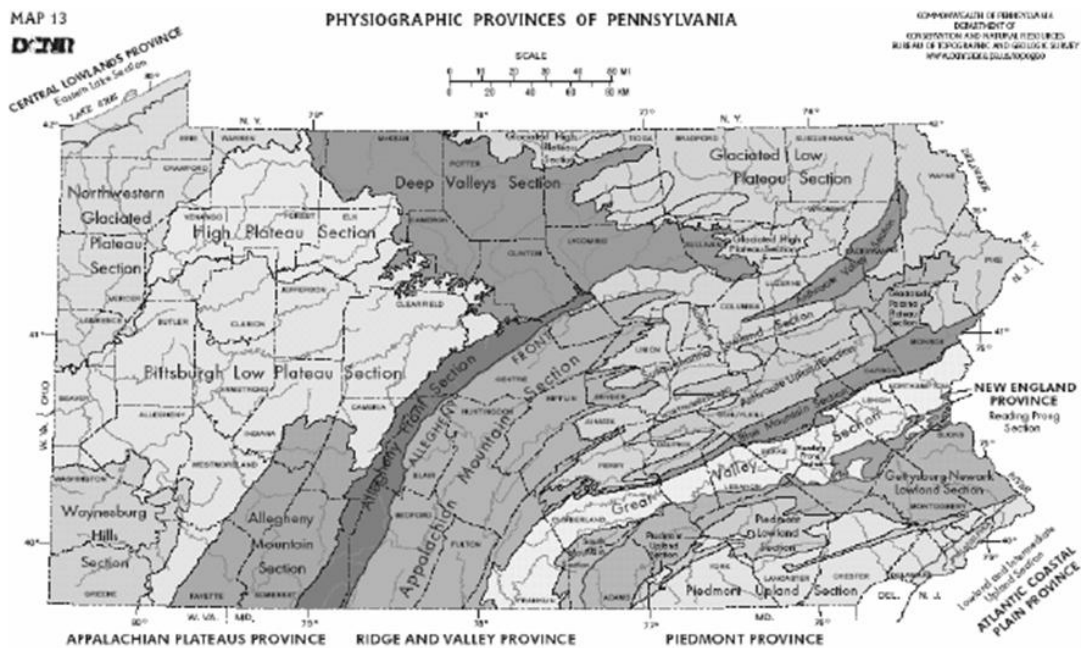


Figure 3: Physiographic provinces of Pennsylvania (Hornberger et al., 2004)

Pennsylvania's bituminous fields are located within the Appalachian Physiographic Province (see Figure 3). Coal bearing rocks within the Allegheny Plateau consist of, from oldest to youngest, the Pottsville, Allegheny, Conemaugh, Monongahela, and Dunkard groups respectively (Hornberger et al., 2004).

Anthracite coal has significantly less sulfur content compared to bituminous coal, 0.7% and 2.0% respectively. Therefore the burning of anthracite coal is more environmentally friendly. Anthracite coal is also much more energy efficient. Burning anthracite coal yields an energy output that is 5% higher per pound. However, due to the geographic location of anthracite, it is considerably more difficult to mine which has economical implications. Anthracite also has a higher ignition and burning temperature which requires more expensive boiling equipment (Dalberto et al., 2004).

Coal mining is an extensive operation in Pennsylvania. As a consequence abandoned/unreclaimed mines, acid mine drainage (AMD), and abandoned coal refuse piles are significant problems. There are more than 5000 abandoned/unreclaimed mine sites which cover a total area in excess of 189000 acres. There are also greater than 820 coal refuse piles which consume approximately 8500 acres and yield 212,465,000 cubic yards. Bituminous refuse piles are known as "gob" and anthracite refuse piles are known as "culm". AMD in Pennsylvania is considered the state's most significant stream pollution problem which is estimated to cost 14.6 billion dollars to remediate (Dalberto et al., 2004).

Coal Fired Power Plants

Coal is used for various applications. Chemicals in coal help to produce plastics, fertilizers, and tar. Coke, a solidified carbon used as fuel in the melting of iron for steel production, is also created from coal. Despite all of its alternate uses, 92% of coal is used to produce electricity. The first steam-electric power plant in the United States was constructed by the Edison Electric Company in New York City in 1882. The plant service approximately 500 residents and produced a total of 600 kilowatts of electricity. Since then, coal fired power plants have grown to produce 56% of the gross electricity in the United States and 36% internationally. Modern plants are capable of producing between 125 MW (megawatts) and 1000 MW. One MW-hour can power in the vicinity of 330 homes for a period of one hour. (Powerspan Corp., 2009)

The methodology behind coal power production is relatively simple. Coal is ignited and burned creating energy. This energy is used to vaporize liquid water. Pressurized water vapor spins a turbine which operates an electrical generator producing electricity.

There are two major types of coal fired power plants in the United States, Fluidized Bed Combustion power plants (FBC) and conventional coal fired power plants (Dalberto et. al., 2004). Figure 4 shows the location of the 21 conventional plants in Pennsylvania.

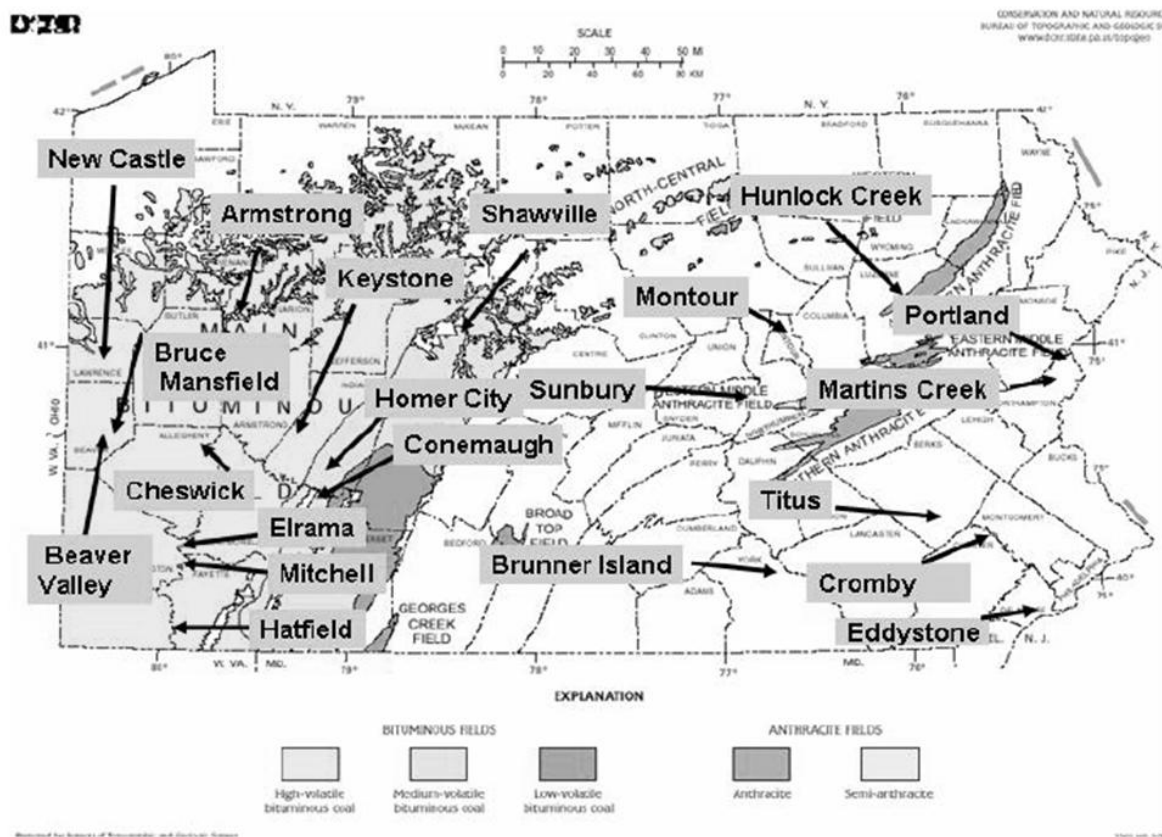


Figure 4: Distribution of conventional coal fired power plants in Pennsylvania (Dalberto et al., 2004)

Conventional (Pulverized) Coal Fired Power Plants

Conventional coal fired power plants burn mined coal. The coal first arrives at the plant and is pulverized into a fine powder (75% less than 75 microns in diameter). This coal powder is injected into the combustion chamber using pressurized air. Since the pulverized coal particles are so fine, the fuel actually behaves like a liquid. The fuel is ignited and burned in the vicinity of 1400°C. This energy is used to heat the liquid water in the boiler to produce steam. The steam then exits the boiler and enters the turbine at pressures between 1800 and 3500 pounds per square inch (psi). The expanding steam through the turbine induces high speed rotation which in turn operates an electro-magnetic generator. In order to produce alternating current with a constant frequency of 60 hertz in the United States, it is essential that the steam be kept at a constant pressure. The steam which passes through the turbine is reused using a condensing process. The steam exits the turbine and enters a condenser which converts the used low pressure steam back into liquid form. The condensing process requires a significant amount of water which explains why many power plants are located adjacent to rivers or lakes. If the power plant is not located within the vicinity of body of water then water is pumped on site and cooling towers are utilized (Powerspan Corp., 2009).

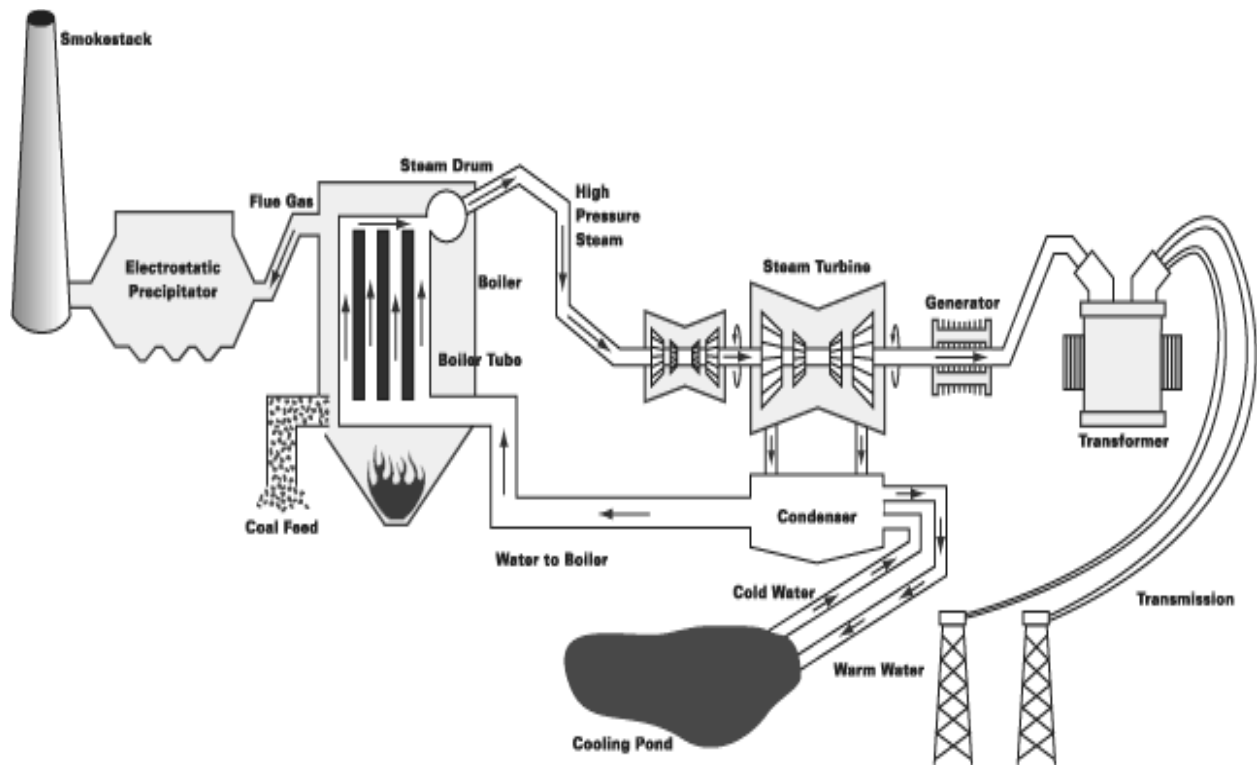


Figure 5: Schematic of coal fired power plant (Powerspan Corp., 2009)

Burning coal for electricity unfortunately produces pollutants which are potentially harmful to the environment as well as human health. The four most significant pollutants are sulfur dioxide (SO_2), nitrogen oxides (NO_x), mercury (Hg), and particulate matter. Sulfur Dioxide forms sulfuric acid which is distributed into the environment via acid rain. Nitrogen oxide can also form acid rain when converted to nitric acid, but its more significant impact is the fact that it aids in ground level ozone production. Particulate matter, referred to as PM_{10} and $\text{PM}_{2.5}$, are particles less than or equal to 10 microns in diameter and less than or equal to 2.5 microns in diameter, respectively. Mercury is released into the air during coal combustion and is then deposited on land or in water. Deposited mercury on land or in water can potentially bioaccumulate in animals and be transferred to humans (Powerspan Corp., 2009).

In 1970, the Clean Air Act authorized the United States Environmental Protection Agency (EPA) to establish National Ambient Air Quality Standards (NAAQS) to protect public health and the environment (Powerspan Corp., 2009). Since then two amendments have been passed, one in 1977 and one in 1990. The Clean Air Act Amendments (CAAA) of 1990 resulted in strict regulations that limit emissions from coal fired power plants. The Acid Rain Program in particular required significant reductions in SO_2 and NO_x . In March 2005, the U.S. EPA issued the Clean Air Interstate Rule and the Clean Air Mercury Rule which were design to achieve a large reduction in air pollution and a permanent cap on mercury emissions, respectively. However, in 2008 the U.S. Court of Appeals voided both of these rules (Powerspan Corp., 2009). There are currently various processes which reduce or eliminate some of the previously described emissions.

Flue Gas Desulfurization (FGD) or Wet Scrubbing is a technique used to control sulfur dioxide emissions. FGD consists of injecting a slurry of calcium carbonate into the combustion chamber. The calcium carbonate is converted to calcium oxide which reacts with the sulfur in the combusting coal and force oxidized. This reaction forms inert calcium sulfate and water which is synthetic gypsum (Dalberto et al., 2004).

Nitrogen Oxide control consists of both pre-combustion and post-combustion techniques. Pre-combustion treatment is administered by lowering the overall combustion temperature which in turn lowers NO_x formation. The fact that the combustion temperature is lowered requires more fuel in order to achieve an equivalent amount of useful energy which results in increased CO_2 emission. Low NO_x burners are also difficult to adapt to current plants which poses a certain economical issue. Post-combustion NO_x control is accomplished by reacting ammonia with nitrogen oxides forming nitrogen and water vapor. This process can be administered in two different ways, the use of thermal energy (heat) or the use of a catalyst. The thermal heat method (selective non-catalytic reduction, SNCR) is difficult to control because the reaction can only take place within a narrow temperature window. If the temperature is too high then the ammonia converts to NO_x and is released into the air. If the temperature is too low both ammonia and NO_x are released into the air.

Using the catalyst method (selective catalytic reduction, SCR), the overall reaction temperature is lowered as well as broadened, making the reaction easier to control (Powerspan Corp., 2009).

Particulate matter release is primarily controlled by using electrostatic precipitators (ESP's). ESP's attract fine particles in the flue gas by producing an opposite electrical charge compared to the particles. This opposite charge attracts the particulate matter to collector plates to be removed. ESP's are approximately 99.5%-99.9% efficient (Powerspan Corp., 2009).

Fluidized Bed Combustion Power Plants

Fluidized Bed Combustion power plants were developed as a result of The Public Utility Regulatory ACT, (PURPA), in response to the fuel crisis of the 1970's. PURPA required utility companies to experiment with the use of non-traditional fuels in order to produce power. Therefore FBC power plants were developed in order to burn coal mine refuse which is considered non-traditional fuel. Figure 6 shows the locations of the 16 FBC plants in Pennsylvania (Dalberto et al., 2004).

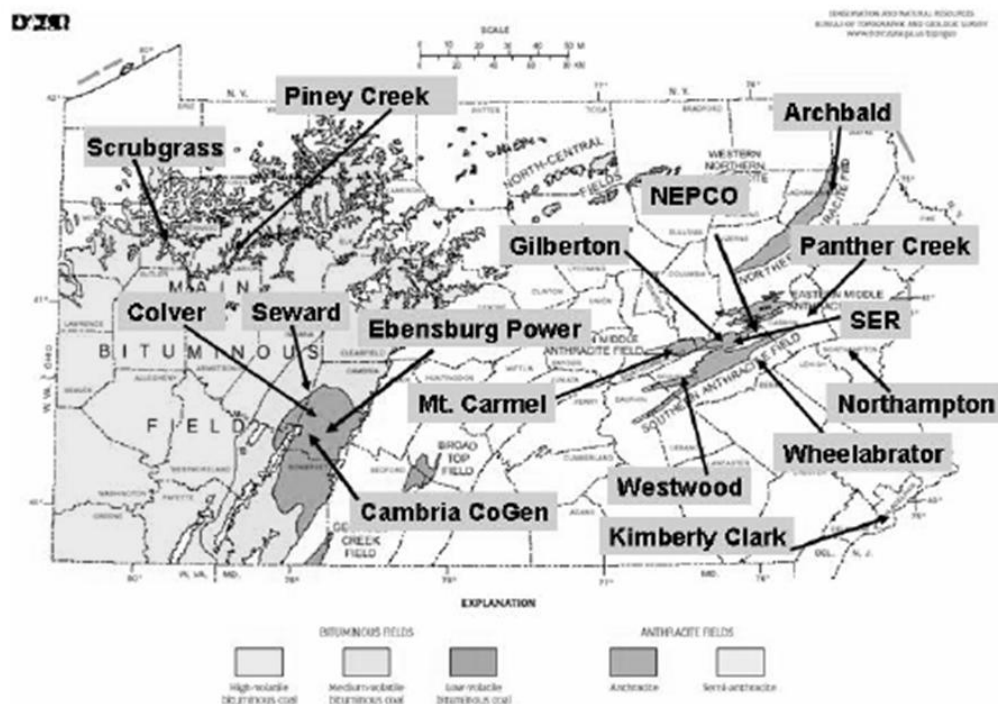


Figure 6: Distribution of FBC power Plants in Pennsylvania (Dalberto et al., 2004)

Coal refuse is first crushed to a top size of 5mm, mixed with air, and then injected into the combustion chamber. This fuel behaves as a liquid hence the name “Fluidized” combustion. Since FBC plants use refuse as the fuel source they are significantly less efficient compared to conventional plants. In fact this refuse, which is essentially waste material, only has about 25% of the heating value of actual coal. However, the FBC burning temperature (800-900°C) is lower than conventional plants which in turn reduce the emission of nitrogen oxides. FBC plants are forecast to burn approximately 11.5 million tons of refuse annually. Figure 7 illustrates the increased use of coal refuse for power production (Dalberto et al., 2004).

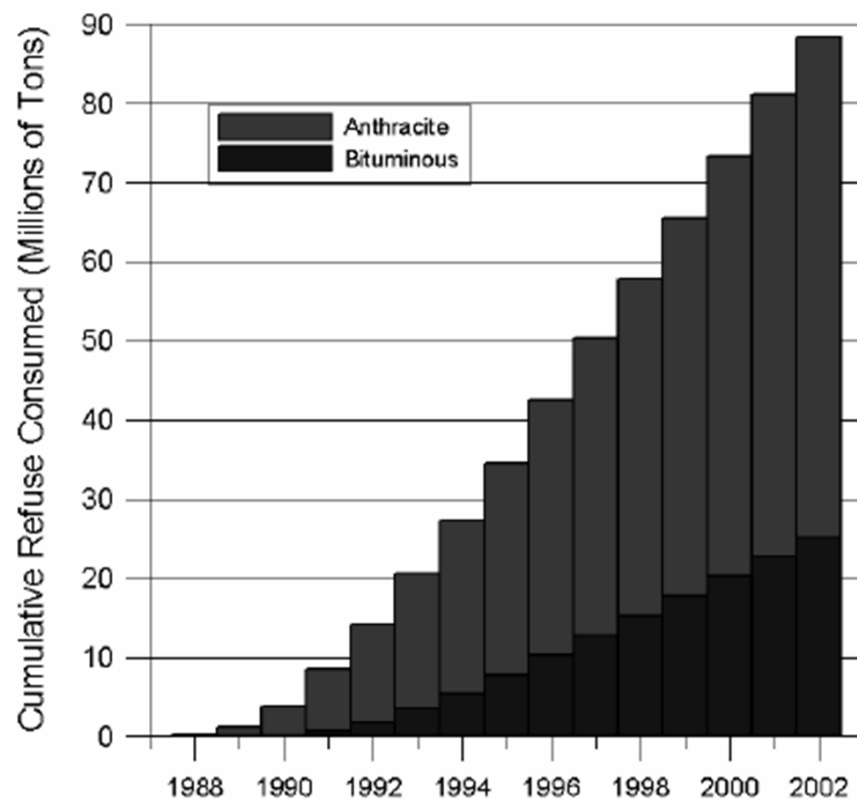


Figure 7: Cumulative coal refuse consumption in both anthracite and bituminous fields in Pennsylvania (Dalberto et al., 2004)

CCP production is highly variable as a function of power plant location, type of power plant (conventional vs. FBC), and the fuel source. The material properties can be very different from one power plant to the next. Therefore it is essential to develop a standard testing framework to qualify these highly variable materials for use in large-volume, engineering applications.

Table 1 outlines various civil engineering applications which utilize CCPs.

Current CCP Applications

Table 1. Outline of CCP Application

CE Application	CCP Type	Comments	Important Material Properties	Reference
Embankment/ Structural Fill	Fly Ash	→Pilot project to study feasibility →Fly ash gained strength with time →Fly ash made an acceptable structural fill	Range of dry densities: 1294-1426 kg/m ³ (80.8-89.0 lbs/ft ³) Range of optimum moisture contents: 24.8%-27.3% CBR (saturated): 2 CBR (unsaturated): 20 CBR swell: 20%	Bacon, 1976
Embankment/ Structural Fill	Fly Ash	→Embankment for a 4 lane concrete highway in Chicago →Construction techniques found to be that same as for naturally occurring soils →GSD resembled a well-graded silty soil, yet compaction was more responsive to vibration than kneading →Significant differences in fly ash density occurred with changes in combustion conditions, fuel source, and plant location →Fly ash proved to be a superior structural fill material compared to naturally occurring soils	N/A	Bacon, 1976
Structural Fill	Fly Ash	→Used as fill under a 1 million gallon fuel tank →Moisture content varied as a function of source	Range of optimum moisture contents: 18%-38% Cohesion at 0 days: 35.85 kPa (5.2 psi) 7 days: 613.63 kPa (89 psi) 28 days: 1172.11 (170 psi)	Joshi et al., 1976
Embankment/ Structural Fill	Fly Ash Bottom Ash	→First major embankment in Ontario to use CCPs as structural fill →Bottom ash and fly ash used to construct a highway embankment →Fly ash proved to be a superior structural fill material →Settlement of the fly ash embankment was negligible	Bottom ash: dry density: 1587 kg/m ³ (99.1 lbs/ft ³) opt. moisture content: 20.6% Fly ash: dry density: 1243 kg/m ³ (77.6 lbs/ft ³) opt. moisture content: 30.5%	Cragg, 1985

Embankment/ Structural Fill	Fly Ash	<p>→10% by weight of ice was added to fly ash during compaction</p> <p>→The ice does not affect compaction and later melts to initiate pozzolanic reactions</p> <p>→The unconfined compressive strength of the ice-added fly ash was 70% greater than fly ash after a 90 day curing period</p>	<p>Unconfined compressive strength w/ ice @ 90 days ~2500 kPa (362.6psi)</p> <p>Unconfined compressive strength w/o ice @ 90 days ~1700 kPa (246.56psi)</p>	Baykal et al., 2004
Embankment/ Structural Fill	FBC Ash Stoker Ash Fly Ash	<p>→Embankment was constructed in order to monitor FBC ash for use as structural fill</p> <p>→The FBC ash exceeded the strength requirements for use as a structural fill</p> <p>→FBC ash has a tendency to swell/expand due to ettringite formation post installation</p>	<p>FBC ash: dry density: 1529 kg/m³ (95.45 lbs/ft³)</p> <p>opt. moisture content: 23.0%</p> <p>Stoker ash: dry density: 1396 kg/m³ (87.15 lbs/ft³)</p> <p>opt. moisture content: 22.0%</p>	Deschamps, 1998
Embankment/ Structural Fill	CCPs	<p>→CCPs are available in bulk quantities</p> <p>→CCPs have greater slope stability factors of safety compared to naturally occurring soils</p> <p>→CCPs have desirable, low unit weights</p> <p>→CCPs have high shear strength/unit weight ratios</p> <p>→CCPs can have various hydraulic conductivity characteristics</p>	N/A	Butalia, 2001

Embankment Fill

Construction of embankments using fly ash has been experimented with as early as the 1960's. In 1964, The Chicago Fly Ash Company proposed the construction of an experimental fly ash embankment in order to study feasibility. The project was planned and supervised by the Illinois Division of Highways. Subsequently in 1965 construction of a 61m (200ft.) long, 12m (40ft.) wide, and 2m (6ft.) tall embankment began. The construction was considered successful and the following observations were made (Bacon, 1976):

- Hardened fly ash lumps must be broken up to obtain full depth compaction.
- Rotary tilling proved to be most effective in breaking up lumps.
- Scarification into the preceding lift was desirable to prevent lensing.
- A 15cm (6in.) loose lift could be best compacted with a rubber tire roller. The sheep's foot tore the surface without providing any additional compaction.
- Within a moisture range of 18%-29%, a narrow range of compaction from 85%-88% was possible using 8-10 passes of a non-vibratory 9000kg (10ton) roller.
- The embankment showed an unconfined compressive strength of 429-482.6 kPa (55.56-62.5 psi)
- Fly ash has a tendency to "age harden", that is gain strength with time.
- Fly ash has a relatively high initial permeability with respect to other similarly graded materials.
- Dusting of fly ash below a moisture content of 13% became a problem.
- Fly ash would not support vegetation satisfactorily.
- Fly ash made an acceptable structural fill.

Table 2. Engineering Properties of Fly Ash (Bacon, 1976)

Engineering Properties of Fly Ash	
Percent Sand-sized Particles	19%
Percent Silt-sized Particles	71%
Percent Clay-sized Particles	10%
Plasticity Index	N.A.
Range of Standard Densities	1294-1426 kg/m ³ (80.8-89 lbs/ft ³)
Range of Optimum Moisture Content	24.8%-27.3%
CBR (Saturated)	2%
CBR (Unsaturated)	20%
CBR Swell	5%

These findings could be considered as some of the first test results and specifications of fly ash for use as a structural material.

In March of 1972, the construction of a four lane concrete highway in Chicago was proposed. The project included a 188,000 cubic meter (245,781 cubic foot) embankment where 85% of the total quantity could be fly ash. Specifications called for electrically precipitated fly ash as the embankment's core with soil placed on top and on the slopes. The fly ash was to be placed at a moisture content of 15%-30%, not exceed 15 cm (6in.) lifts, be scarified to a depth of 18cm (7in.), and compacted to at least 85% of the laboratory dry density. A minimum shear strength of 239.4 kPa (5000 lb/ft.²) was required and measured with a pocket penetrometer.

The following construction and post-construction observations were made (Bacon, 1976):

- Electrically precipitated fly ash is an acceptable material to use as an alternate to naturally occurring soils as an embankment material above the water table, and in some cases would be a superior structural material.
- The methods of construction may be essentially those used for natural soils, that is, compaction in thin lifts, scarification of the preceding lift surface, and compaction to a predetermined minimum relative compaction.
- While the grain size of fly ash most resembles a well-graded silty soil, compaction is more responsive to vibration than kneading, loading, or tamping and in this respect acts like a granular soil.
- Significant differences in standard laboratory densities of fly ash should be expected, particularly when changes occur with source or combustion conditions.

- The use of large quantities of water is required for controlling dust and obtaining compaction.
- The pocket penetrometer was a very helpful tool for use in conjunction with other standard tests in maintaining job control over compaction operations.
- Environmental hazards, real or purely speculative, must be solved or fly ash usage may never reach its full potential. Dusting is a very real problem, causing excessive wear to contractors' equipment and possible objections from adjacent land owners. The actual occurrence of ground water pollution by fly ash is more in the speculative category and has not been confirmed by field experience.

Another early study involved the use of fly ash as structural fill where a 1 million gallon fuel tank was to be constructed. The existing subsurface consisted of soft clay to a depth of 20 ft. followed by a dense sand layer to 80 ft. The soft clay was considered inappropriate for construction and needed to be replaced. Since there was a large quantity of fly ash stockpiled nearby it seemed a logical choice.

The clay material was removed and the fly ash fill was placed and compacted in 8in. to 10in. lifts. The moisture content of the fly ash source varied from 18%-38%. Despite this large variation in moisture content, problems with compaction were not encountered and 95% relative compaction proved to be easily attainable. Minimum and maximum settlements were 0.5in. and 1in. respectively. Table 3 references lab and field test results obtained from the fly ash fill material.

Table 3. Influence of Age on Values of Cohesion and Angle of Internal Friction for Compacted Fly Ash (Joshi et. al., 1976)

Age in Days	Laboratory Tests		Field Tests	
	c_u (psi)	Φ_u (degrees)	c_u (psi)	Φ_u (degrees)
0	5.2	29	NA	NA
7	89	45	4	43
28	170	45	67	43

Another study conducted by Cragg, 1985 examined the behavior of fly ash used as structural fill for a highway embankment. The embankment was monitored for settlement, frost penetration, and frost heave. The embankment was part of the construction of an over pass on highway 402 which links Canada to the United States in Sarnia, Ontario. This was considered the first major highway embankment in Ontario to use coal combustion products as a structural material. In fact 82,640Mg (91,095 tons) of bottom ash and 164,210Mg (181,004 tons) of fly ash were used for construction. The embankment consisted of a base layer of bottom ash, a fly ash core, and a top layer of bottom ash. The bottom ash served as a drainage blanket for the fly ash as well as prevent the fly ash from wicking ground water. An outer layer of naturally occurring soil was placed on the sides of the embankment in order to prevent erosion and support vegetation growth. The ash was compacted in lifts reaching relative compaction using moderate effort. Laboratory dry densities were 1587 kg/m^3 (99.1 lb/ft.^3) at 20.6% water content for the bottom ash and 1243 kg/m^3 (77.6 lb/ft.^3) at 30.5% water content for the fly ash. (Cragg, 1985)

Instruments were installed throughout the site in order to monitor natural soil settlement below the embankment, settlement of the actual fill, frost penetration, and frost heave at the top of the embankment.

Observations of the use of fly ash for fill material on this project were positive. Settlement of the fly ash embankment was negligible and frost heave minimal. Fly ash used a structural fill is recommended by the results of this particular paper. (Cragg, 1985)

A paper written by Baykal et al., 2004 explains a technique which “balances” the sensitive amount of water required for fly ash compaction and the excess amount of water required to initiate pozzolanic reactions of the material. The technique involves the addition of snow or ice during the compaction of fly ash at optimum water content. Theoretically, the ice does not affect compaction and later melts to initiate chemical reactions. Samples of fly ash were prepared at optimum moisture content with the addition of 10% by weight of ice. The Harvard Miniature Compaction Device was used to create the samples which were 3.6cm in diameter and 7.6cm in height. Some interesting results were obtained.

Table 4. Comparison of the Properties of Compacted Fly Ash and Compacted Fly Ash with Snow (Baykal et al., 2004)

	Fly ash (FA)	Fly ash + snow (FI)	Change
Dry unit weight (kN/m^3)	13.41	11.78	14% decrease
Water content (%)	19.54	28.89	48% increase
Void ratio (e)	0.90	1.17	30% increase

One can observe from Table 4 the altered properties of the fly ash with snow addition. A 14% decrease in dry unit weight will decrease the overall settlement of an embankment. The 30% increase in void ratio will allow less fly ash to fill an equivalent volume resulting in a more economic practice.

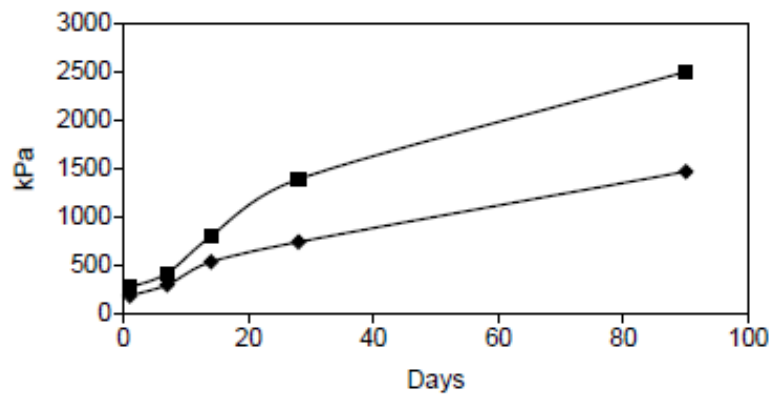


Figure 8: Variation of unconfined compressive strength values of fly ash (FA) and snow-added fly ash (FI) with time (Baykal et al., 2004)

By observing Figure 8, one can clearly see the increased unconfined compressive strength of the snow-added fly ash due to continued chemical reactivity over the 90 day test period. In fact, the strength of the snow-added fly ash was 70% greater than the fly ash at 90 days. (Baykal et al., 2004)

During highway pavement design, tensile stresses become a very important parameter. In order to test this behavior, splitting tensile tests were also conducted. Refer to Figure 8 to notice a similar strength gain trend compared to the results of the unconfined compression test. The tensile strength of the snow-added fly ash is approximately 85% greater than the fly ash and is generally 10% of the unconfined compressive strength. (Baykal et al., 2004)

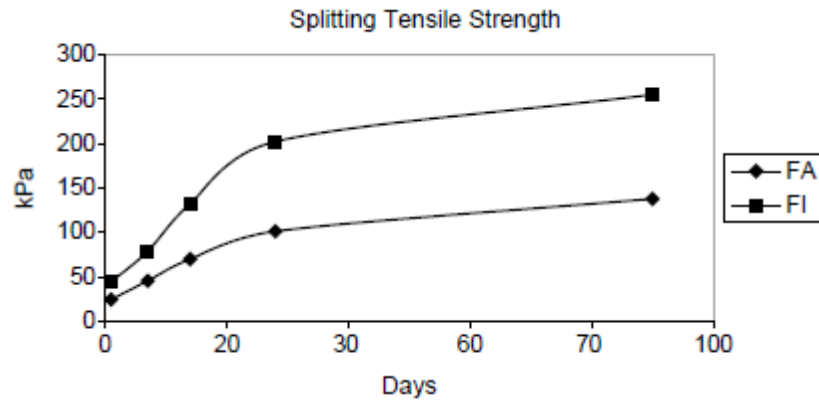


Figure 9: Variation of splitting tensile strength values of fly ash (FA) and snow-added fly ash (FI) with time (Baykal et al., 2004)

Butalia et. al. examined the benefits of using CCPs for the construction and repair of highways in Ohio. The use of CCPs in embankments/structural fills provided various advantages including:

- Availability of materials in bulk quantities
- Higher slope stability factors of safety compared to naturally occurring soils
- Suitable for construction on low-bearing strength soils due to their lower unit weight compared to naturally occurring soils
- High shear strength/unit weight ratio resulting in ideal placement under foundations
- Availability of free draining materials such as bottom ash (Butalia, 2001)

Fluidized Bed Combustion (FBC) ash can also be utilized as embankment fill yet different considerations must be taken into account compared to only using fly ash. A large-volume embankment was constructed at Purdue University consisting of 60% FBC ash, 35% stoker ash, and 5% fly ash. The embankment was approximately 20 m in length and 10 m in height. The purpose of this project was to monitor the performance of FBC ash for use as a fill material. Table 5 outlines the compaction characteristics of the material used. Table 6 illustrates the permeability characteristics of the material used (Deschamps, 1998).

Table 5. Optimum Water Content and Maximum Dry Density from Standard Proctor Compaction Test (Deschamps, 1998)

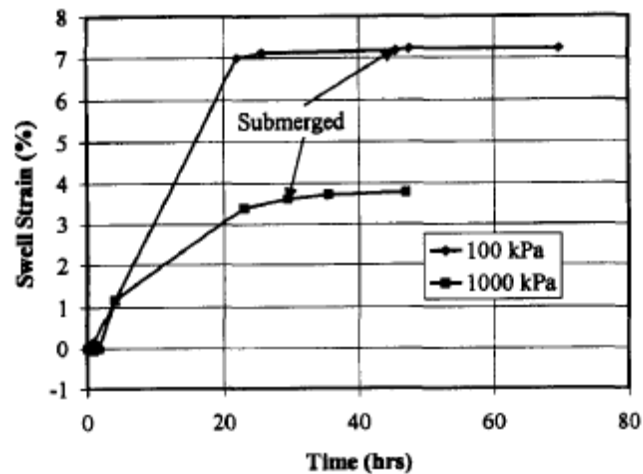
CCB (1)	Optimum water content (%) (2)	Maximum dry density (kg/m ³) (3)
FBC	23.0	1,529
Stoker	22.0	1,396
50/50	22.5	1,437

Table 6. Hydraulic Conductivity of Uncured Samples using Falling Head Test (Deschamps, 1998)

Tested material (1)	Dry density from standard Proctor* (% maximum) (2)	Hydraulic conductivity (cm/s) (3)
Stoker ash	96	8.7E-5
Stoker ash	97	8.6E-5
Atmospheric FBC ash	93	1.2E-5
Atmospheric FBC ash	91	6.4E-5
50/50 mixture	100	2.4E-5
50/50 mixture	96	8.1E-5
50/50 mixture	93	1.5E-4
50/50 mixture	90	3.3E-4

During construction, the ash reached appropriate relative compaction at various moisture contents, the most efficient being close to optimum. Due to the cementitious nature of the material, the ash in the cured condition became extremely hard. Therefore it was almost impossible to excavate a hole to administer the sand cone test or drive the stake of a nuclear density gauge in order to verify compaction and moisture content. This being stated, the ash material far exceeds the strength requirements for use as a structural fill (Deschamps, 1998).

The major issue with regard to using FBC ash as structural fill is its tendency to swell/expand after installation. Figure 10 demonstrates the materials swell strain as a function of time. Figure 11 illustrates the vertical movement of a manhole on top of the embankment at various dates post-construction (Deschamps, 1998).

**Figure 10:** Swell stain vs. time at 100 and 1000kPa (Deschamps, 1998)

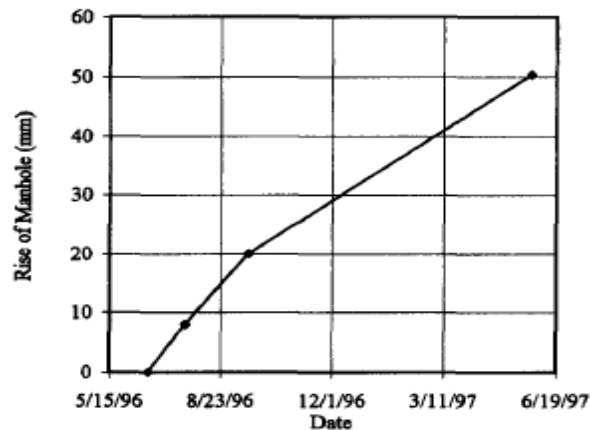


Figure 11: Vertical movement of manhole (Deschamps, 1998)

FBC ash has a high concentration of calcium and sulfur compared to fly ash. These elements lead to the formation of ettringite causing an increase in volume which subsequently produces swelling pressures (Yoon, 2007). The potential for swelling can be reduced by stockpiling the material at an adequate moisture exposure for several months prior to installation (Deschamps, 1998).

The Electric Power Research Institute (EPRI) in collaboration with Duquesne Light Company and GAI Consultants constructed a 1490 ft long structural embankment to support a section of highway in Pittsburgh, PA. Approximately 255000 cubic yards of CCPs were utilized in this project predominately class F fly ash. The class F fly ash exhibited properties similar to naturally occurring silty soils therefore conventional construction techniques could be implemented. The fly ash was placed in 8 in lifts and compacted with a vibratory roller. The material consistently reached 100% of standard Proctor maximum dry density. The project demonstrated that roadway embankments can be designed and constructed of fly ash using conventional engineering practices. The fly ash embankment has performed as well as or better than design estimates with respect to settlement, deformation, and slope stability. The following observations were made (Brendel, 1989):

- Conventional analytical procedures can be used to predict embankment performance.
- The design parameters for fly ash are equal to or better than many naturally occurring soils.
- Preliminary leachate analysis stated that the fly ash is non-toxic and non-hazardous.
- Fly ash is most efficiently compacted using vibratory compactors.
- The use of heavy compactors extends the moisture range over which fly ash can be appropriately compacted.
- Fly ash will pump moisture when the moisture content exceeds the optimum moisture content.

- The use of fly ash saved the Commonwealth of Pennsylvania and the contractor \$100,000 each. Duquesne Light Company saved \$750,000.

Based on the current literature review and case studies the main advantages and disadvantages of using CCPs for civil engineering applications are summarized below.

Main Advantages

- An excess amount of CCPs exist which could potentially be used for large-volume engineering applications
- CCPs are cementitious and gain strength with time
- Low unit weights
- High slope stability factor of safety
- High shear strength/unit weight ratio
- High permeability
- Conventional construction methods can be used for installation

Main Disadvantages

- CCPs are variable (chemical and mechanical properties) as a function of power plant location, type of power plant (conventional vs. FBC), and the fuel source
- High permeability
- Some CCPs have expansive characteristics
- Large volumes of water are required to control dusting and achieve compaction
- CCP leachate can have negative environmental impact

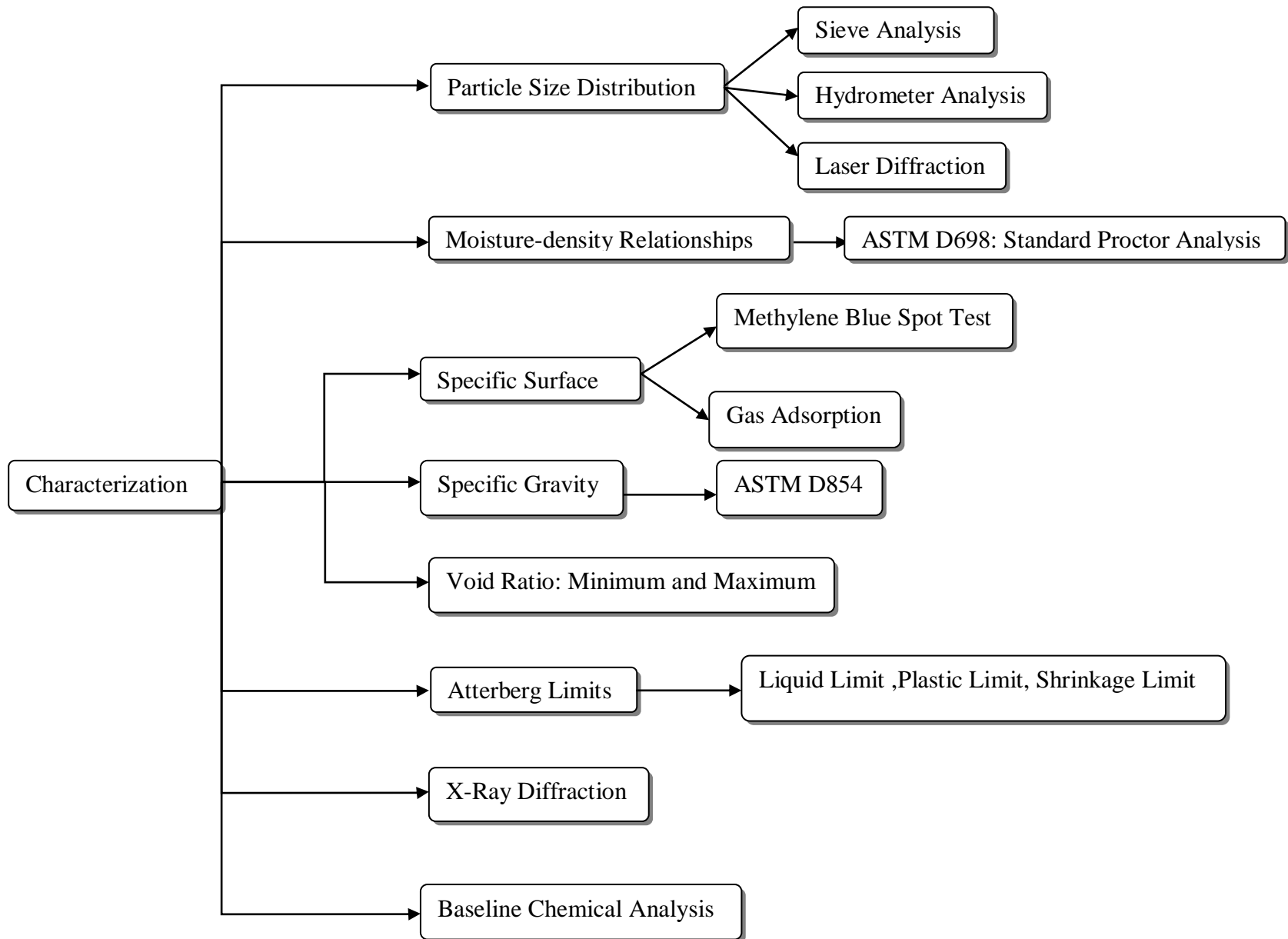
Chapter 3: PRELIMINARY TESTING FRAMEWORK

Due to the fact that CCPs are variable as a function of power plant location, type of power plant (conventional vs. FBC), and the fuel source it is imperative to develop a specific testing framework in order to quality their use for large-volume, engineering applications. CCPs need to be characterized, examined from a chemical basis, and then tested mechanically to ensure their viability for various applications such as embankment/structural fills and mine land reclamation.

The Department of Environmental Protection outlines regulations for the beneficial use of coal ash in 25 Pa. Code Chapter 290. The Department of Environmental Protection Bureau of Mining and Reclamation also has document entitled Certification Guidelines for the Chemical and Physical Properties of Coal Ash Beneficially Used at Mines. Both documents provide very limited guidelines with respect to mechanical characterization and performance. Chapter 290 states the following mechanical requirements to use coal ash as structural fill:

- The slope of a structural fill may not be greater than 2.5 horizontal to 1.0 vertical. The Department may approve a greater slope based on a demonstration of structural stability.
- Coal ash must achieve a minimum compaction of 90% of the maximum dry density as determined by the Modified Proctor Test, or 95% of the maximum dry density as determined by the Standard Proctor Test. Ash from each source must be tested individually. The Proctor Test must be conducted by a certified laboratory.
- Coal ash shall be spread uniformly and compacted in layers not exceeding 2 feet in thickness. The coal ash shall be spread and compacted within 24 hours of its delivery to the site unless stored in accordance to Subchapter E (relating to coal ash storage).

These requirements are extremely vague from a characterization and strength perspective. Figure 12 outlines the possible tests which could be used for embankments and mine land reclamation. The purpose of this research is to identify the most appropriate and accurate tests to characterize and predict the performance of CCPs. Once the testing framework has been established, three types of CCPs will be chosen and tested for a particular application to ensure the functionality of the framework.



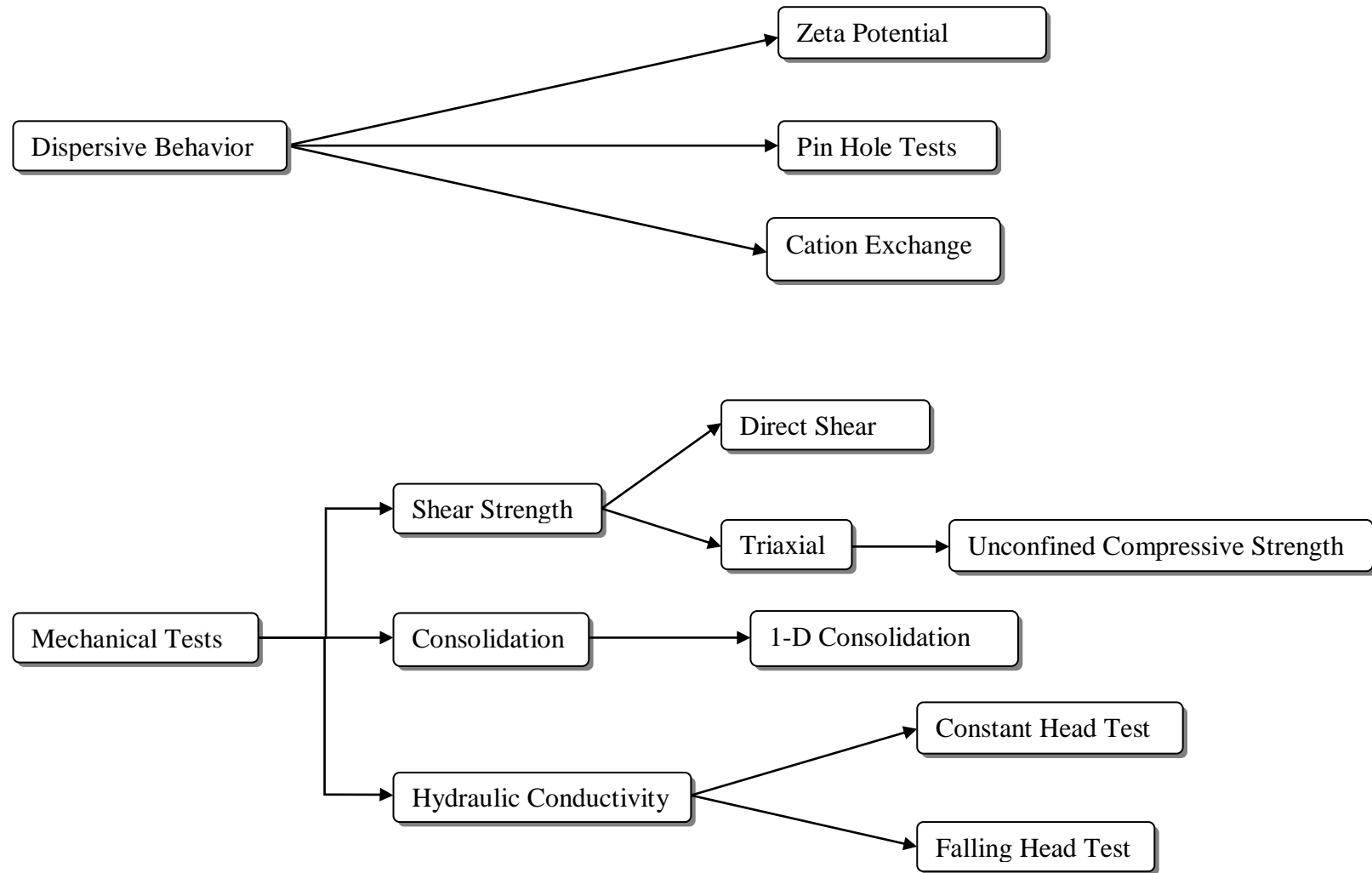


Figure 12: Possible Tests for Using CCPs in Embankment Construction

Material characterization is an imperative process for any material and/or application. Geotechnical engineering materials, typically naturally occurring soil, are specifically characterized for various values relevant to particular applications. CCPs should also be characterized as such. One important property that should always be considered is grain or particle size distribution (PSD). PSD influences other material properties like hydraulic conductivity, density, and subsequently strength. Knowing a material's PSD can provide an initial idea about how the material will perform. PSD's can be determined using standard sieve and hydrometer analysis or particle size analyzer machines. Since CCPs are typically fine-grained in nature, hydrometer analysis would generally be used. However, certain CCPs exhibit properties which could render hydrometer results inaccurate. For example, FGD material is soluble in water therefore hydrometer analysis is not appropriate. Laser diffraction particle analysis techniques (dry method) provide accurate particle size distributions and do not require water-particle interaction.

The specific surface is another important property especially as it relates to fine-grained materials. Specific surface of a particle is the ratio of its surface area to its mass. When the specific surface of a material exceeds $1 \text{ m}^2/\text{g}$ the physical processes that govern soil behavior significantly change. Soils with higher specific surface experience sedimentation and fabric formation controlled by environmental factors, shrinkage and stiffening in unsaturated conditions, and mechanical-chemical coupling (Santamarina et al., 2002). Specific surface can also be an important property for CCPs. Typically, the higher the specific surface the more reactive the material in the presence of fluid (water). For a highly reactive CCP, FBC ash for example, specific surface is a very useful parameter.

Another important parameter of geotechnical materials are moisture-density relationships. Every material has the ability to reach a certain maximum density or packing configuration. In order to reach this maximum density a particular amount of water is required for lubrication. This relationship is determined using the Proctor Test. Materials compacted to their maximum density reflect their highest strength characteristics. While the DEP code only specifies monitoring compaction as a means of strength justification, additional strength parameters need to be obtained for the design of structures like embankments.

Examining the dispersive behavior of a geotechnical material is also relevant. The electrical charges of particles can promote attraction or repulsion which influences material fabric. Fabric influences density, strength, and permeability (Mitchell and Soga, 2005). Another standard property in characterizing naturally occurring soils is specific gravity and should be determined in CCP characterization as well.

Naturally occurring soils possess intrinsic, inert properties that typically do not change over short periods of time (less than 50 years). For example, the unconfined compressive strength of a particular clay and gradation can be considered constant over a particular time frame given the material was compacted in a similar manner. CCPs differ in that they gain strength over a short

period of time (months) (Deschamps, 1998). Therefore strength parameters should be examined as a function of time in order to predict current and future material behavior. Various processes govern this possible strength gain behavior. Changes in the mineralogical composition can influence the strength characteristics. It would be beneficial to examine these processes in order to understand the relevant mechanisms using x-ray diffraction techniques.

The hydraulic conductivity is another important parameter for geotechnical materials. CCP hydraulic conductivity can also vary as a function of time and needs to be examined at various curing intervals to quantify behavior. Since some CCPs can produce hazardous leachate, the effluent from hydraulic conductivity testing should be examined.

Material characterization and specification will vary with respect to the desired application. Embankments and mine land reclamation are inherently different in nature. Mine land reclamation is similar to a backfill structure where fill is placed below grade in confined spaces. Usually these applications do not have slope stability components. However, if structures are to be built on CCP fill materials other considerations like bearing capacity and consolidation/settlement need to be examined. The following is Terzaghi's equation for ultimate bearing capacity for shallow foundations (Das, 2007):

$$q_u = c'N_c + qN_q + \frac{1}{2}\gamma BN_\gamma$$

The ultimate bearing capacity (q_u) is a function of cohesion (c'), equivalent surcharge (q), the unit weight of the soil (γ), the width of the foundation (B), and the terms N_c , N_q , N_γ which are determined by the soil friction angle (ϕ). The unit weight of the soil can easily be determined and used to compute the equivalent surcharge which is simply the unit weight of the soil multiplied by the proposed depth of the foundation. Cohesion and soil angle need to be determined using shear strength tests. Unconfined compression testing provide an undrained cohesion value but no friction angle. Direct shear testing provides values for both cohesion and friction angle. The friction angle provided by direct shear testing however tends to over estimate shear strength compared to triaxial testing. This can overestimate strength and subsequently bearing capacity as well. The most accurate way to obtain cohesion and friction angle values is the triaxial test. The triaxial test does not force a specific failure plane as the direct shear test does and provides a more realistic value. Also consolidated-drained, consolidated-undrained, and unconsolidated-undrained tests can be conducted which accurately mimic specific in situ conditions. If both the cohesion and friction angle are required for design then triaxial tests would most likely be most appropriate for CCPs with cementitious characteristics. Triaxial samples could be prepared and then cured indefinitely before testing. This would not be possible if using the direct shear test. The engineer should decide which test is most appropriate for each particular project.

Consolidation is another important parameter when examining fill materials. Consolidation is mainly an issue in saturated clays since pore water can take significant time to dissipate.

Consolidation can be an issue in CCP fill materials as well. 1-D consolidation tests should be performed in order to examine and quantify consolidation in CCPs.

Embankments are typically laterally unsupported fills placed on top of the natural ground surface. Various types of embankments can be constructed each with different complexities and cost. Some types of embankments include:

- Dumped fill
- Hydraulic fill
- Selected fill
- Equipment-compacted embankment
- Rolled earth fill
- Vibratory-compacted embankment
- Blended earth fill
- Modified soil fill (Bureau of Reclamation, 1998)

Although these different types may have different specifications, the material characterization process should be similar. Embankment design should include bearing capacity and consolidation analyses but include a slope stability study as well. Internal friction angles are required for slope stability calculation and can be obtained using direct shear or triaxial testing (Brendel, 1989).

Chapter 4: MATERIALS

Three specific materials were selected for the purpose of this study. The materials include Flue Gas Desulfurization (FGD) material, Fluidized Bed Combustion (FBC) ash (45% bottom ash, 55% fly ash), and Class F fly ash. Table 7 lists the facility and location where the materials were produced.

Table 7. CCP Source Locations

Material	Facility	Source Location
FGD Material	PPL Montour Power Plant	Washingtonville, PA
FBC Ash	Reliant Energy Seward Power Plant	Johnstown, PA
Class F Fly Ash	PPL Montour Power Plant	Washingtonville, PA

FGD Material. Burning coal for electricity produces pollutants which are potentially harmful to the environment as well as to human health, and regulations are in place to minimize the release of these pollutants into the environment. The Clean Air Act Amendments of 1990 and the Environmental Protection Agency's (EPA's) Clean Air Interstate Rule (CAIR) limit the emissions of sulfur dioxide into the atmosphere. Coal-fired power plants comply with this regulation implementing a lime or limestone reagent in combination with a forced oxidation system to act as a "scrubber" (FGDProducts.org, 2008). This process is known as flue gas desulfurization (FGD) and consists of injecting a slurry of calcium carbonate into the combustion chamber. The calcium carbonate is converted to calcium oxide which reacts with the sulfur in the combusting coal. This reaction forms inert calcium sulfate and water also known as synthetic gypsum or FGD material by-product (Dalberto et. al., 2004). In 2007, over 33 million tons of FGD materials were produced in the U.S. with only 31% beneficially used, mostly in the manufacture of wall board for the housing and building industry (ACAA, 2007). The FGD material was obtained in a dry state. This particular FGD material is considered to be pure synthetic gypsum and meets the standard requirements to be used in the production of wall board.

Fluidized Bed Combustion. FBC ash is produced at FBC power plants which typically burn coal mine refuse. Coal mine refuse, or waste coal, is low BTU material discarded by the mining industry. Coal mine refuse from bituminous and anthracite mining is referred to as gob and culm respectively (Dalberto et. al., 2004). The Reliant Energy Seward Power Plant near Johnstown, PA is one of the largest FBC Plants and therefore produces a substantial quantity of ash on a daily basis. For this reason, FBC ash was examined for use in alternate applications. FBC ash also has interesting strength characteristics. FBC ash has been observed to gain strength as a function of time (Deschamps, 1998). In this study, a blend of 45% bottom ash and 55% fly ash was used. Bottom ash consists of heavier, courser particles which collect on the bottom of the combustion chamber and are removed via a conveyer system. Fly ash particles are much lighter and finer. Fly ash travels up through the flue gas and is removed via electrostatic precipitators.

Class F Fly Ash. Class F fly ash is produced at conventional coal fired power plants and is removed from the flue gas using electrostatic precipitators. Class F fly ash, as defined by ASTM, is fly ash normally produced from burning anthracite or bituminous coal which has pozzolanic properties. Class C fly ash, as defined by ASTM, is fly ash normally produced from lignite or sub bituminous coal which has both pozzolanic properties and some cementitious properties. Class F fly ash is very well studied and has various standards which allow it to be used in various applications. Therefore class F fly ash was chosen as a point of comparison with FGD material and FBC ash.

Chapter 5: TESTING METHODOLOGY

Material Characterization

Scanning Electron Microscopy. SEMs (Hitachi S-3000H) at Penn State's Materials Research Institute were utilized in order to obtain images of the materials, Figure 13. The images were examined to observe the particle structure, particle surface topography, and particle size. SEMs scan the specimen with a finely focused electron beam of kilovolt energy. Portions of electrons are either adsorbed or reflected. An image is formed by scanning a cathode-ray tube in synchronism with the beam and by modulating the brightness of the tube with beam excited signals. The image is therefore built point by point as the specimen is scanned by the electron beam (Cahn, 2005). Since the samples were nonconductive a pretreatment process called gold sputter application was required. This process consists of applying an extremely thin coating of gold onto the sample which renders the sample conductive. 20.0kV were used along with varying degrees of magnification which was dependent on how the sample wanted to be viewed.

Particle Size Distribution. The particle size distribution (PSD) was determined using monochromatic laser light diffraction. Small particles scatter a monochromatic beam where the scattering angle is a function of particle size. As the particle size decreases the scattering angle increases logarithmically (Cahn, 2005). The resulting measurement is essentially a volume distribution where various particle diameters are given as a percentage of the total volume of the sample. A machine called a Malvern Mastersizer was used in this study. The Mastersizer has the ability to measure particles ranging from 0.02 μm to 2000 μm in diameter. Particle size distributions or gradations are important because they describe the range of particle sizes present. Whether a material is uniformly, gap, or well graded influences the mechanical properties of density, permeability and strength.

BET Specific Surface. Specific surface is important as it influences how reactive a particular material will be. If a particular material has appropriate mineralogical constituents which could interact with pore fluid then specific surface must be considered. The higher the specific surface the more the particle is exposed to the pore fluid causing the material to be more reactive. The specific surface was determined using the Brunauer-Emmett-Teller (BET) method. Gas molecules in the vicinity of a solid can experience attractive forces resulting in an enhanced concentration of molecules at the solid surface. This mechanism of the BET method is called gas adsorption. The quantity of gas adsorbed by the solid is a function of temperature and pressure and also is dependent on the solids' surface. Below the critical temperature, the adsorbed layer resembles a thin film potentially several molecule diameters thick. The specific surface can be estimated by determining the quantity of adsorbed gas which would sufficiently form a close-packed layer one molecule diameter thick (Cahn, 2005). The BET equation describes the volume adsorbed V as a function of vapor pressure p :

$$V = \frac{V_m cx}{(1-x)[1+(c-1)x]}$$

Where $x=p/p_o$ is the relative vapor pressure, V_m is the monolayer capacity, and c is related to the strength of the adsorption forces (Cahn, 2005). Since the size and number of gas molecules required to cover the particle sample is known, the specific surface can be calculated (Fagerlund, 1973). In this case, nitrogen gas was used which has a surface area of 16.2 \AA^2 .

Zeta Potential. The Zeta potential is a term for the electric potential of colloidal systems. This electric potential is at the interface of the double layer (the location of the shear or slipping plane) and the bulk fluid of the system (Lyklema, 1995). The Zeta potential can be related to the stability of colloidal systems as it indicates the degree of repulsion between adjacent particles. High Zeta potential values indicate stable systems where the solution is dispersed. Low Zeta potential values cause attraction forces between particles to exceed dispersion causing the system to flocculate or aggregate (Russel et al., 1992). Table 8 relates the Zeta potential in mV to the stability of the system. A Brookhaven Zeta Potential Analyzer was used in this study.

Table 8. Zeta Potential and System Stability (ASTM Standard D 4187-82)

Zeta Potential (mV)	Stability of Colloid
0 to 5	Rapid coagulation/flocculation
10 to 30	Instable
30 to 40	Moderately stable
40 to 60	Good stability
greater than 60	Excellent stability

Moisture/Density Relationships. The moisture/density relationships of the materials were determined using ASTM Standard D698 “Standard Test Methods for Laboratory Compaction Characteristics of Soil Using Standard Effort.” Samples were compacted in three lifts at 25 blows per lift using a standard proctor mold and standard hammer, see Figure 14. Compacting at varying moisture contents allowed the development of moisture/density curves where optimum moisture content and maximum dry density could be determined.

Specific Gravity. Specific gravity was determined following ASTM Standard D854 “Standard Test Methods for Specific Gravity of Soil Solids by Water Pycnometer.”



Figure 13: Hitachi S-3000H SEM



Figure 14: Standard Proctor mold and hammer

Chemical Analysis

Baseline chemical analysis and leachate chemical analysis was contracted to ACT Labs who are based in Ontario Canada. Refer to appendix F for complete chemical analysis. Various methods were used in the analysis.

Instrumental Neutron Activation Analysis (INAA). Activation analysis is an analytical technique used to analyze trace elements quantitatively by activating naturally occurring isotopes of these elements. Neutron activation analysis is generally used for heavy metals and uses neutrons to activate the atoms in the sample (Cahn, 2005). The primary source of neutrons for irradiation is usually a nuclear reactor. Each element which is activated emits a "fingerprint" of gamma radiation which can be measured and quantified. Multi-element analyses of practically any material from the smallest sample which can be weighed accurately to very large samples have been analyzed routinely by INAA (www.actlabs.com).

Inductively coupled plasma mass spectroscopy (ICP-MS). ICP-MS is an analytical technique used for trace elemental determinations of solids. The technique was commercially introduced in 1983 and has gained general acceptance in many types of laboratories. ICP-MS is a hybrid technique combining a high power laser for sampling solids, high temperature inductively coupled plasma for ionization, and a mass spectrometer for mass separation and detection. Laser sampling allows a solid specimen to be sampled without dissolving the specimen. The laser causes material vaporization. This vapor enters the mass spectrometer where it is atomized and ionized. The ion signal which is measured is representative of the composition of the original specimen (Cahn, 2005).

Combustion Infrared Detection (IR). IR was used when analyzing samples for sulfur content. Accelerator material is added to a 0.2 g sample. The inductive elements of the sample and accelerator couple with the high frequency field of the induction furnace. The pure oxygen environment and the heat generated by this coupling cause the sample to combust. During combustion, carbon-bearing elements are reduced, releasing the carbon, which immediately binds with the oxygen to form CO and CO₂, the majority being CO₂. Also, sulfur-bearing elements are reduced, releasing sulfur, which binds with oxygen to form SO₂. Sulfur is measured as sulfur dioxide in the first IR cell. A small amount of carbon monoxide is converted to carbon dioxide in the catalytic heater assembly; SO₂ is converted to SO₃, while sulfur trioxide is removed from the system in the filter. Carbon is measured as carbon dioxide in the IR cell as gases flow through the IR cells. Carbon dioxide absorbs IR energy at a precise wavelength within the IR spectrum. Energy from the IR source is absorbed as the gas passes through the cell, preventing it from reaching the IR detector. All other IR energy is prevented from reaching the IR detector by a narrow filter. Because of the filter, the absorption of IR energy can be attributed only to carbon dioxide (CO₂). The concentration of CO₂ is detected as a reduction in the level of energy at the detector. An Eltra CS-2000 is used for the analysis (www.actlabs.com).

Mechanical Tests

Unconfined Compression Testing. Unconfined compression (UC) strength tests were performed to obtain minimum strength characteristics for the FGD material, FBC ash, and class F fly ash. UC tests were completed for each material at various curing durations to quantify any strength changes with time. The materials were cured for 1, 3, 7, 14, 28, 56, 90, and 180 days. Three samples of each material were prepared for each curing period to ensure repeatable results. The tests were carried out in accordance to ASTM Standard D 2166-00 with the following exceptions:

- Samples were prepared at optimum water content using a Standard Proctor Mold. Samples were compacted in the proctor mold in 3 equal lifts using a Standard Proctor hammer at 25 blows per lift.
- FGD and Class F fly ash samples were tested using a Geocomp Load Trac II frame, see Figure 15. A constant strain rate of 0.5 % per minute was applied until failure. Failure was defined at the point where the specimen could no longer carry a load after the peak value was reached.
- FBC samples could not be tested in the Geocomp Load trac II frame because the strength of the material exceeded the capacity of the frame. Therefore the FBC samples were tested on a concrete compression testing machine manufactured by Boart Longyear model cm-625, see Figure 16. Due to limitations of the Boart Longyear machine, a constant strain rate could not be applied. Alternatively, a constant loading rate of 6.9 kPa to 20.7 kPa per second (1 psi to 3 psi per second) was applied until failure. This was the lowest range of loading rate achievable with this device. Failure was defined at the point where the specimen could no longer carry a load after the peak value was reached.



Figure 15: Boart Longyear frame



Figure 16: Geocomp Load Trac II frame

Hydraulic Conductivity. Permeability was measured using a specially designed pressurized permeability cell shown in Figure 17. The permeability cell consists of a hollow metal cylinder which holds the sample. The sample is compacted into a Tygon tube segment (Figure 18). High pressure water lines are connected to the cell to provide confining and driving pressures independently. The test is run using distilled water which is pressurized with nitrogen gas. Water is supplied through an external reservoir with an inner piston (Figure 19). The nitrogen gas pushes on the piston which pressurizes the water in the reservoir, thus preventing nitrogen-water interaction. Confining pressure is applied to the sample prior to the driving pressure. The sample is allowed to saturate and reach a steady-state flow rate at the sample exit. Manipulation of Darcy's law allows calculation of the hydraulic conductivity based on the driving pressure and the outflow assuming a constant head condition. Refer to Appendix A for a detailed procedure of the test. The following expression describes the hydraulic conductivity, k :

$$k = \frac{Q \cdot L}{A \cdot (h_a - h_b)}$$

The hydraulic conductivity k is a function of the volumetric flow rate Q , the length of the sample L , the cross-sectional area of the sample A , the equivalent pressure head at the inlet of the sample h_a , and the equivalent pressure head at the outlet (atmospheric pressure) of the sample h_b .

Two samples per curing duration were prepared at optimum moisture content and compacted in 3 equal lifts using a tamper. Samples were compacted to their maximum density to attempt consistent void ratios between samples. Samples were tested at curing durations of 1, 3, 7, 14, 28, 56, 90, and 180 days. Table 9 outlines the test parameters for each material. Note that a lower driving pressure was used for the FGD material to prevent dissolution during measurement.

Using this pressurized hydraulic conductivity cell has the following advantages:

- Hydraulic conductivity of fine-grained materials can be measured in a timely manner compared to conventional falling head tests.
- The system is applicable to cementitious materials.
- Confining pressure minimizes the development of preferential flow paths at the material/cell wall interface.
- Samples can be prepared and cured in Tygon tubing for indefinite time intervals

Table 9. Hydraulic Conductivity Test Parameters

Material	Driving Pressure	Confining Pressure	Outlet Pressure
FGD Material	345 kPa (50 psi)	689 kPa (100 psi)	101 kPa (14.7 psi)
FBC Ash	1034 kPa (150 psi)	1379 kPa (200 psi)	101 kPa (14.7 psi)
Class F Fly Ash	1034 kPa (150 psi)	1379 kPa (200 psi)	101 kPa (14.7 psi)

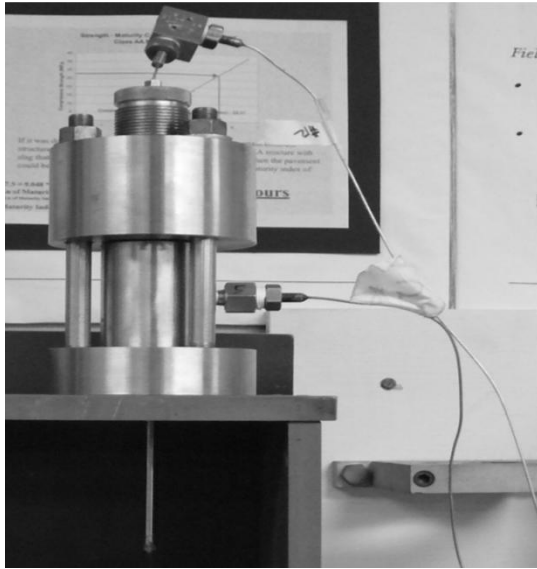


Figure 17: Pressurized permeability cell



Figure 18: Sample preparation

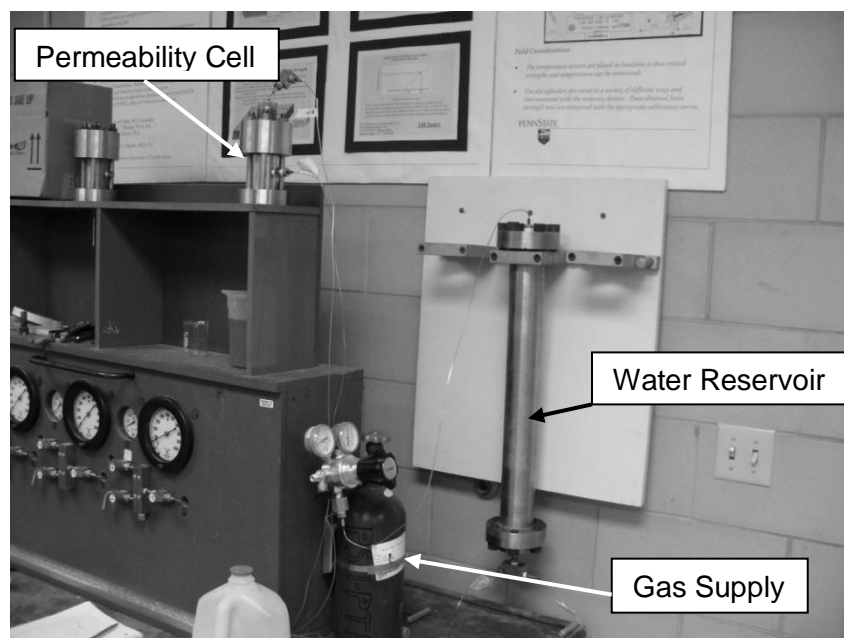


Figure 19: Hydraulic conductivity test configuration

Effluent Chemical Analysis. The effluent from the permeability tests was collected for each specimen for each curing duration for chemical analysis. The chemical composition of the materials is important in examining changes in strength and permeability as well as identifying potentially harmful constituents. Activation Laboratories in Ontario, Canada conducted the analysis using inductively coupled plasma mass spectroscopy (ICP-MS).

X-Ray Diffraction. X-ray diffraction (XRD) techniques were employed in order to examine how the materials' mineralogical characteristics change as a function of time. XRD samples were taken from the UC test samples for each material at each curing duration. Therefore, explanation of how strength and hydraulic conductivity change with time could be provided from a mineralogical perspective. When x-rays interact with a substance an XRD pattern results. The x-rays are reflected off of the structure of the substance at a particular angle and intensity. The resulting pattern consists of graphical peaks which are a function of that angle and intensity. Each XRD pattern is unique for a given substance, therefore the pattern could be considered a "finger print" for that particular substance. Once the patterns have been plotted for a sample, modern pattern databases are examined to find a perfect match or fingerprint to identify the substances in the sample. Not only do the patterns signify various chemical/mineralogical phases present, but the area under the peaks represents the magnitude of the presents phases (UC Santa Barbara, 2010).

Chapter 6: RESULTS AND DISCUSSION

Characterization

Figure 20 shows the optimum water content and maximum dry density relationships for FGD material, FBC ash, and Class F fly ash. The maximum dry density of each material can be related to their respective particle size distributions. Table 10 outlines the maximum dry densities and optimum water contents for the three materials. The material with the highest maximum dry density is the Class F fly ash at 1582 kg/m^3 (98.81 lb/ft^3). The Class F fly ash has a fairly well graded particle size distribution. The d_{10} and the d_{90} are $1.79 \text{ }\mu\text{m}$ and $70.07 \text{ }\mu\text{m}$ respectively, see table 11. This broad range of particle sizes allows smaller particles to fill the voids between the larger particles creating a denser particle packing. Compare the Class F fly ash particle size distribution to that of the FGD material. The d_{10} and the d_{90} are $22.94 \text{ }\mu\text{m}$ and $65.00 \text{ }\mu\text{m}$, respectively. This correlates to a more uniform particle size distribution since the majority of particles are similar in size. Uniform distributions cannot achieve as high a density as well graded distributions since there are no small particles to fill the voids between the large particles. Consequently, the FGD material is less dense at 1470.0 kg/m^3 (91.78 lb/ft^3) compared to the Class F fly ash. The FBC ash has a fairly well graded particle size distribution like the Class F fly ash. The d_{10} and the d_{90} are $3.19 \text{ }\mu\text{m}$ and $65.96 \text{ }\mu\text{m}$ respectively. However, the FBC ash has the lowest maximum dry density. This is due to the fact the 45% bottom ash in the mixture is significantly larger in particle size compared to the 55% fly ash. The structure of the FBC is also different in a way that could promote this lighter dry density. Figure 23 shows an SEM image of FBC ash at 3.0k magnification. The surface of the particle appears to be very porous. This porous structure proves to be lighter in weight which describes the lower dry density of the material.

The optimum water content is essentially the amount of water required for a material to reach its maximum density. The water serves as a lubricant for the particles to slide past one another and into the tightest packing allowed by the particle size distribution. The FGD material and Class F fly ash have similar optimum water contents at 18% and 19% respectively, see table 10. However, the FBC ash required a much higher water content of 25%. This can be explained by referring to figure 23. The porous structure requires a large amount of water to initially fill the structure along with an additional amount of water which provides the compaction lubrication.

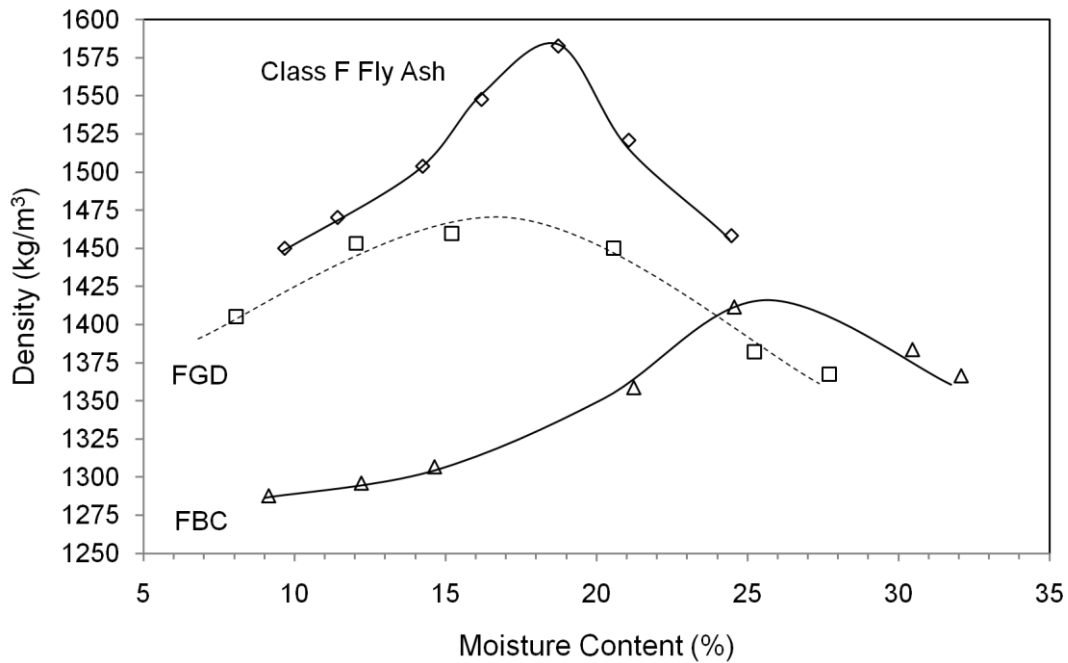


Figure 20: Proctor curves for FGD material, FBC ash, and class F fly ash

Table 10. Proctor Test Results for FGD Material, FBC Ash, and Class F Fly Ash

Material	Optimum Moisture Content, %	Max. Dry Density, kg/m ³ (lb/ft ³)
FGD	17.0	1470.0 (91.8)
FBC	26.0	1415.0 (88.1)
Class F	19.0	1582.0 (98.8)

Table 11. d₁₀, d₅₀, and d₉₀ values for FGD material, FBC ash, and Class F Fly ash

Material	Particle Size (μm)		
	d ₁₀	d ₅₀	d ₉₀
FGD Material	22.94	40.18	65.00
FBC Ash	3.19	18.19	65.96
Class F Fly Ash	1.79	15.27	70.07

Table 12 outlines the specific gravity and specific surface characteristics for the materials used in this study. The values of specific gravity for all three materials can vary within an acceptable range. According to the literature, the specific gravities obtained in this study were within acceptable ranges.

The FGD material had the highest specific surface of the three materials at $9.14 \text{ m}^2/\text{g}$. This is somewhat surprising considering the “sponge like”, pitted structure of the FBC ash ($7.20 \text{ m}^2/\text{g}$) as seen in Figure 23. However, $7.20 \text{ m}^2/\text{g}$ is still a high specific surface and large portions of the particles are in contact with the pore fluid. The mineralogical properties of FBC ash dictate high hydration potential in the presence of water, therefore this value is very important. Class F fly ash has the lowest specific surface at $2.69 \text{ m}^2/\text{g}$.

Figure 21 illustrates the Zeta potential of the materials as a function of pH. It is important to note that both the FGD material and the FBC ash have net negative charges. The class F fly ash is more sensitive to pH conditions as it fluctuates between positive and negative charges with an isoelectric point at pH 8.

Table 12. Specific Gravity (G_s) and Specific Surface (S_a) of the Materials Used in this Study

Material	G_s	$S_a (\text{m}^2/\text{g})$
FGD Material	2.57	9.14
FBC Ash	3.09	7.20
Class F Fly Ash	2.62	2.69

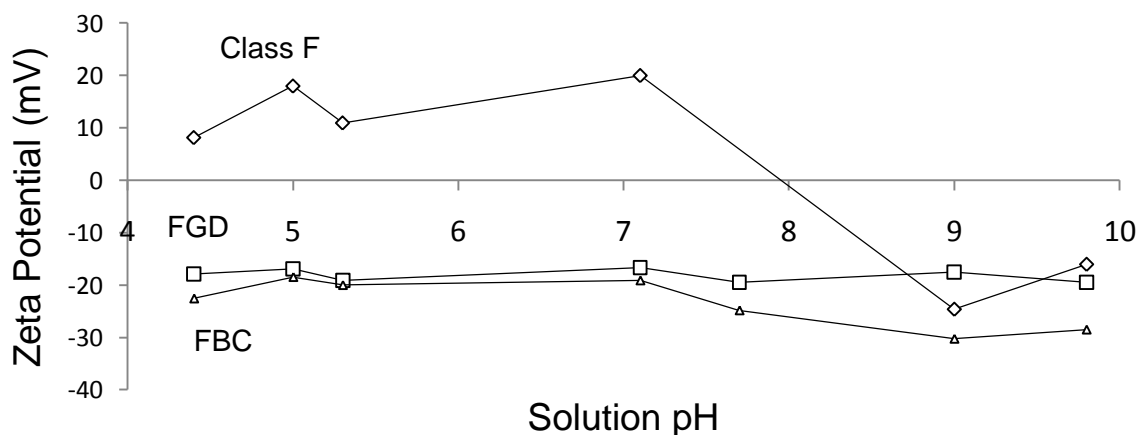


Figure 21: Zeta potential vs. solution pH for FGD material, FBC ash, and class F fly ash

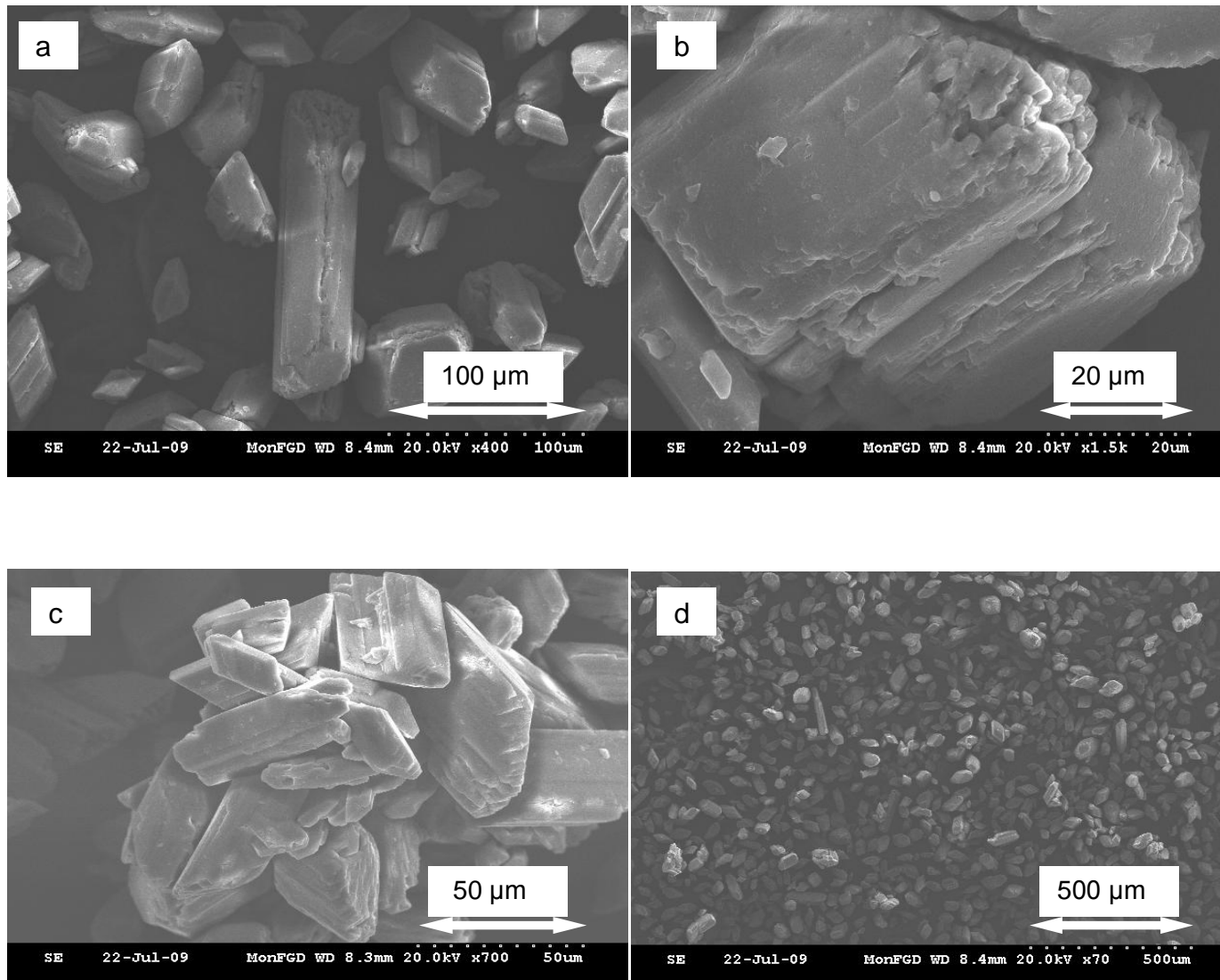


Figure 22: Scanning electron micrographs of FGD material (a) 400x, (b) 1500x, (c) 700x, (d) 70x

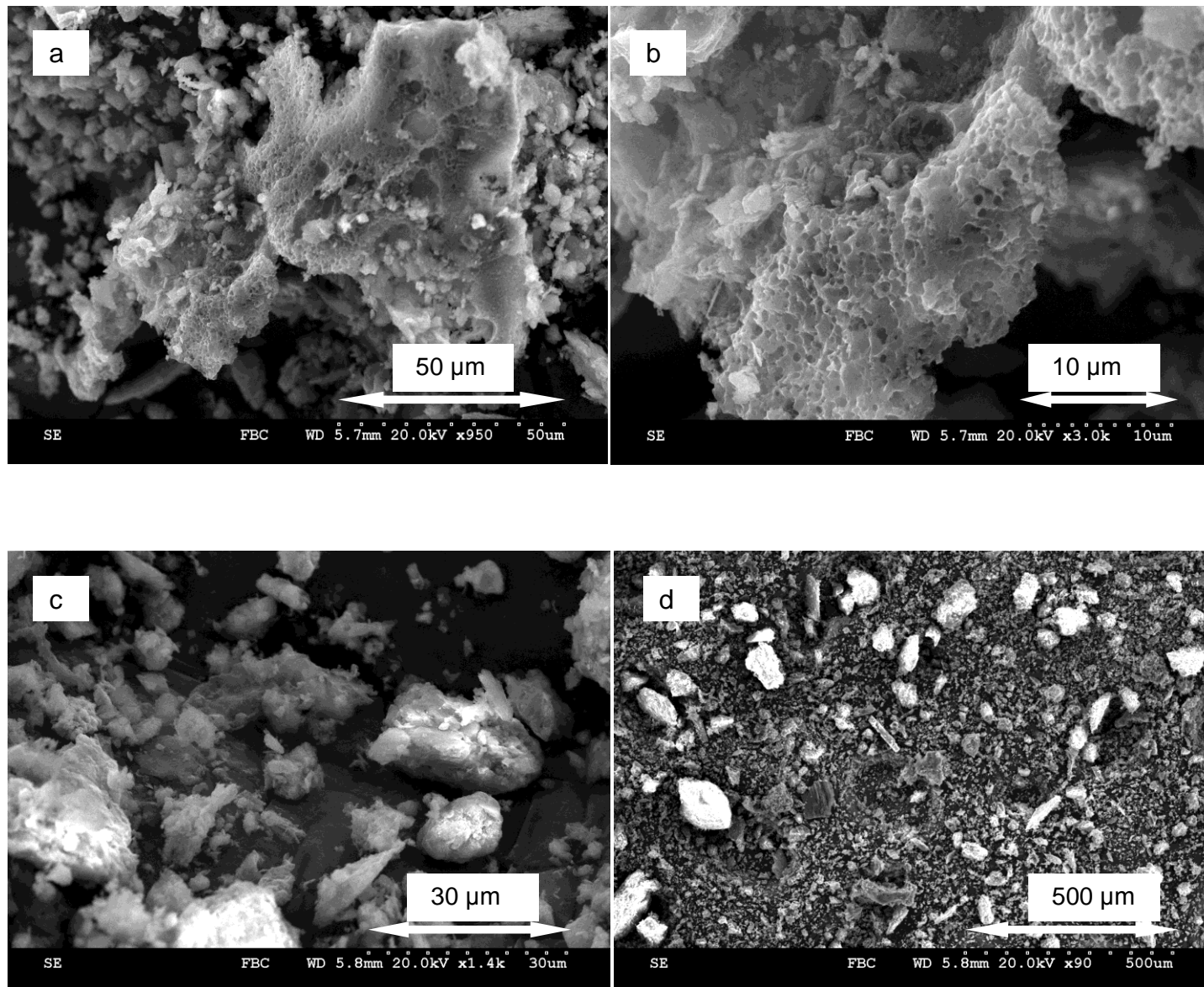


Figure 23: Scanning electron micrographs of FBC ash (a) 950x, (b) 3000x, (c) 1400x, (d) 90x

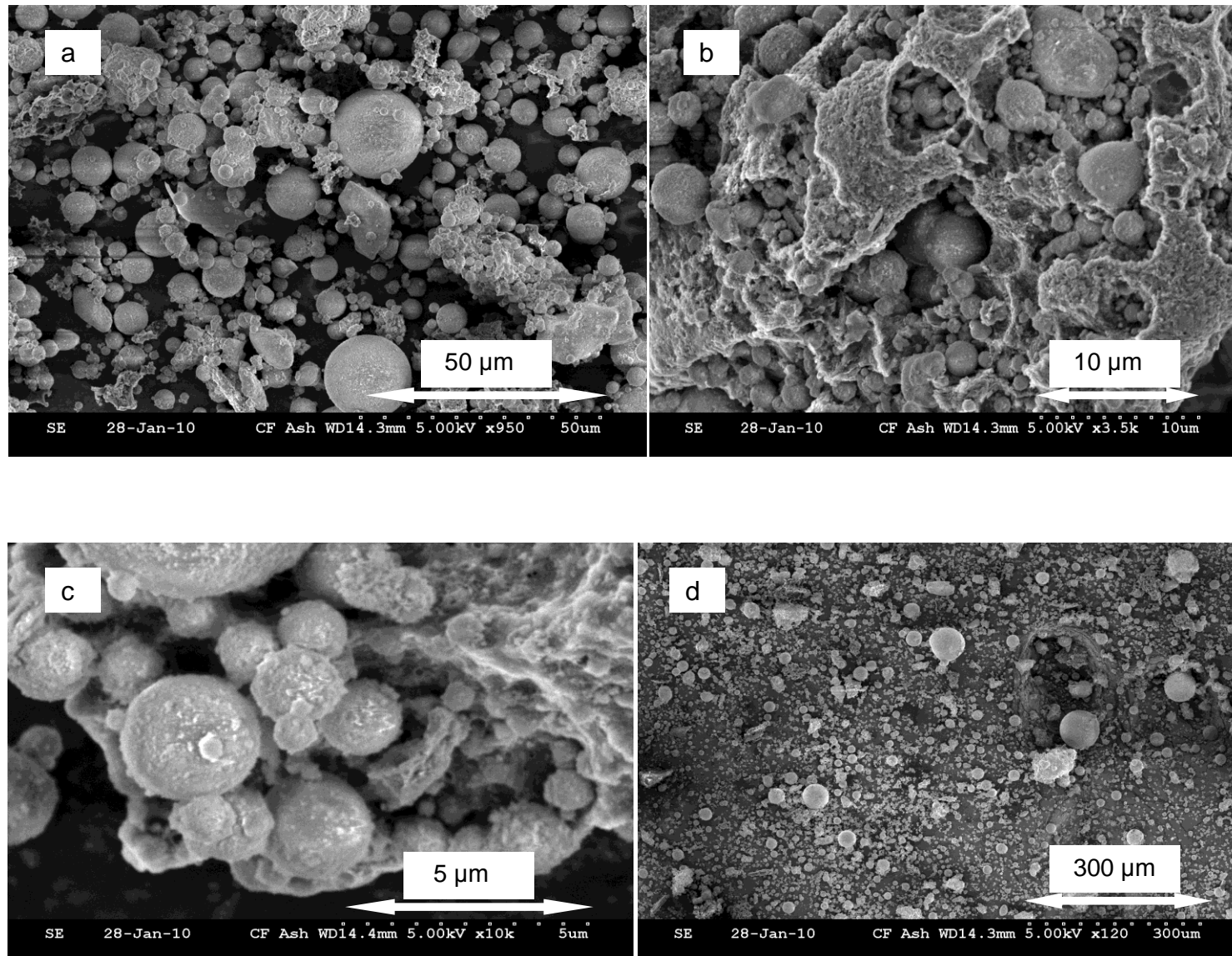


Figure 24: Scanning electron micrographs of class F ash (a) 950x, (b) 3500x, (c) 10000x, (d) 120x

Mechanical Tests

Unconfined compressive (UC) tests were performed on the FGD material, FBC ash, and class F fly ash at various curing durations to obtain minimum strength characteristics. Figure 25 illustrates the peak strength (log scale) for all three materials as a function of curing time (log scale). The peak strength values represent the average of three samples for each material and curing duration. The peak strength of the FGD material remains relatively constant with respect to curing time. Figure 31 shows the XRD patterns for the FGD material over a curing period of 90 days. The only mineralogical component in the FGD material is gypsum. Furthermore, the intensity of the peaks corresponding to gypsum do not change in magnitude indicating that the amount of gypsum remains the same over the curing duration. Therefore, the material has an inherent strength of approximately 68.9 kPa (10 psi) without subsequent strength gain. This is comparable to a clay of medium consistency with UC strength ranging from 48.23 to 96.46 kPa (7 to 14 psi) (Das, 1994). The failure modes of the FGD material proved to be similar to that of naturally occurring clay in that 45° shear cracks commonly developed as in figure 26. Other failure modes included high compressibility of the samples resulting in significant deformation up to 0.25 in., refer to appendix D for sample load and deformation data.

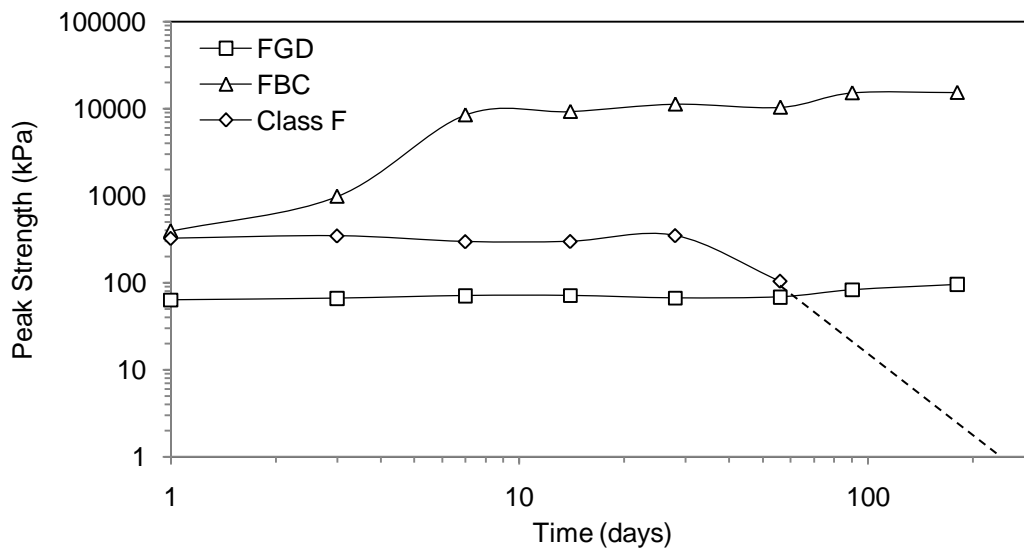


Figure 25: Peak strength vs. curing time for FGD material, FBC ash, and Class F fly ash

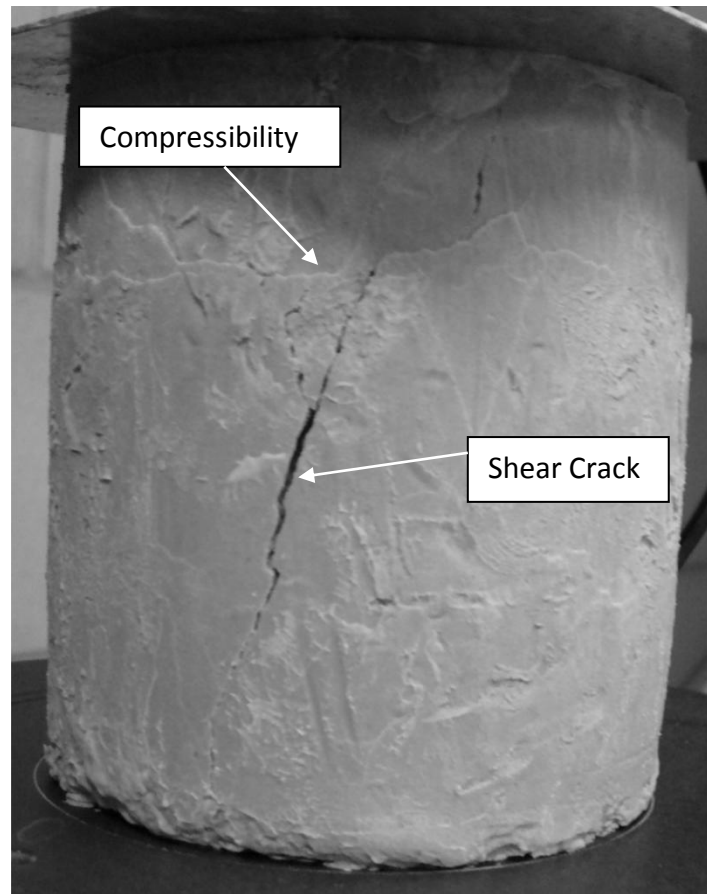


Figure 26: Typical shear crack failure mode for FGD material

FBC ash experiences significant strength gain characteristics as a function of curing time as seen in Figure 25. The peak strength approaches 17225 kPa (2500 psi) after a period of 180 days. Figure 32 outlines the XRD patterns for the FBC ash over a curing period of 180 days. The magnitude of the gypsum and ettringite peaks increase as a function of time explaining the early strength gain of the material. The ettringite peak at 7 days of curing is much higher compared to the 3 day peak, hence the significant strength gain at 7 days. As the quantity of gypsum increases, the anhydrite decreases accordingly. Muscovite, halloysite, and phlogopite are indicative of clay components which increase with time. These clays eventually change into calcium silicate hydrate (CSH) and contribute to long term material strength. The high cementation and subsequent compressive strength of the FBC ash causes the material to behave similar to a Portland cement concrete. Failure modes included vertical cracking and spalling as seen in figures 27 and 28, respectively.

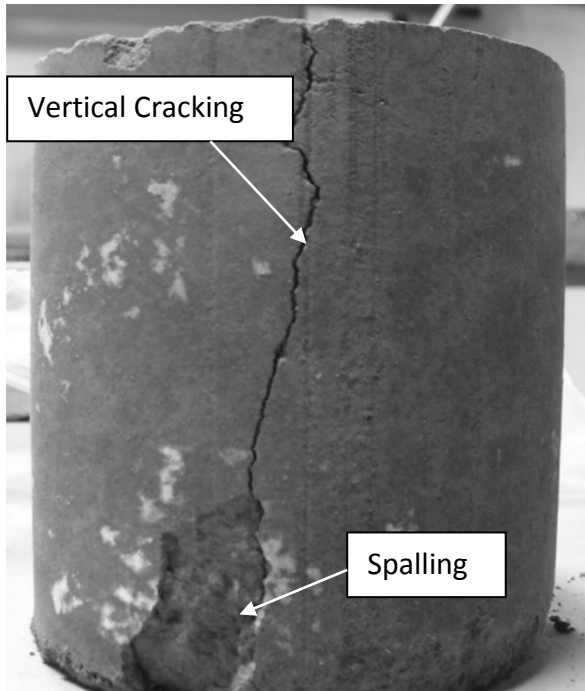


Figure 27: Typical spalling failure

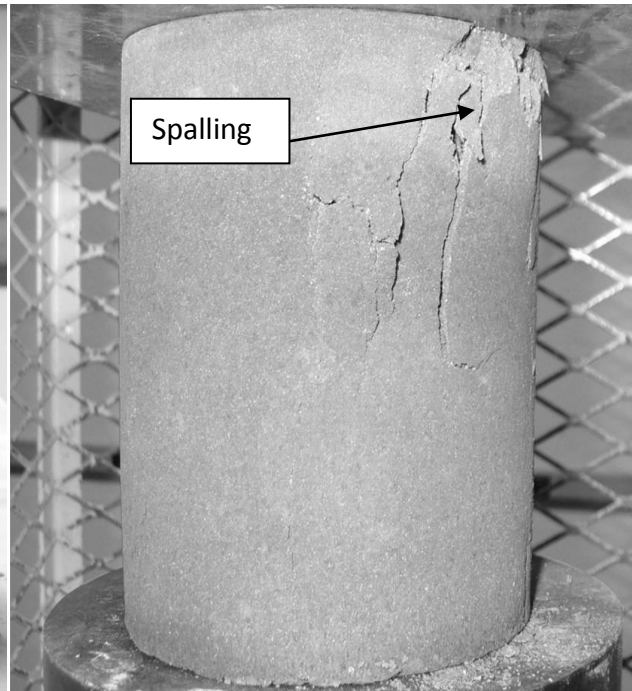


Figure 28: Typical vertical cracking failure

The class F fly ash fluctuates between 276 and 345 kPa (40 and 50 psi) over a period of 28 days which is comparable to a very stiff clay (Das, 1994). The gypsum present remains relatively constant with respect to curing time as seen in Figure 33. The formation of gypsum accounts for the strength in the material. Since the amount of gypsum does not increase the strength does not increase. The class F fly ash experienced an interesting phenomena after 56 days of curing. The samples became extremely fractured and cracked as in Figure 29. This fracturing caused the decrease in strength at 56 days of curing and subsequently prevented the 180 day samples from being loaded. Class F fly ash does not possess intrinsic cementation characteristics which could describe this late term fracturing. Moisture loss after 56 days of curing could also describe this behavior as the material losses its effective cohesion and behaves as a granular material.



Figure 29: Class F fly ash sample after 56 days of curing

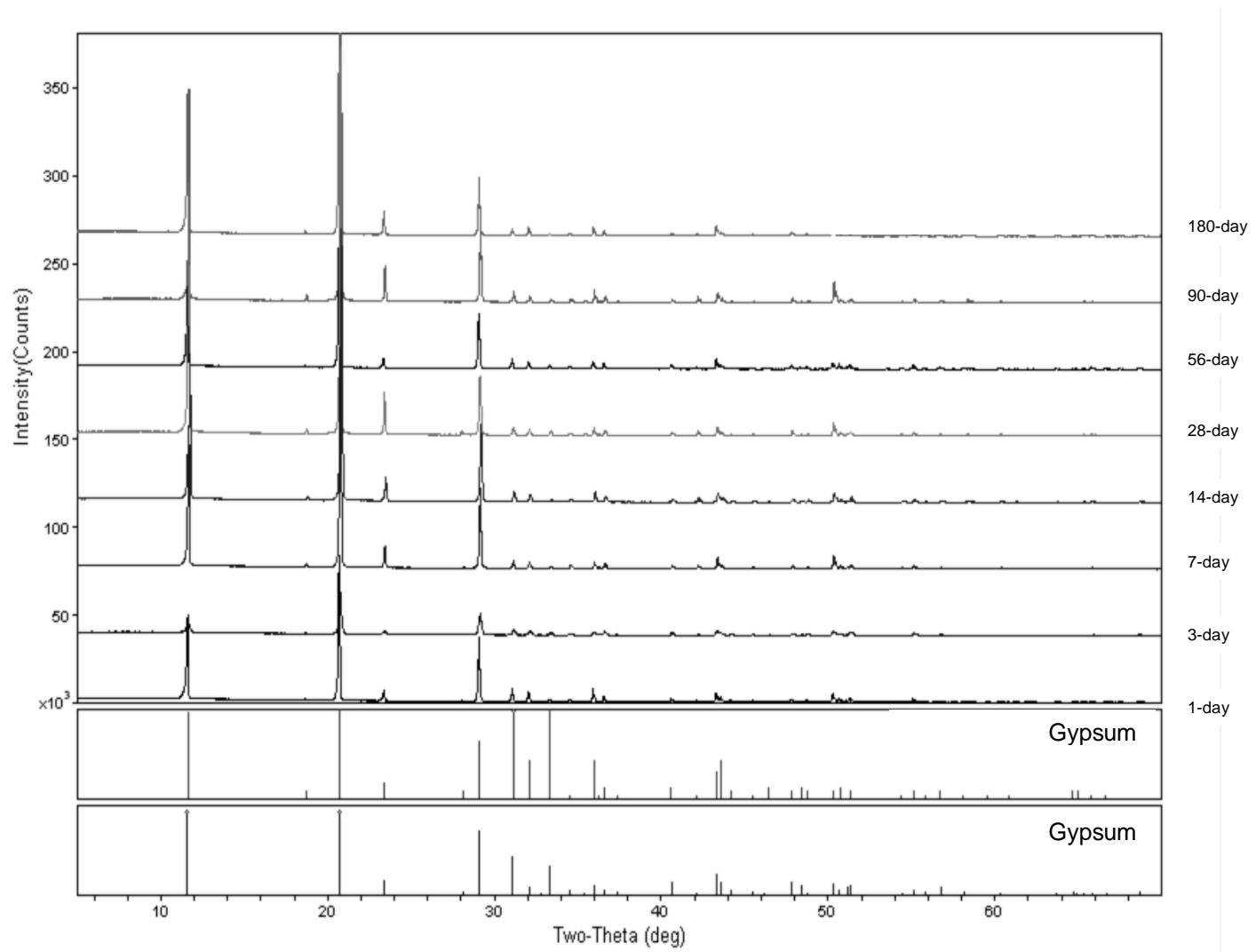


Figure 30: XRD Patterns for FGD material initially mixed at optimum water content. Samples cured for 1-180 Days

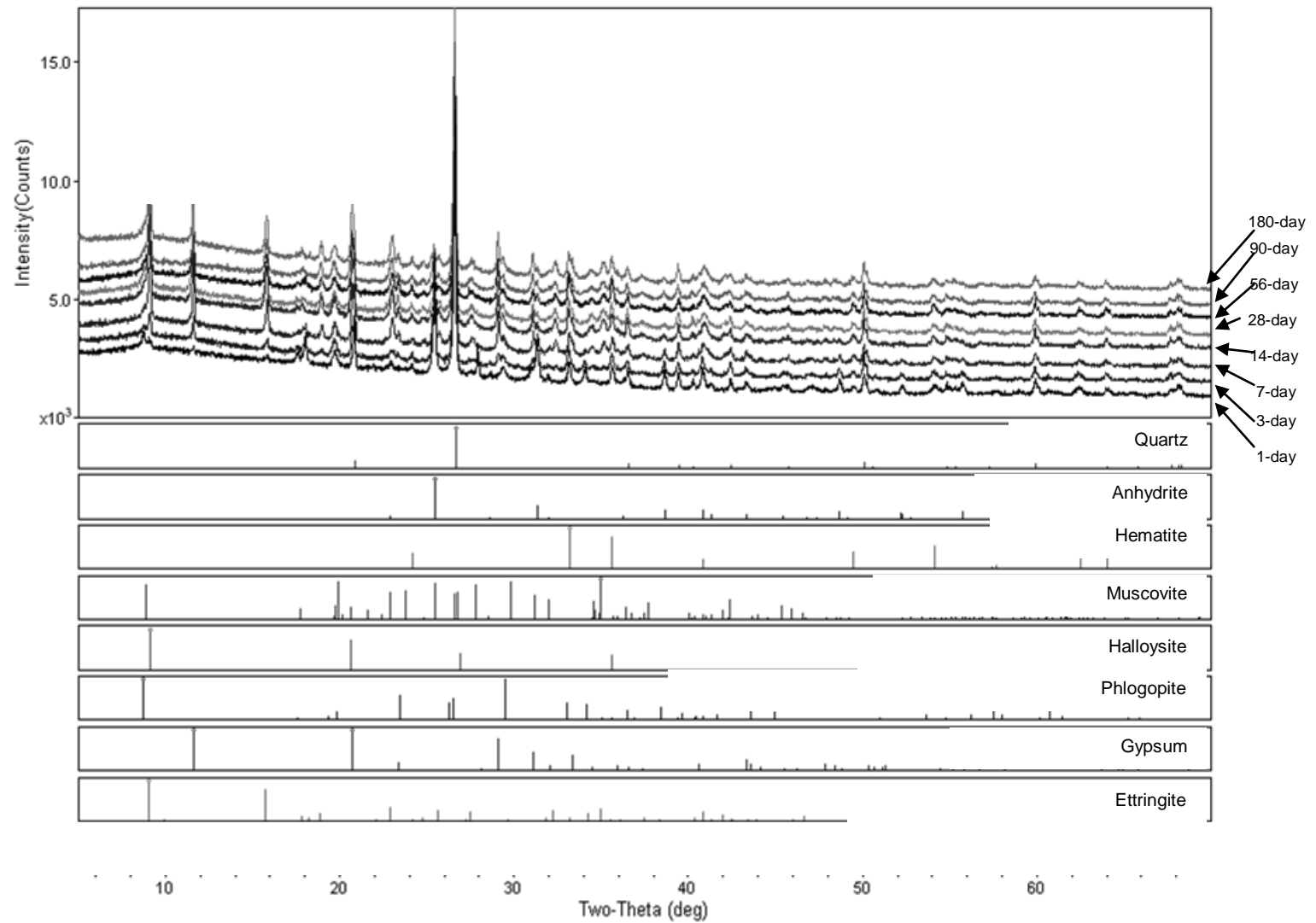


Figure 31: XRD Patterns for FBC ash initially mixed at optimum water content. Samples cured for 1-180 Days

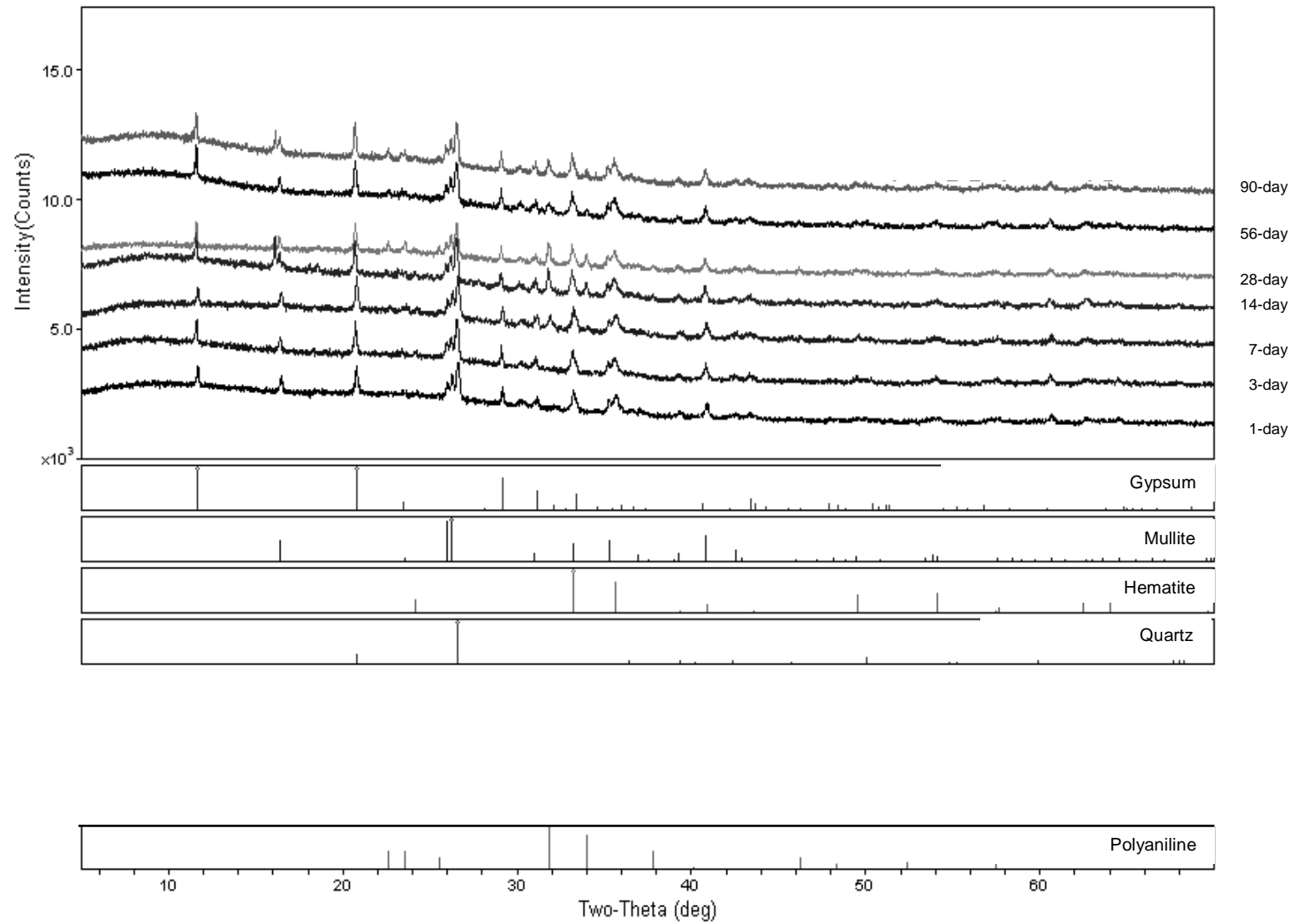


Figure 32: XRD Patterns for class F fly ash initially mixed at optimum water content. Samples cured for 1-90 Days

Permeability analysis was done to examine how the permeability characteristics of FGD material, FBC ash, and class F fly ash change with respect to curing time. The hydraulic conductivity (log scale) as a function of curing time is shown in Figure 30. Permeability of the FGD material remains relatively constant as a function of time. Values range from $1.25\text{E-}4$ to $1.59\text{E-}4$ cm/s. This result makes sense since the FGD material experiences no mineralogical change over the curing duration. Class F fly ash permeability slightly increases as a function of time with values ranging from $1.87\text{E-}5$ to $3.90\text{E-}5$ cm/s. Again, the limited mineralogical changes relate to the consistent hydraulic conductivity. FBC ash experiences a wide range of permeability characteristics. Initially, the permeability decreases over the first 28 days to a value of $4.06\text{E-}7$ cm/s. Then permeability increases over 56 and 90 days to a value of $3.04\text{E-}5$ cm/s. This significant change in hydraulic conductivity may be due to certain chemical components becoming more soluble with time subsequently increasing permeability. Naturally occurring materials with similar permeability values ($\text{E-}3$ to $\text{E-}7$ cm/s) include very fine sands, organic and inorganic silts, sand mixtures, silt and clay, glacial till, and stratified clay deposits (Al-Khafaji and Andersland, 1992).

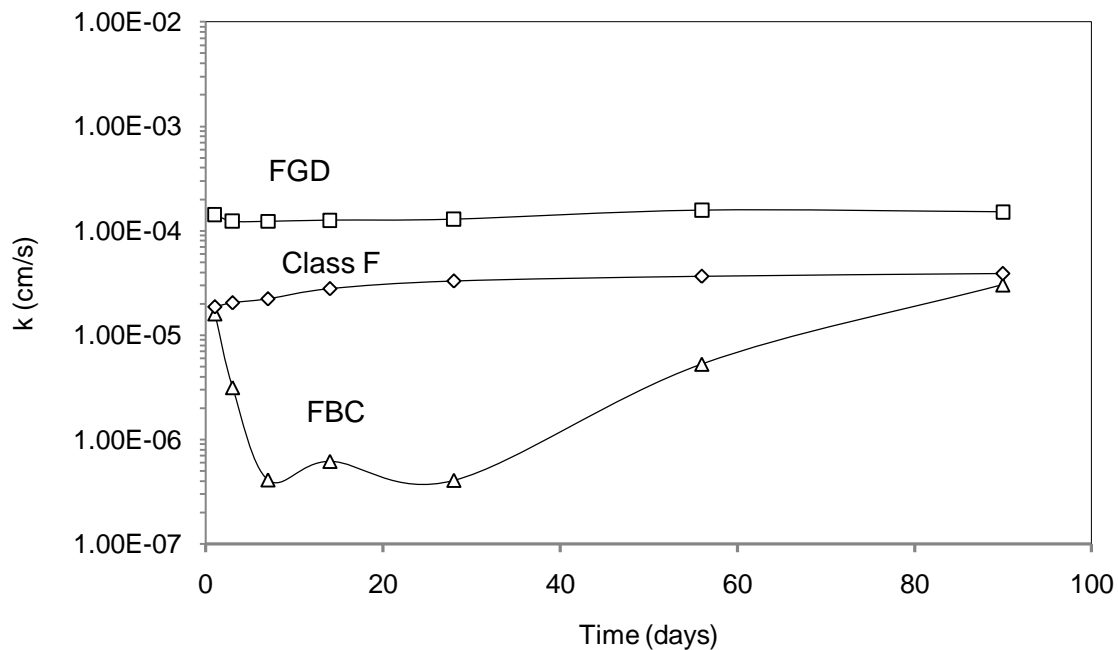


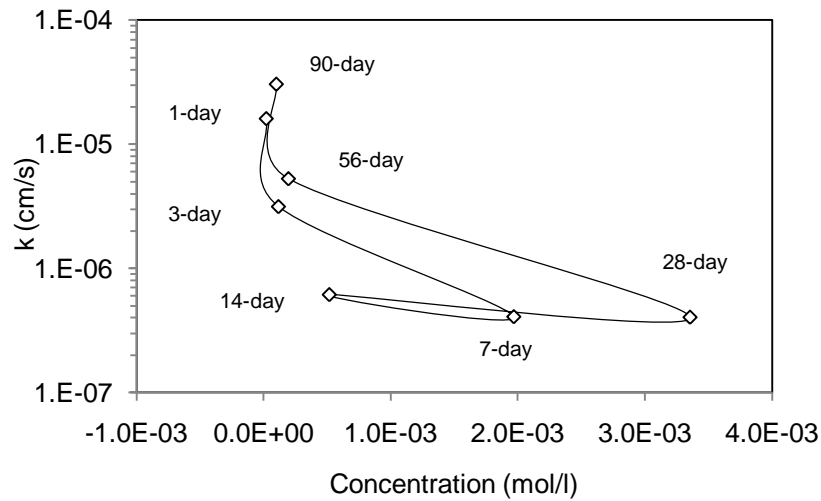
Figure 33: Hydraulic conductivity as a function of time

The effluent from permeability testing was retained for chemical analysis. Effluent from each material at each curing duration was examined. The Department of Environmental Protection has published certification guidelines for the chemical and physical properties of coal ash beneficially used at mine sites (DEP, 2009). Table 14 outlines the maximum acceptable leachate concentrations for mine land reclamation as well as the observed concentrations from the effluent analysis. All of the observed concentrations are below the maximum acceptable leachate concentrations. The effluent chemical analysis also describes the high variation in the hydraulic conductivity of the FBC ash. The hydraulic conductivity seems to be related to the concentration of Chloride (Cl), Sodium (Na), Potassium (K), and Thallium (Tl). The hydraulic conductivity decreases with increasing concentration of each component. The following figures illustrate the components' concentration as a function of hydraulic conductivity. It is important to note how the concentration trends for each component are similar. There seems to be an indirect relationship between the hydraulic conductivity of the FBC ash the concentrations of these three components. As the concentration increases, the hydraulic conductivity decreases. However, further investigation is required in order to confirm this result. The fact that the concentration increases during lower permeability also could be attributed to the fact the material is in contact with the pore fluid for a longer period of time.

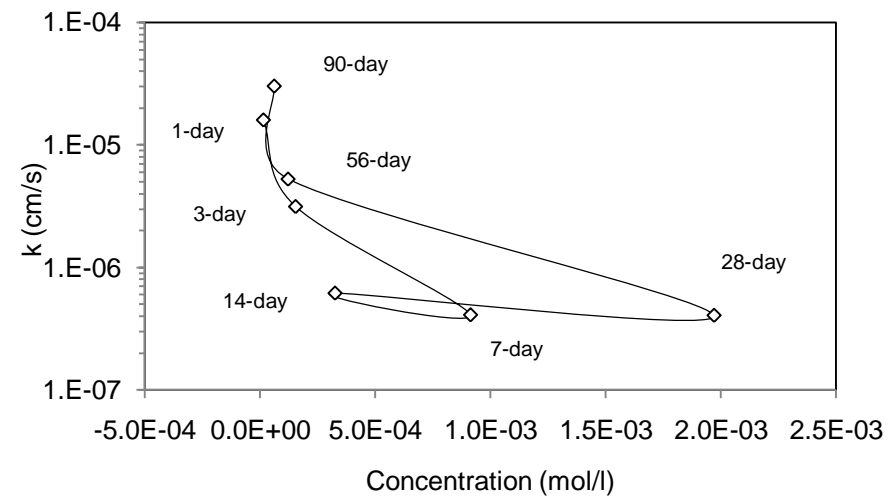
Table 13. Maximum Observed Concentrations and DEP Maximum Acceptable Leachate Concentrations

Component	Max. Concentration Observed in FGD (mg/L)	Max. Concentration Observed in FBC (mg/L)	Max. Concentration Observed in Class F fly ash (mg/L)	DEP Max. Acceptable Concentration (mg/L)
Aluminum (Al)	0.028(1)	2.04(56)	2.7(1)	5.00
Antimony (Sb)	0.0001(1-56)	0.00024(90)	0.0066(1)	0.15
Arsenic (As)	0.00085(90)	0.0157(90)	0.036(90)	0.25
Barium (Ba)	0.0034(1-3)	0.167(3)	0.0875(1)	50.00
Beryllium (Be)	0.001(1-56)	0.001(1-56)	0.001(1-56)	0.10
Boron (B)	0.03(1-56)	0.039(7)	2.37(1)	15.00
Cadmium (Cd)	0.00056(90)	0.00063(7)	0.0001(1-56)	0.125
Chromium (Cr)	0.005(1-56)	0.065(7)	0.005(1-56)	2.500
Cobalt (Co)	0.00023(56)	0.00009(7)	0.00005(1-56)	17.500
Copper (Cu)	0.0044(28)	0.0502(56)	0.002(1-56)	25.000
Fluoride (F)	0.00143(1)	0.0003(1)	0.00093(1)	4.000
Iron (Fe)	0.18(1)	0.1(1)	0.1(1)	7.500
Lead (Pb)	0.00103(28)	0.00251(3)	0.0001(1)	0.375
Manganese (Mn)	0.12(90)	0.214(90)	0.851(1)	2.50
Mercury (Hg)	0.002(1)	0.002(1)	0.002(1)	0.05
Molybdenum (Mo)	0.001(1)	0.224(7)	0.0333(1)	4.375
Nickel (Ni)	0.003(1)	0.003(1)	0.003(1)	2.50
Selenium (Se)	0.0257(1)	0.0171(1)	0.0974(1)	0.50
Silver (Ag)	0.002(1)	0.002(1)	0.002(1)	2.50
Thallium (Tl)	0.000014(90)	0.00025(28)	0.00016(1)	0.05
Zinc (Zn)	0.089(1)	0.0344(56)	0.0088(90)	50.00
Sulfate (SO ₄)	1460(90)	1610(28)	867(1)	2500.00
Chloride (Cl)	0.3(1-90)	119(28)	0.3(1)	2500.00
Nitrate (NO ₃)	0.1(1-90)	0.3(1-7)	0.1(1)	10.00
Nitrite (NO ₂)	0.1(1-90)	0.97(3)	0.1(1)	1.00
Ammonia	-	-	-	30.00
Calcium (Ca)	200(1-56)	200(1-7)	200(1)	-
Magnesium (Mg)	0.12(90)	0.214(90)	0.851(1)	-
Potassium (K)	0.3(1-56)	200(28)	1.24(1)	-
Sodium (Na)	0.199(90)	45.3(28)	3.43(1)	-
Vanadium (V)	0.001(1-56)	0.0403(28)	0.0616(7)	6.50

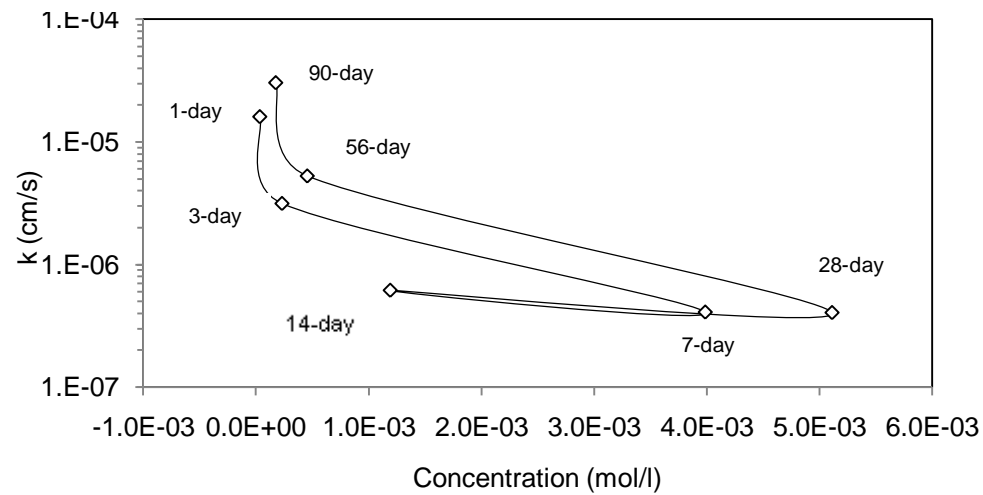
Note: numbers in parenthesis indicate the curing duration (days) at which the maximum concentration was observed



Cl concentration vs. FBC hydraulic conductivity



Na concentration vs. FBC hydraulic conductivity



K concentration vs. FBC hydraulic conductivity

Figure 34: Hydraulic conductivity vs. concentration

Chapter 7: RECOMMENDED TESTING FRAMEWORK

After the three materials had been examined certain tests and certain testing techniques were realized to be appropriate for CCPs. Figure 37 outlines the recommended testing framework in order to use CCPs in embankment and mine land reclamation applications.

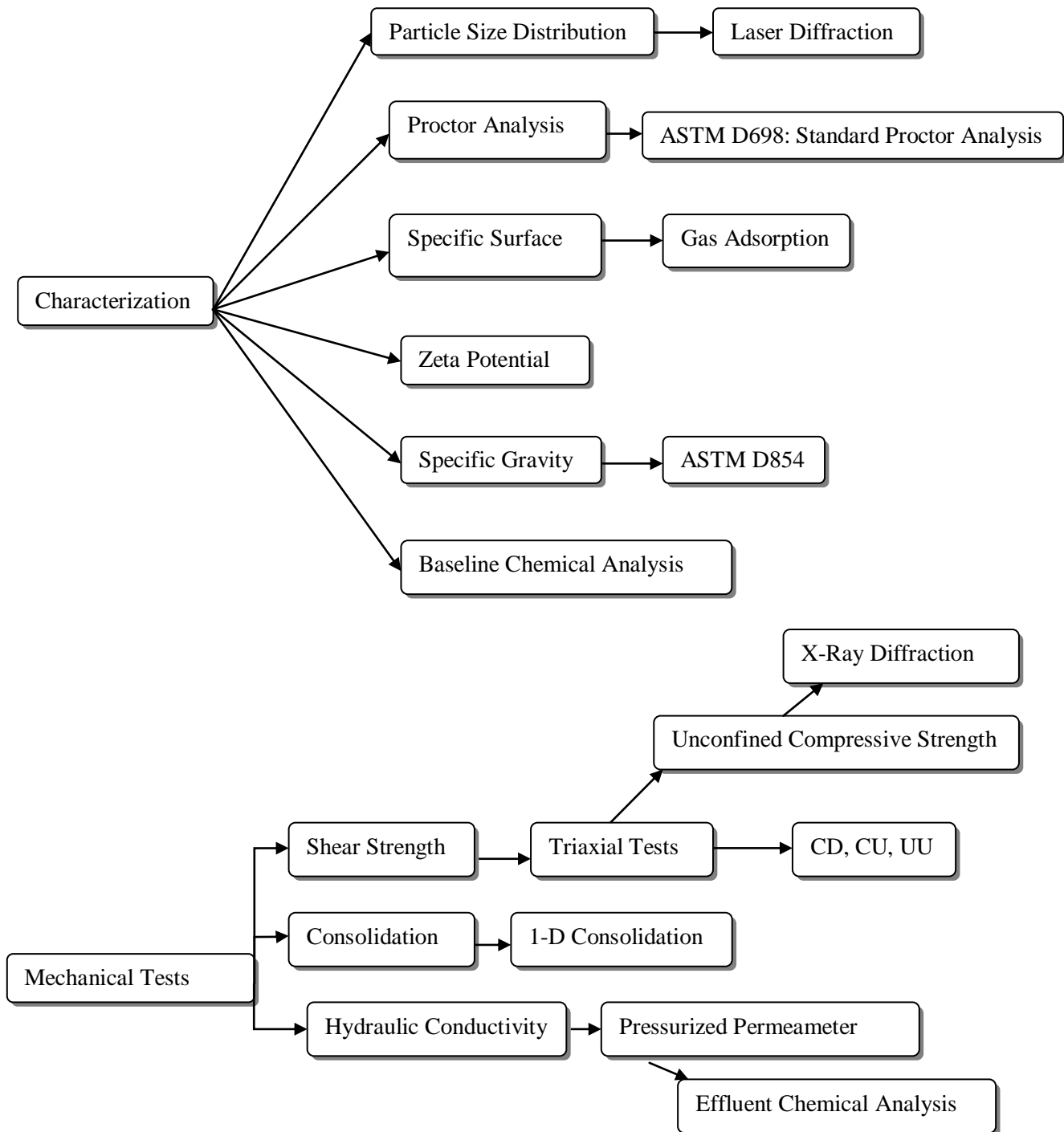


Figure 35: Test framework for embankment construction and mine land reclamation

This framework addresses the appropriate characterization and strength parameters required to properly predict CCP performance as a material for embankments or mine land reclamation. Determining particle size distributions using laser diffraction proved to be the most accurate method for CCPs. FGD material for example is soluble in water which makes hydrometer analysis results inaccurate. The possibility of entrained air within the porous structure of the FBC ash could also affect hydrometer results. Since laser diffraction is a dry technique it is most appropriate. Standard techniques for determining moisture-density relationships and specific gravity were fine for use with CCPs. The BET gas adsorption technique for specific surface proved to work well with CCPs since it is a dry method, eliminating the variability of material solubility.

CCPs can be dynamic materials and it is imperative to examine their strength and hydraulic conductivity characteristics as a function of time. The unconfined compressive strength test is a simple way to determine short and long term strength trends. Samples are easily prepared and can be cured for indefinite time intervals in order to quantify strength with time. The systematic use of x-ray diffraction in order to examine mineralogical change as a function of time is also an imperative tool. Mineralogical changes in CCPs describe where strength and permeability change and can also be used to predict future strength parameters. Sample storage would also be useful in examining extremely long term performance. While unconfined compression testing is great to describe changing strength characteristics, it lacks the results necessary to design structures. In order to design foundations or analyze slope stability the angle of internal friction is required. To obtain the angle of internal friction, triaxial tests at various levels of confinement must be done. Consolidation is another important design parameter which must be examined.

The pressurized permeameter used in this study proved quite effective in measuring the hydraulic conductivity of CCPs. It allow hydraulic conductivity measurement in a timely manner. Due to the applied confining pressure, preferential flow path development at the material/cell wall interface was significantly reduced if not eliminated. Since CCPs can potentially produce hazardous leachate, capturing and chemically analyzing the effluent from the hydraulic conductivity testing can be beneficial. The effluent analysis can also help describe any changing hydraulic conductivity characteristics.

This framework addresses relevant parameters and tests which describe the characteristics of CCPs and help to predict performance. The value of the information obtained from this framework greatly exceeds the mechanical requirements for a structural fill as described in DEP's Chapter 290: Beneficial Use of Coal Ash.

Chapter 8: CONCLUSIONS

In this day in age, it is becoming more practical and sustainable to implement green technologies in various aspects of human existence. The construction industry is no different. The manufacture, transportation, and installation of materials require significant cost and natural resource consumption. The reuse and recycling of alternate, human-made materials can reduce costs and environmental impacts. Coal combustion products (CCPs) can be reused and recycled in large volume civil engineering structures like embankment and fill applications. In some cases CCPs can even out-performed natural materials for these applications (Bacon, 1976). Typical intrinsic CCP properties present various advantages. These advantages include the potential cementitious nature of CCPs (strength gain with time), low unit weight, high factor of safety for slope stability, high shear strength per unit weight ratio, and the immediate availability of large volumes of material (Butalia and Wolfe, 2001) (ACAA, 2009). However, CCPs can be highly variable as a function of power plant type (conventional vs. FBC) and fuel source. In order for CCPs to be reused they must be carefully examined via a specific testing framework. The development of this framework was the main purpose of this study. The main conclusions of this study are:

- CCPs can be properly tested for implementation from a characterization, chemical, and mechanical standpoint. The more that is known about a particular material, the more accurately performance can be predicted. Accurate performance prediction justifies reasons for implementation.
- Monitoring CCP characteristics as a function of time is essential. CCPs can be dynamic. Studying strength, hydraulic conductivity, and mineralogical change with respect to time is necessary to predict behavior and performance. Storage of samples provides a means of examining very long term performance.
- Some typical soil testing techniques are not appropriate for testing CCPs. Some CCPs are soluble which limit the accuracy of tests involving water, hydrometer analysis for example. The high strength of some CCPs exceed the capacity of many typical soil loading frames and load cells.

Chapter 9: RECOMMENDATIONS FOR FUTURE WORK

- Characteristics of CCPs blended with naturally occurring materials
- How CCP properties change as a function of fuel source
- CCP usage in transportation applications
- Development of a database consisting of various CCP properties
- Triaxial testing program to determine design friction angles for various CCPs and various applications
- Pilot embankment and fill projects utilizing CCPs and monitoring long term stability
- Techniques to stabilize FBC ash as a low permeability material
- How often do CCPs need to be tested for different applications, every time a new CCP is used, every time the fuel source changes?

REFERENCES

Activation Laboratories, <http://www.actlabs.com>, Date accessed: January 2010.

Al-Khafaji, A.W., Andersland, O.B., Geotechnical Engineering and Soil Testing., copyright 1992 Saunders College Publishing p.138.

American Coal Ash Association (ACAA), <http://www.acaa-usa.org/#>, Date accessed: March 2009.

ASTM Standard C 618 “Standard Specification for Coal Fly Ash and Raw or Calcined Natural Pozzolan for Use as a Mineral Admixture in Concrete.”

ASTM Standard D 4187-82 “Zeta Potential of Colloids in Water and Waste Water.”

ASTM Standard D 698 “Standard Test Methods for Laboratory Compaction Characteristics of Soil Using Standard Effort.”

ASTM Standard D 854 “Standard Test Methods for Specific Gravity of Soil Solids by Water Pycnometer.”

ASTM Standard D 2166-00 “Standard Test Method for Unconfined Compressive Strength of Cohesive Soil.”

Babykal, G., Edincliler, A., and Saygili, A., “Highway Embankment Construction Using Fly Ash in Cold Regions.” *Resources, Conservation, and Recycling*, vol. 42, 2004, pp 209-222.

Bacon, L.D. (1976). Fly Ash for Construction of Highway Embankments. Proc. 4th International Ash Utilization Symposium, Energy Research and Development Administrations, Report No. MERC/SP-76/4, Morgantown WV: 262-292.

Butalia, T.S. and Wolfe, W.E. (2001). Utilization of Coal Combustion Products in Ohio for Construction and Repair of Highways. Beneficial Use of Recycled Materials in Transportation Applications, Proc. of the International Conf. on Beneficial Use of Recycled Materials in Transportation Applications, Washington, DC, Nov. 13-15, 2001: 803-812.

Brendel, G. F., “Ash Utilization in Highways: Pennsylvania Demonstration Project.”EPRI Report GS-6431 Project 2422-19, June 1989.

Dalberto, A.D., B.E. Scheetz, R.J. Hornberger, T.C. Kania, M.J. Menghini, and S.E. Walters (2004). Chapter 1. Overview: Coal Ash Beneficial Use at Mine Sites. In: Coal Ash Beneficial Use in Mine Reclamation and Mine Drainage Remediation in Pennsylvania, DEP Publication #5600-UK-DEP3132: 1-19.

Das, B.M., Principles of Geotechnical Engineering, copyright 1994 PWS publishing company, Boston, MA, p. 351.

DEP (2009). Certification Guidelines for the Chemical and Physical Properties of Coal Ash Beneficially Used at Mines, PA Dept. of Environmental Protection Bureau of Mining and Reclamation, Doc. No. 563-2112-224, Interim Final Report, April 2009.

Department of Environmental PA Code 25 Chapter 290: Beneficial Use of Coal Ash.

Deschamps. R.J., "Using FBC and Stoker Ashes as Roadway Fill: A Case Study." *Journal of Geotechnical and Geoenvironmental Engineering*, vol. 24, No. 11, November, 1998, pp 1120-1127.

Cahn, R., Concise Encyclopedia of Materials Characterization, copyright 2005 Elsevier, The Boulevard, Langford Lane Kidlington, Oxford OX5 1GB UK.

Cragg, C., "Fly Ash Speeds Bridge Construction." United States Department of Energy, Morgantown Energy Technology Center (Report) DOE/METC, vol. 2, 1985, pp 487-501.

Fagerlund, G., "Determination of Specific Surface by the BET Method." *Materials and Structures*, vol. 6, No. 3, May, 1973, pp 239-245.

FGDProducts.org, Date accessed: September 2009

Hornberger, R., Loop, C.M., Brady, K.B.C., and Houtz, N.A., "Chapter 2. Geology of the Pennsylvania Coal Regions." Coal Ash Beneficial Use in Mine Reclamation and Mine Drainage Remediation in Pennsylvania, 2004.

Joshi, R.C., Duncan, D.M., and Durbin, W.L. "Performance Record of Fly Ash as a Construction Material." *U.S. Symposium on Rock Mechanics.*, 1976, pp 300-320.

Kumar, S., Patil, C.B. "Estimation of Resource Savings Due to Fly Ash Utilization in Road Construction." *Resources, Conservation, and Recycling*, vol. 48, 2006, pp 125-140.

Loop, C.M., White, W.B., Scheetz, B.S., "Chapter 8. The Knickerbocker Demonstration Project." Coal Ash Beneficial Use in Mine Reclamation and Mine Drainage Remediation in Pennsylvania, 2004.

Lyklema, J. "Fundamentals of Interface and Colloid Science", vol.2, page.3.208, 1995 ISBN 012460529X.

Mitchell, J.K. and Soga, K., Fundamentals of Soil Behavior, copyright 2005 John Wiley & Sons.

Nichols, Herbert L., "Moving the Earth." McGraw-Hill Publishing Company, New York, New York, 1976.

Powerspan Corp., <http://www.powerspan.com/home/index.shtml>, Date accessed: March 2009.

Russel, W.B., Saville, D.A. and Schowalter, W.R. "Colloidal Dispersions", Cambridge University Press, 1992 ISBN 0521426006.

Santamarina, J.C., Klein, K.A., Wang, Y.H., Prencke E. "Specific Surface: Determination and Relevance." *Canadian Geotechnical Journal*, vol. 39, 2002, pp 233-241.

University of California Materials Research Laboratory <http://www.mrl.ucsb.edu>, Date accessed: December 2009.

USGS, <http://minerals.cr.usgs.gov/icpms/intro.html>, Date accessed: January 2010.

U.S. Department of Interior Bureau of Reclamation., Earth Manual. United States Government Printing Office, Denver 1998.

Yoon, S., Balunaini, U., Prezzi, M., "Forensic Examination of Severe Heaving of an Embankment Constructed with Fluidized Bed Combustion Ash." *Transportation Research Record: Journal of the Transportation Research Board*, no. 2026, 2007, pp 9-17.

Appendix A: HYDRAULIC CONDUCTIVITY PROCEDURE

Sample Preparation

1. Mix the material in a bowl with the amount of water needed for desired water content.
2. Place empty Tygon tube on compaction stand, see Figure 1.

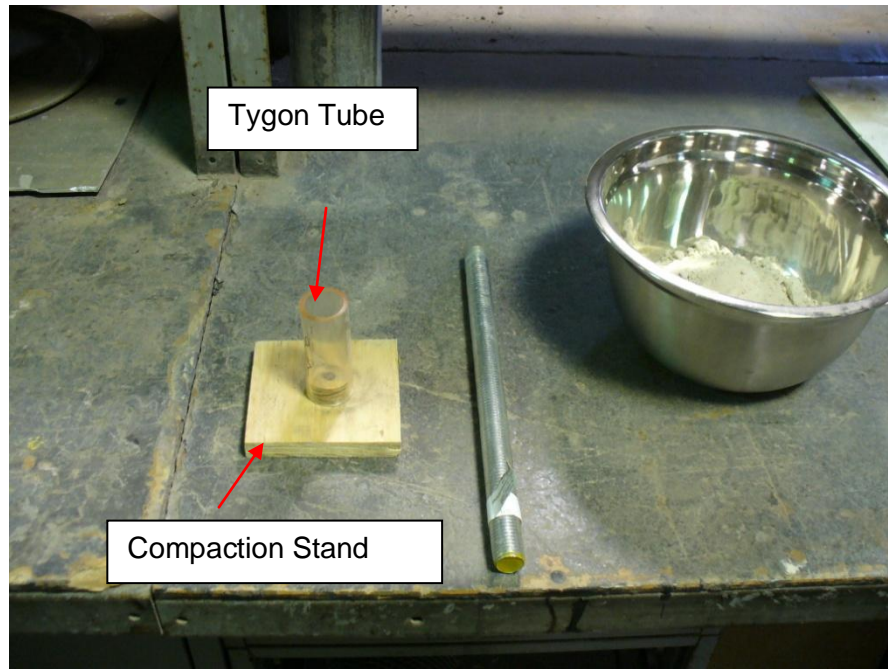


Figure 1: Tygon tube on compaction stand

3. Compact sample in 3 equal lifts with 25 blows per lift from the tamping rod, see Figure 2.
4. Remove sample from compaction stand.

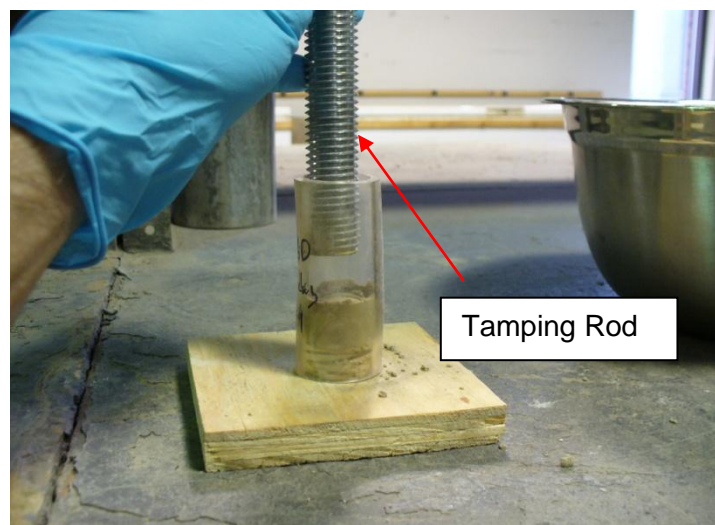


Figure 2: Sample compaction



Figure 3: Finished samples

Prime Water Vessel

1. Remove top cap, see Figure 4.

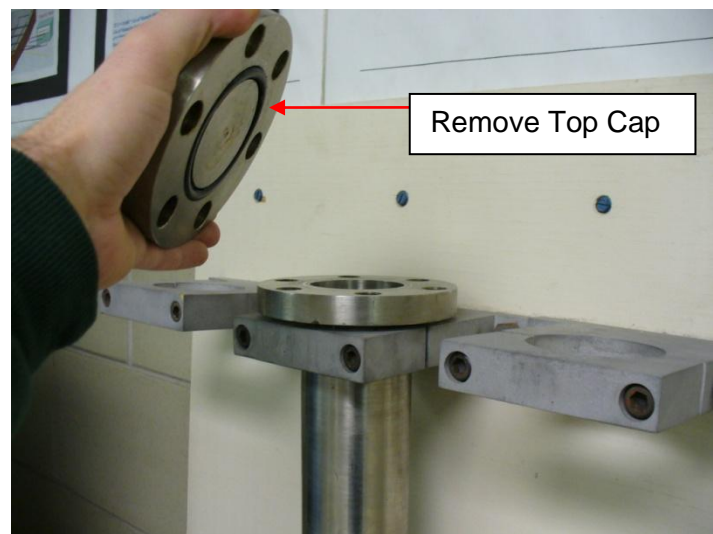
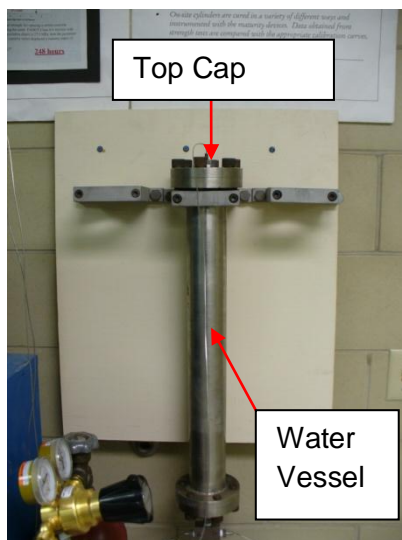


Figure 4: Top cap removal

2. Located extended flat head screw driver and threaded rod, see Figure 5.

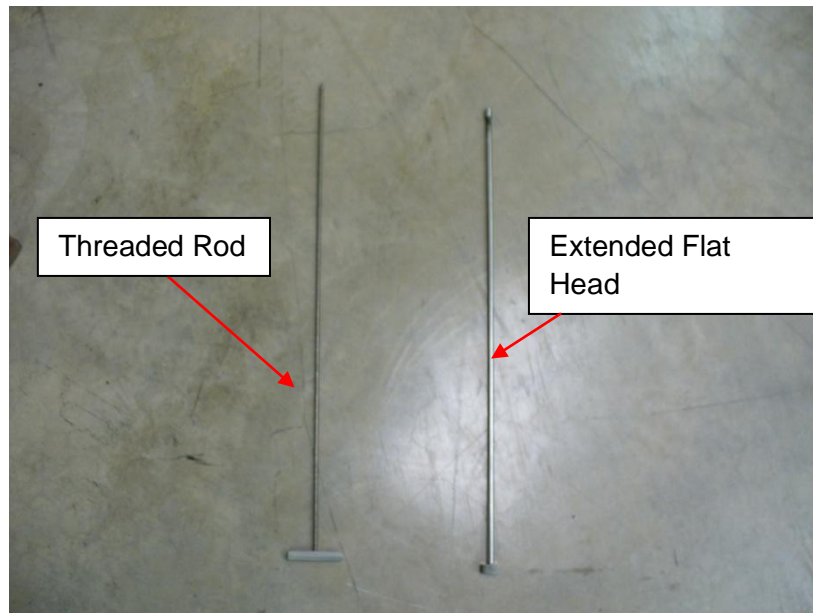


Figure 5: Extended flat head and threaded rod

3. Remove inner cylinder by: 1. opening valve using extended flat head turning counter clockwise, see Figure 6. 2. inserting threaded rod and pulling cylinder up and out of water vessel, see Figure 7.



Figure 6: Open valve using extended flat head

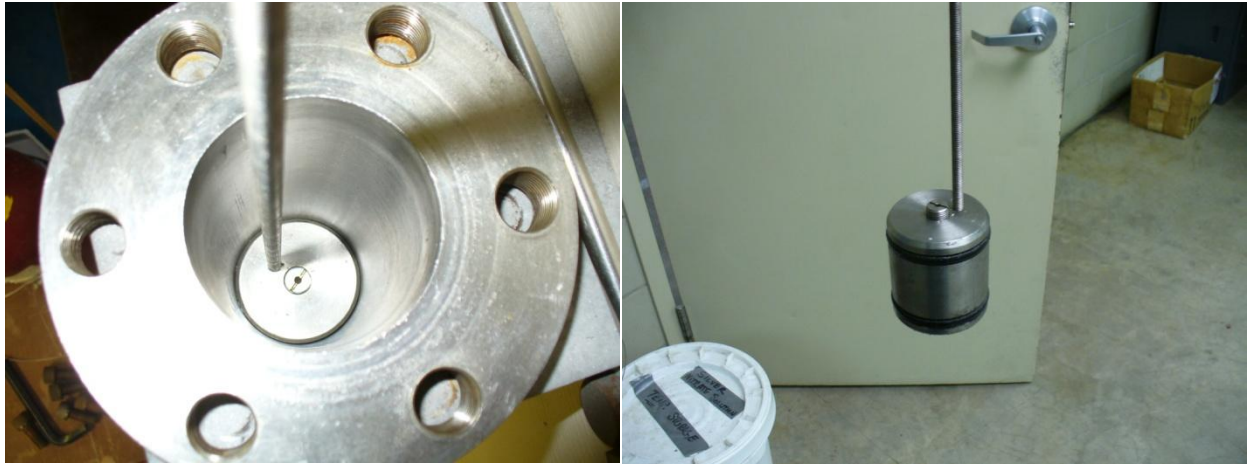


Figure 7: Remove cylinder with threaded rod

4. Fill water vessel with distilled water, see Figure 8.



Figure 8: Fill with water

5. Insert cylinder into water vessel with valve open until water comes out of the valve, then close the valve (this expels all air from the inside of the water vessel), see Figure 9.

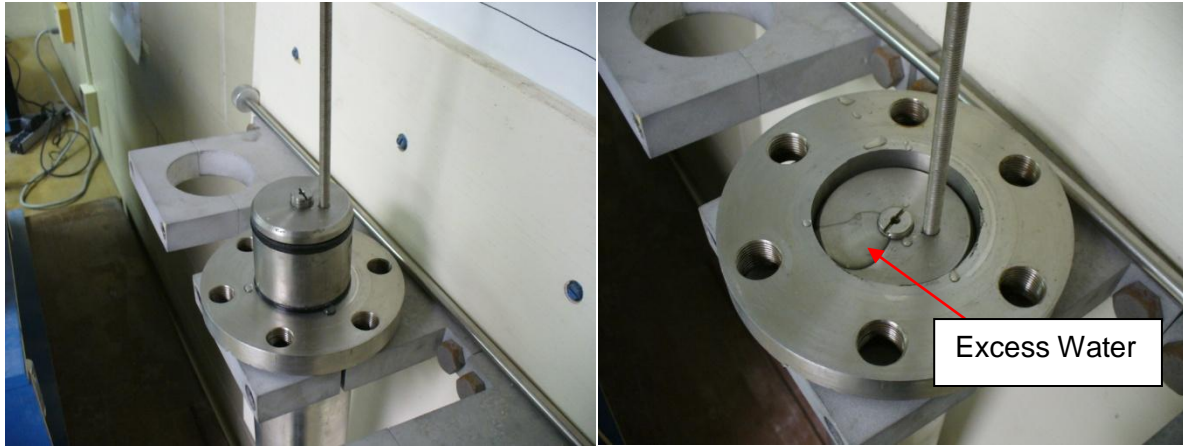


Figure 9: Insert cylinder back into water vessel

6. Dry up the excess water.
7. Replace top cap on vessel and tighten, see fig 10.

Permeability Chamber Set-up

1. Measure the length and diameter of the sample, see fig 11. Cut a piece of filter paper 1 in. in diameter and place on bottom of sample inside tygon tube.



Figure 10: Replace vessel top cap



Figure 11: Sample measurement

2. Insert sample into metal cylinder, see fig 12.

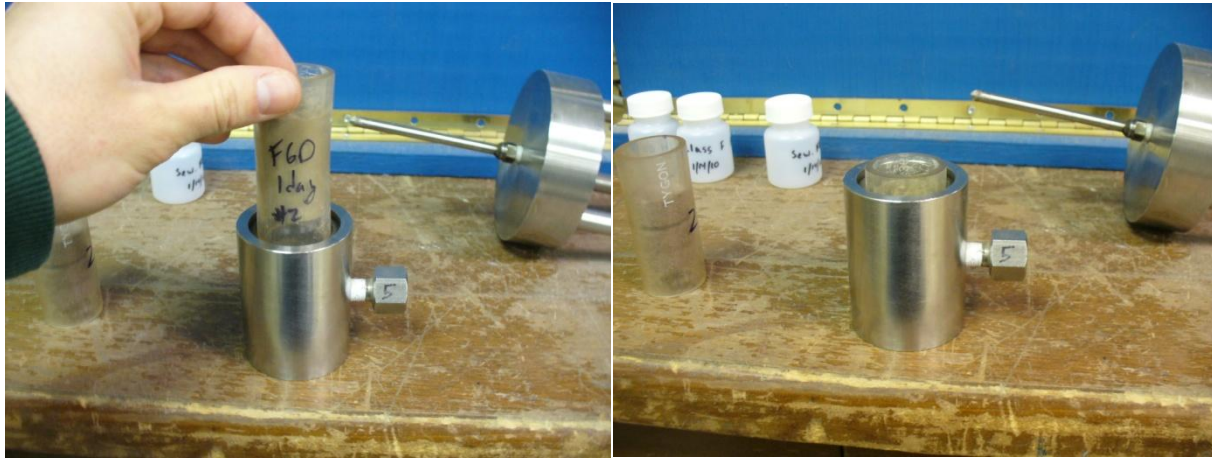


Figure 12: Sample installation

3. Place metal cylinder with sample into frame, be sure specimen is properly seated into the base of the frame, see Figure 13.



Figure 13: Sample Inside Metal Cylinder on Base of Frame

4. Insert water injector into the top of the sample, see fig 14.

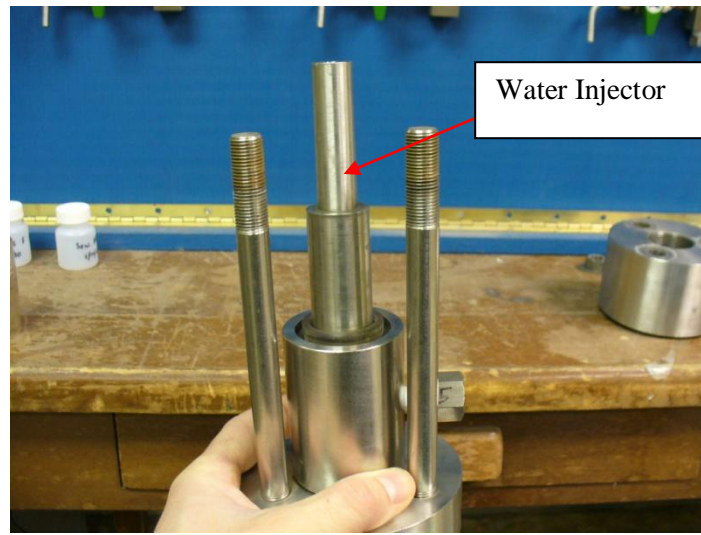


Figure 14: Insert water injector

5. Place top cap on frame and tighten. Be sure the frame top cap is properly seated on top of the sample, see Figure15.

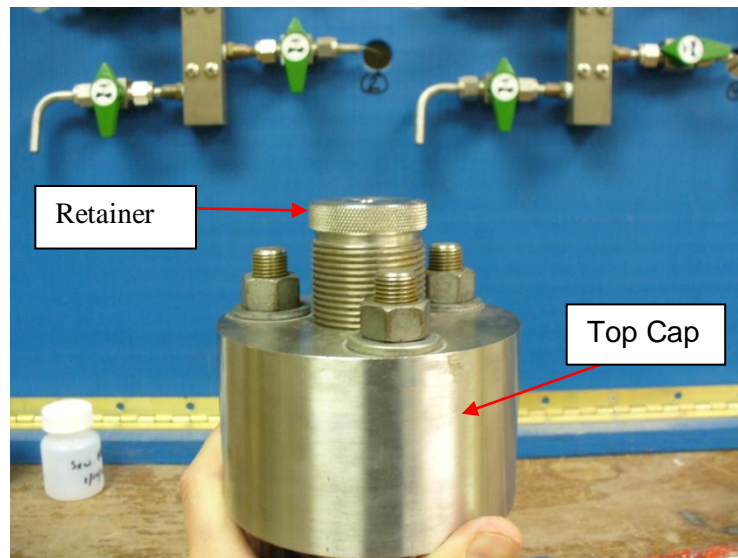


Figure 15: Secure the top cap

6. Screw water injector retainer into top cap, see Figure 15.
7. Attach confining pressure line to the side of the metal cylinder, see Figure 16.



Figure 16: Confining pressure line

8. Attach driving pressure line into the top of the water injector, see Figure 17.



Figure 17: Driving pressure line

Run Permeability Test

1. Open main valve completely on nitrogen tank by turning counter clockwise, see Figure 18.



Figure 18: Nitrogen gas valve

2. Make sure valves 5 and 6 on panel are open, pointed to the left, see Figure 19.

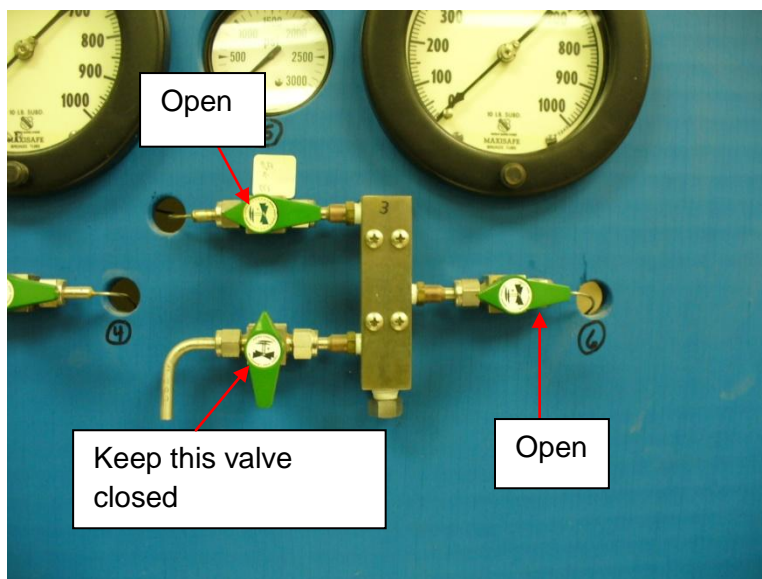


Figure 19: Valves 5 and 6 open

3. Open regulator until desired confining pressure is reached by turning regulator knob clockwise, see Figure 20.

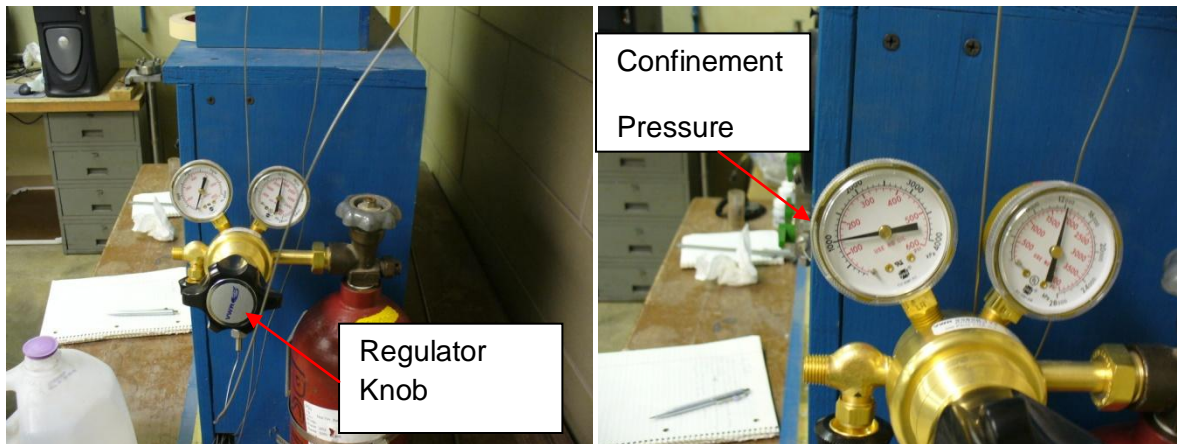


Figure 20: Open regulator

4. Close valve 5 to keep constant confining pressure.
5. Reduce pressure on regulator until desired driving pressure is reached.
6. Allow time for sample saturation
7. Record the time (t) required for a known volume (v) of water to pass through the sample.
Use a graduated cylinder to measure the volume.
8. When finished, close regulator by turning the regulator knob counter clockwise.
9. Remove the excess pressure in the system by opening the bleed valve on the regulator, see Figure 21.



Figure 21: Opening bleed valve

Appendix B: PROCTOR DATA

Soil Description: Montour FGD (synthetic gypsum)

Test Date: July 24, 2009

Test Location: CITEL Building (Penn State)

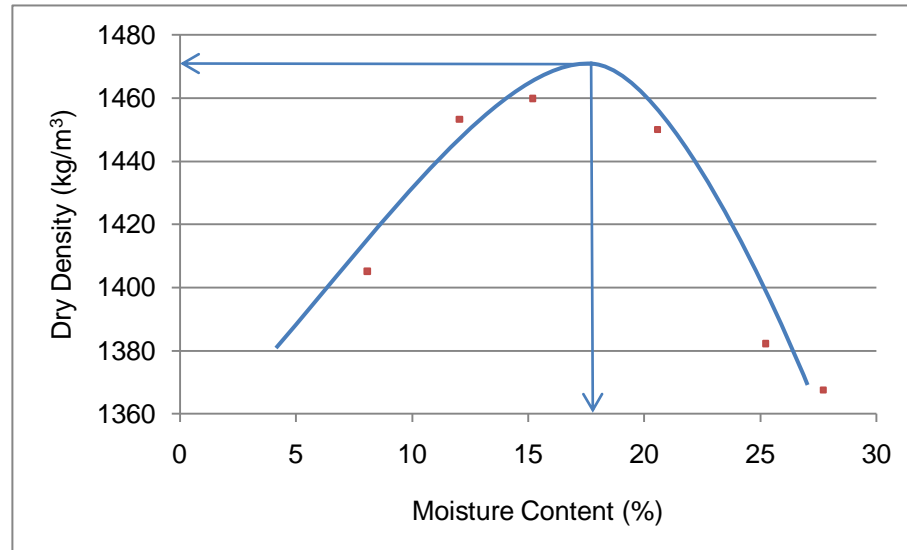
Vol. of Mold: $9.439 \times 10^{-4} \text{m}^3$ ($1/30 \text{ft}^3$)

Hammer Mass 2494.76 g

No. Blows/Lift: 25

No. Lifts: 3

Material dried at a maximum of 95°C



Trial Number	1	2	3	4	5	6
Mass of Mold (g)	4370.40	4370.40	4370.40	4370.40	4370.40	4370.40
Mass of Mold + Moist Soil (g)	5803.70	5907.30	5957.80	6020.70	6004.40	6019.00
Mass of Moist Soil (g)	1433.30	1536.90	1587.40	1650.30	1634.00	1648.60
Moist Density (kg/m^3)	1518.49	1628.24	1681.75	1748.38	1731.12	1746.58
Mass of Moisture Can (g)	19.80	20.90	19.70	20.80	20.50	20.60
Mass of Moisture Can + Moist Soil (g)	33.20	45.10	43.20	41.90	47.30	60.70
Mass of Moisture Can + Dry Soil (g)	32.20	42.50	40.10	38.30	41.90	52.00
Moisture Content	8.06	12.04	15.20	20.57	25.23	27.71

Dry Density of Compaction (kg/m^3)	1405.17	1453.31	1459.90	1450.08	1382.31	1367.65
Optimum Moisture Content	17%					
Maximum Dry density	1470.00 kg/m^3 (91.78 lb/ft^3)					

Soil Description: Seward FBC Ash

(45% ba, 55% fa)

Test Date: September 30, 2009

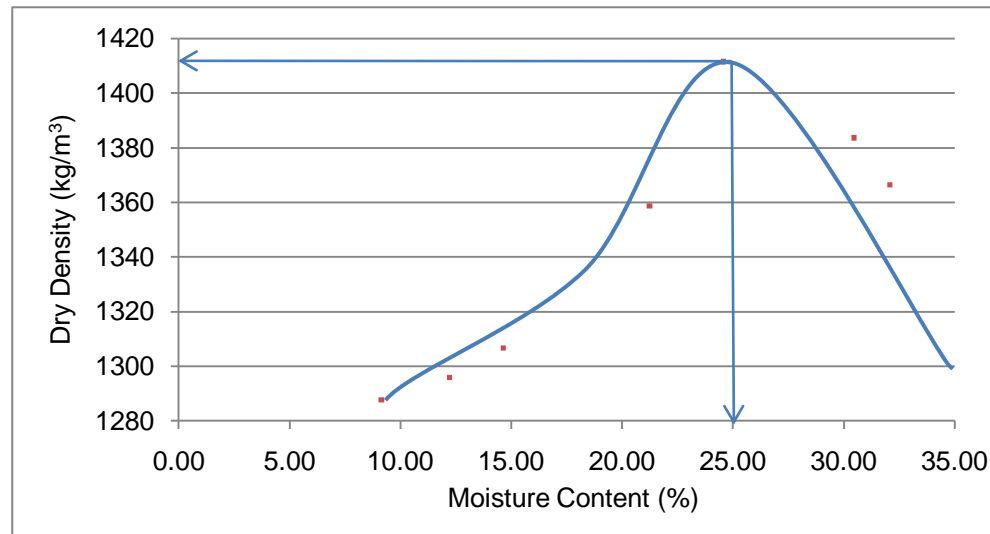
Test Location: CITEL

Vol. of Mold: $9.439 \times 10^{-4} \text{m}^3$ (1/30ft³)

Hammer Mass 2494.76 g

No. Blows/Lift: 25

No. Lifts: 3



Mass of Mold (g)	4368.80	4368.80	4368.80	4368.80	4368.80	4368.80	4368.80
Mass of Mold + Moist Soil (g)	5695.30	5741.40	5782.70	5923.60	6028.50	6072.70	6072.30
Mass of Moist Soil (g)	1326.50	1372.60	1413.90	1554.80	1659.70	1703.90	1703.50
Moist Density (kg/m³)	1405.34	1454.18	1497.93	1647.21	1758.34	1805.17	1804.75
Mass of Moisture Can (g)	20.70	19.80	20.90	20.70	19.70	19.70	20.70
Mass of Moisture Can + Moist Soil (g)	39.80	39.10	39.70	38.40	48.10	39.40	55.70
Mass of Moisture Can + Dry Soil (g)	38.20	37.00	37.30	35.30	42.50	34.80	47.20
Moisture Content	9.14	12.21	14.63	21.23	24.56	30.46	32.08

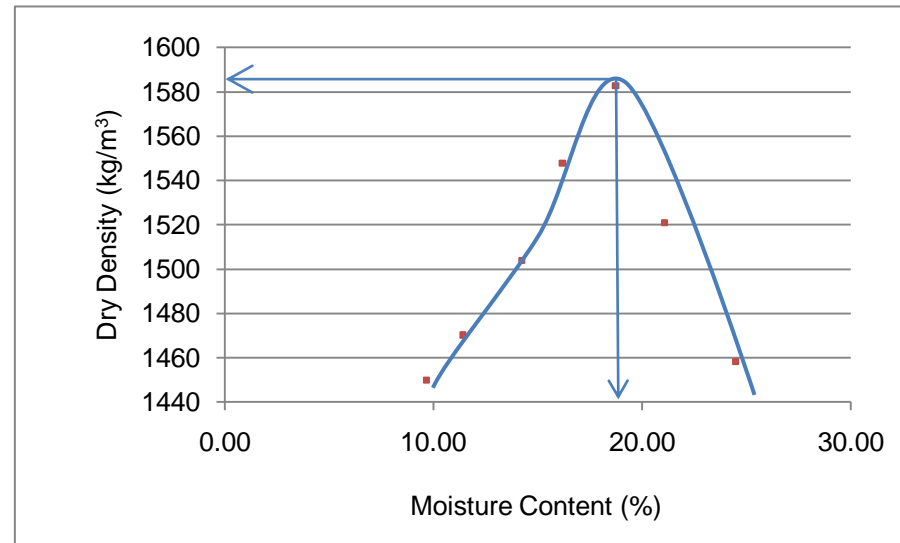
Dry Density of Compaction (kg/m³)	1287.61	1295.95	1306.71	1358.71	1411.63	1383.66	1366.45
Optimum Moisture Content	25%						
Maximum Dry density	1415.00 kg/m ³ (88.13lb/ft ³)						

Test Date: November 12, 2009

Test Location: CITEL Building (Penn State)

Vol. of Mold: $9.439 \times 10^{-4} \text{m}^3$ ($1/30 \text{ft}^3$)

Hammer Mass 2494.76 g

No. Blows/Lift: 25**No. Lifts: 3**

Trial Number	1	2	3	4	5	6	7
Mass of Mold (g)	4371.40	4371.40	4371.40	4371.40	4371.40	4371.40	4371.40
Mass of Mold + Moist Soil (g)	5872.30	5917.60	5993.00	6068.90	6145.30	6109.50	6084.70
Mass of Moist Soil (g)	1500.90	1546.20	1621.60	1697.50	1773.90	1738.10	1713.30
Moist Density (kg/m³)	1590.10	1638.10	1717.98	1798.39	1879.33	1841.40	1815.13
Mass of Moisture Can (g)	20.60	20.80	19.80	21.00	20.50	20.70	19.70
Mass of Moisture Can + Moist Soil (g)	50.10	53.00	54.30	57.60	61.70	56.90	67.00
Mass of Moisture Can + Dry Soil (g)	47.50	49.70	50.00	52.50	55.20	50.60	57.70
Moisture Content	9.67	11.42	14.24	16.19	18.73	21.07	24.47

Dry Density of Compaction (kg/m³)	1449.96	1470.22	1503.85	1547.79	1582.83	1520.94	1458.24
Optimum Moisture Content	19%						
Maximum Dry density	1582.00 kg/m ³ (98.81 lb/ft ³)						

Appendix C: HYDRAULIC CONDUCTIVITY DATA

1-day Hydraulic Conductivity (2/18/2010)		FBC #1	FBC #2	Class F #1	Class F #2	FGD #1	FGD #2
Volume of Water	v(cm ³)	20	20	20	20	20	20
Time	t(s)	74.63	144.75	100.60	78.28	44.93	50.16
Measured Flow Rate (q/t)	q(cm ³ /s)	0.2680	0.1382	0.1988	0.2555	0.4451	0.3987
Measured Flow Rate	q(in ³ /s)	0.0163	0.0084	0.0121	0.0156	0.0272	0.0243
Specimen Diameter	D(in)	1	1	1	1	1	1
Specimen Area	A(in ²)	0.785	0.785	0.785	0.785	0.785	0.785
Specimen Length	L(in)	1.45	1.606	1.609	1.534	1.78	1.55
Inlet Pressure	P _a (lb/in ²)	150	150	150	150	50	50
Outlet Pressure	P _b (lb/in ²)	14.7	14.7	14.7	14.7	14.7	14.7
Unit Weight of Water	γ _w (lb/in ³)	0.0361	0.0361	0.0361	0.0361	0.0361	0.0361
Equivalent Pressure Head (Inlet) (P _a /γ _w)	h _a (in)	4155.12	4155.12	4155.12	4155.12	1385.04	1385.04
Equivalent Pressure Head (Outlet)(P _b /γ _w)	h _b (in)	407.20	407.20	407.20	407.20	407.20	407.20
Hydraulic Conductivity, k=(Q*L)/A*(h _a -h _b)	k (in/sec)	8.06E-06	4.60E-06	6.63E-06	8.13E-06	6.30E-05	4.91E-05
Hydraulic Conductivity, k=(Q*L)/A*(h _a -h _b)	k (cm/sec)	2.05E-05	1.17E-05	1.68E-05	2.06E-05	1.60E-04	1.25E-04
3-day Hydraulic Conductivity (1/16/2010)		FBC #1	FBC #2	Class F #1	Class F #2	FGD #1	FGD #2
Volume of Water	v(cm ³)	20	20	20	20	20	0
Time	t(s)	560.34	434.97	72.66	80.91	56.85	0
Measured Flow Rate (q/t)	q(cm ³ /s)	0.0357	0.0460	0.2753	0.2472	0.3518	0.0000
Measured Flow Rate	q(in ³ /s)	0.0022	0.0028	0.0168	0.0151	0.0215	0.0000
Specimen Diameter	D(in)	1	1	1	1	1	0
Specimen Area	A(in ²)	0.785	0.785	0.785	0.785	0.785	0
Specimen Length	L(in)	1.588	1.367	1.382	1.611	1.735	0
Inlet Pressure	P _a (lb/in ²)	150	150	150	150	50	0
Outlet Pressure	P _b (lb/in ²)	14.7	14.7	14.7	14.7	14.7	0
Unit Weight of Water	γ _w (lb/in ³)	0.0361	0.0361	0.0361	0.0361	0.0361	0
Equivalent Pressure Head (Inlet) (P _a /γ _w)	h _a (in)	4155.12	4155.12	4155.12	4155.12	1385.04	0.00
Equivalent Pressure Head (Outlet)(P _b /γ _w)	h _b (in)	407.20	407.20	407.20	407.20	407.20	0.00
Hydraulic Conductivity, k=(Q*L)/A*(h _a -h _b)	k (in/sec)	1.18E-06	1.30E-06	7.89E-06	8.26E-06	4.85E-05	0.00E+00
Hydraulic Conductivity, k=(Q*L)/A*(h _a -h _b)	k (cm/sec)	2.98E-06	3.31E-06	2.00E-05	2.10E-05	1.23E-04	0.00E+00

7-day Hydraulic Conductivity (1/20/2010)		FBC #1	FBC #2	Class F #1	Class F #2	FGD #1	FGD #2
Volume of Water	$v(\text{cm}^3)$	20	20	20	0	60	60
Time	$t(\text{s})$	5580.33	2671.45	58.91	0	146.67	103.78
Measured Flow Rate (q/t)	$q(\text{cm}^3/\text{s})$	0.0036	0.0075	0.3395	0.0000	0.4091	0.5781
Measured Flow Rate	$q(\text{in}^3/\text{s})$	0.0002	0.0005	0.0207	0.0000	0.0250	0.0353
Specimen Diameter	$D(\text{in})$	1	1	1	1	1	1
Specimen Area	$A(\text{in}^2)$	0.785	0.785	0.785	0.785	0.785	0.785
Specimen Length	$L(\text{in})$	1.366	1.423	1.25	1.25	1.488	1.82
Inlet Pressure	$P_a(\text{lb}/\text{in}^2)$	150	150	150	150	50	50
Outlet Pressure	$P_b(\text{lb}/\text{in}^2)$	14.7	14.7	14.7	14.7	14.7	14.7
Unit Weight of Water	$\gamma_w(\text{lb}/\text{in}^3)$	0.0361	0.0361	0.0361	0.0361	0.0361	0.0361
Equivalent Pressure Head (Inlet) (P_a/γ_w)	$h_a(\text{in})$	4155.12	4155.12	4155.12	4155.12	1385.04	1385.04
Equivalent Pressure Head (Outlet) (P_b/γ_w)	$h_b(\text{in})$	407.20	407.20	407.20	407.20	407.20	407.20
Hydraulic Conductivity, $k=(Q*L)/A*(h_a-h_b)$	$k (\text{in}/\text{sec})$	1.02E-07	2.21E-07	8.80E-06	0.00E+00	4.84E-05	8.36E-05
Hydraulic Conductivity, $k=(Q*L)/A*(h_a-h_b)$	$k (\text{cm}/\text{sec})$	2.58E-07	5.61E-07	2.23E-05	0.00E+00	1.23E-04	2.12E-04
14-day Hydraulic Conductivity (1/27/2010)		FBC #1	FBC #2	Class F #1	Class F #2	FGD #1	FGD #2
Volume of Water	$v(\text{cm}^3)$	20	20	20	20	20	20
Time	$t(\text{s})$	7200	1786.32	56.63	55.31	52.33	51.32
Measured Flow Rate (q/t)	$q(\text{cm}^3/\text{s})$	0.0028	0.0112	0.3532	0.3616	0.3822	0.3897
Measured Flow Rate	$q(\text{in}^3/\text{s})$	0.0002	0.0007	0.0215	0.0221	0.0233	0.0238
Specimen Diameter	$D(\text{in})$	1	1	1	1	1	1
Specimen Area	$A(\text{in}^2)$	0.785	0.785	0.785	0.785	0.785	0.785
Specimen Length	$L(\text{in})$	1.575	1.7	1.4	1.567	1.581	1.658
Inlet Pressure	$P_a(\text{lb}/\text{in}^2)$	150	150	150	150	50	50
Outlet Pressure	$P_b(\text{lb}/\text{in}^2)$	14.7	14.7	14.7	14.7	14.7	14.7
Unit Weight of Water	$\gamma_w(\text{lb}/\text{in}^3)$	0.0361	0.0361	0.0361	0.0361	0.0361	0.0361
Equivalent Pressure Head (Inlet) (P_a/γ_w)	$h_a(\text{in})$	4155.12	4155.12	4155.12	4155.12	1385.04	1385.04
Equivalent Pressure Head (Outlet) (P_b/γ_w)	$h_b(\text{in})$	407.20	407.20	407.20	407.20	407.20	407.20
Hydraulic Conductivity, $k=(Q*L)/A*(h_a-h_b)$	$k (\text{in}/\text{sec})$	9.07E-08	3.95E-07	1.03E-05	1.17E-05	4.80E-05	5.13E-05
Hydraulic Conductivity, $k=(Q*L)/A*(h_a-h_b)$	$k (\text{cm}/\text{sec})$	2.30E-07	1.00E-06	2.60E-05	2.98E-05	1.22E-04	1.30E-04

28-day Hydraulic Conductivity (2/10/2010)		FBC #1	FBC #2	Class F #1	Class F #2	FGD #1	FGD #2
Volume of Water	v(cm ³)	20	20	20	20	20	20
Time	t(s)	4282	4102	53.53	44.12	47.31	48.96
Measured Flow Rate (q/t)	q(cm ³ /s)	0.0047	0.0049	0.3736	0.4533	0.4227	0.4085
Measured Flow Rate	q(in ³ /s)	0.0003	0.0003	0.0228	0.0277	0.0258	0.0249
Specimen Diameter	D(in)	1	1	1	1	1	1
Specimen Area	A(in ²)	0.785	0.785	0.785	0.785	0.785	0.785
Specimen Length	L(in)	1.486	1.735	1.618	1.436	1.521	1.55
Inlet Pressure	P _a (lb/in ²)	150	150	150	150	50	50
Outlet Pressure	P _b (lb/in ²)	14.7	14.7	14.7	14.7	14.7	14.7
Unit Weight of Water	γ _w (lb/in ³)	0.0361	0.0361	0.0361	0.0361	0.0361	0.0361
Equivalent Pressure Head (Inlet) (P _a /γ _w)	h _a (in)	4155.12	4155.12	4155.12	4155.12	1385.04	1385.04
Equivalent Pressure Head (Outlet)(P _b /γ _w)	h _b (in)	407.20	407.20	407.20	407.20	407.20	407.20
Hydraulic Conductivity, k=(Q*L)/A*(h _a -h _b)	k (in/sec)	1.44E-07	1.75E-07	1.25E-05	1.35E-05	5.11E-05	5.03E-05
Hydraulic Conductivity, k=(Q*L)/A*(h _a -h _b)	k (cm/sec)	3.66E-07	4.45E-07	3.18E-05	3.43E-05	1.30E-04	1.28E-04
56-day Hydraulic Conductivity (2/1/2010)		FBC #1	FBC #2	Class F #1	Class F #2	FGD #1	FGD #2
Volume of Water	v(cm ³)	20	60	20	20	20	20
Time	t(s)	198.03	1454.47	50.09	46.25	48.12	45.22
Measured Flow Rate (q/t)	q(cm ³ /s)	0.1010	0.0413	0.3993	0.4324	0.4156	0.4423
Measured Flow Rate	q(in ³ /s)	0.0062	0.0025	0.0244	0.0264	0.0254	0.0270
Specimen Diameter	D(in)	1	1	1	1	1	1
Specimen Area	A(in ²)	0.785	0.785	0.785	0.785	0.785	0.785
Specimen Length	L(in)	1.325	1.615	1.713	1.64	1.845	1.78
Inlet Pressure	P _a (lb/in ²)	150	150	150	150	50	50
Outlet Pressure	P _b (lb/in ²)	14.7	14.7	14.7	14.7	14.7	14.7
Unit Weight of Water	γ _w (lb/in ³)	0.0361	0.0361	0.0361	0.0361	0.0361	0.0361
Equivalent Pressure Head (Inlet) (P _a /γ _w)	h _a (in)	4155.12	4155.12	4155.12	4155.12	1385.04	1385.04
Equivalent Pressure Head (Outlet)(P _b /γ _w)	h _b (in)	407.20	407.20	407.20	407.20	407.20	407.20
Hydraulic Conductivity, k=(Q*L)/A*(h _a -h _b)	k (in/sec)	2.77E-06	1.38E-06	1.42E-05	1.47E-05	6.09E-05	6.26E-05
Hydraulic Conductivity, k=(Q*L)/A*(h _a -h _b)	k (cm/sec)	7.05E-06	3.51E-06	3.60E-05	3.73E-05	1.55E-04	1.59E-04

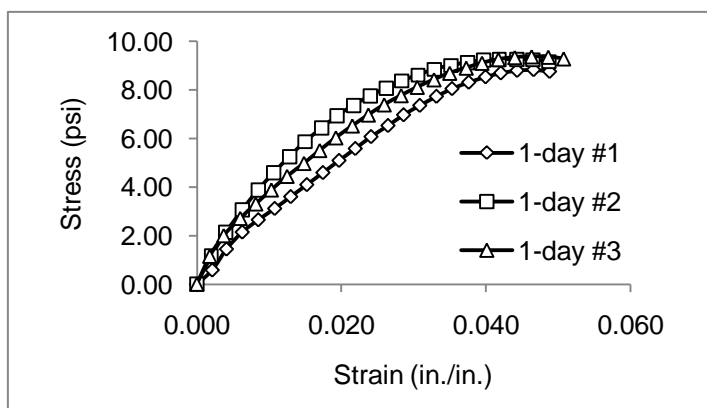
90-day Hydraulic Conductivity (3/11/2010)		FBC #1	FBC #2	Class F #1	Class F #2	FGD #1	FGD #2
Volume of Water	v(cm ³)	20	20	20	20	20	20
Time	t(s)	36.66	74.9	47.78	48.5	43.03	49.59
Measured Flow Rate (q/t)	q(cm ³ /s)	0.5456	0.2670	0.4186	0.4124	0.4648	0.4033
Measured Flow Rate	q(in ³ /s)	0.0333	0.0163	0.0255	0.0252	0.0284	0.0246
Specimen Diameter	D(in)	1	1	1	1	1	1
Specimen Area	A(in ²)	0.785	0.785	0.785	0.785	0.785	0.785
Specimen Length	L(in)	1.409	1.45	1.862	1.7	1.661	1.804
Inlet Pressure	P _a (lb/in ²)	150	150	150	150	50	50
Outlet Pressure	P _b (lb/in ²)	14.7	14.7	14.7	14.7	14.7	14.7
Unit Weight of Water	γ _w (lb/in ³)	0.0361	0.0361	0.0361	0.0361	0.0361	0.0361
Equivalent Pressure Head (Inlet) (P _a /γ _w)	h _a (in)	4155.12	4155.12	4155.12	4155.12	1385.04	1385.04
Equivalent Pressure Head (Outlet)(P _b /γ _w)	h _b (in)	407.20	407.20	407.20	407.20	407.20	407.20
Hydraulic Conductivity, k=(Q*L)/A*(h _a -h _b)	k (in/sec)	1.59E-05	8.03E-06	1.62E-05	1.45E-05	6.14E-05	5.78E-05
Hydraulic Conductivity, k=(Q*L)/A*(h _a -h _b)	k (cm/sec)	4.05E-05	2.04E-05	4.10E-05	3.69E-05	1.56E-04	1.47E-04
180-day Hydraulic Conductivity		FBC #1	FBC #2	Class F #1	Class F #2	FGD #1	FGD #2
Volume of Water	v(cm ³)	20	20				
Time	t(s)	38	37.52				
Measured Flow Rate (q/t)	q(cm ³ /s)	0.5263	0.5330				
Measured Flow Rate	q(in ³ /s)	0.0321	0.0325				
Specimen Diameter	D(in)	1	1				
Specimen Area	A(in ²)	0.785	0.785				
Specimen Length	L(in)	1.475	1.795				
Inlet Pressure	P _a (lb/in ²)	150	150				
Outlet Pressure	P _b (lb/in ²)	14.7	14.7				
Unit Weight of Water	γ _w (lb/in ³)	0.0361	0.0361				
Equivalent Pressure Head (Inlet) (P _a /γ _w)	h _a (in)	4155.12	4155.12				
Equivalent Pressure Head (Outlet)(P _b /γ _w)	h _b (in)	407.20	407.20				
Hydraulic Conductivity, k=(Q*L)/A*(h _a -h _b)	k (in/sec)	1.61E-05	1.98E-05				
Hydraulic Conductivity, k=(Q*L)/A*(h _a -h _b)	k (cm/sec)	4.09E-05	5.04E-05				

Appendix D: UNCONFINED COMPRESSION TEST DATA

Montour FGD #1

Initial Parameters

Curing Duration	1-day
Date	8/14/2009
Diameter, in	4
Area, in²	12.57
Length, in	5
Ini mass, g	36.1
Fin mass, g	33.5
Moisture Content	7.8



Time,	Deformation,	Vertical Strain,	Load,	Corrected Area	Stress,
sec	ΔL , in	$\epsilon = \Delta L/L$	lb	$A_c = A_o/(1-\epsilon)$, in ²	σ , lb/in ²
0	0.0000	0.0000	0.00	12.57	0.00
30	0.0107	0.0021	7.33	12.60	0.58
60	0.0205	0.0041	18.25	12.62	1.45
90	0.0314	0.0063	27.14	12.65	2.15
120	0.0426	0.0085	33.62	12.68	2.65
150	0.0539	0.0108	39.62	12.71	3.12
180	0.0650	0.0130	45.94	12.74	3.61
210	0.0761	0.0152	52.34	12.76	4.10
240	0.0873	0.0175	58.81	12.79	4.60
270	0.0984	0.0197	65.36	12.82	5.10
300	0.1097	0.0219	71.83	12.85	5.59
330	0.1206	0.0241	78.31	12.88	6.08
360	0.1323	0.0265	84.39	12.91	6.54
390	0.1431	0.0286	90.32	12.94	6.98
420	0.1543	0.0309	95.54	12.97	7.37
450	0.1659	0.0332	100.61	13.00	7.74
480	0.1767	0.0353	104.98	13.03	8.06
510	0.1882	0.0376	108.65	13.06	8.32
540	0.1999	0.0400	111.85	13.09	8.54
570	0.2104	0.0421	114.19	13.12	8.70
600	0.2217	0.0443	115.82	13.15	8.81
630	0.2331	0.0466	116.53	13.18	8.84
660	0.2442	0.0488	115.82	13.22	8.76

Montour FGD #2
Initial Parameters

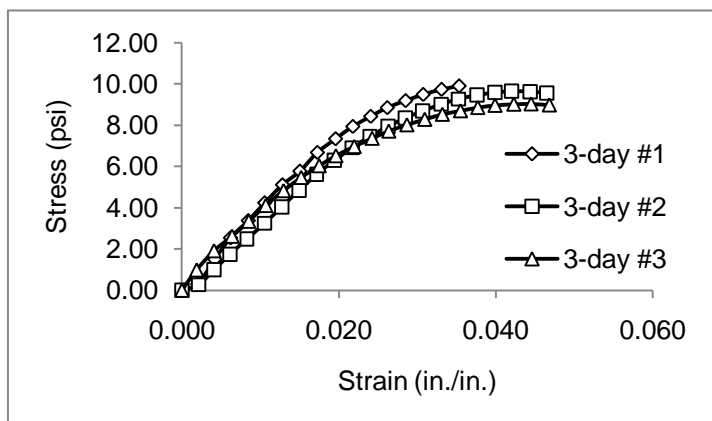
Curing Duration	1-day				
Date	8/14/2009				
Diameter, in	4				
Area, in²	12.57				
Length, in	5				
Ini mass, g	36.9				
Fin mass, g	34.1				
Moisture Content	8.2				
Time,	Deformation,	Vertical Strain,	Load,	Corrected Area	Stress,
sec	ΔL, in	$\epsilon = \Delta L/L$	lb	$A_c = A_o/(1-\epsilon)$, in²	σ, lb/in²
0	0.0000	0.0000	0.00	12.57	0.00
30	0.0100	0.0020	14.66	12.60	1.16
60	0.0201	0.0040	26.91	12.62	2.13
90	0.0315	0.0063	38.76	12.65	3.06
120	0.0425	0.0085	49.29	12.68	3.89
150	0.0533	0.0107	58.42	12.71	4.60
180	0.0641	0.0128	66.92	12.73	5.26
210	0.0749	0.0150	74.95	12.76	5.87
240	0.0863	0.0173	82.21	12.79	6.43
270	0.0972	0.0194	88.92	12.82	6.94
300	0.1085	0.0217	94.69	12.85	7.37
330	0.1199	0.0240	99.91	12.88	7.76
360	0.1310	0.0262	104.28	12.91	8.08
390	0.1418	0.0284	108.34	12.94	8.37
420	0.1531	0.0306	111.69	12.97	8.61
450	0.1643	0.0329	115.04	13.00	8.85
480	0.1758	0.0352	117.38	13.03	9.01
510	0.1873	0.0375	119.33	13.06	9.14
540	0.1984	0.0397	120.74	13.09	9.22
570	0.2093	0.0419	121.60	13.12	9.27
600	0.2215	0.0443	121.75	13.15	9.26
630	0.2327	0.0465	121.91	13.18	9.25
660	0.2437	0.0487	121.13	13.21	9.17

Montour FGD #3
Initial Parameters

Curing Duration	1-day				
Date	8/14/2009				
Diameter, in	4				
Area, in²	12.57				
Length, in	5				
Ini mass, g	34.5				
Fin mass, g	32				
Moisture Content	7.8				
Time,	Deformation,	Vertical Strain,	Load,	Corrected Area	Stress,
sec	ΔL, in	ε = ΔL/L	lb	Ac = Ao/(1-ε), in²	σ, lb/in²
0	0.0000	0.0000	0.00	12.57	0.00
30	0.0089	0.0018	14.51	12.59	1.15
60	0.0186	0.0037	25.27	12.62	2.00
90	0.0300	0.0060	34.32	12.65	2.71
120	0.0408	0.0082	41.96	12.67	3.31
150	0.0516	0.0103	49.37	12.70	3.89
180	0.0625	0.0125	56.62	12.73	4.45
210	0.0741	0.0148	63.57	12.76	4.98
240	0.0850	0.0170	70.51	12.79	5.51
270	0.0962	0.0192	77.37	12.82	6.04
300	0.1076	0.0215	83.85	12.85	6.53
330	0.1187	0.0237	89.85	12.88	6.98
360	0.1297	0.0259	95.47	12.90	7.40
390	0.1414	0.0283	100.61	12.94	7.78
420	0.1525	0.0305	105.29	12.97	8.12
450	0.1641	0.0328	109.58	13.00	8.43
480	0.1750	0.0350	113.33	13.03	8.70
510	0.1864	0.0373	116.37	13.06	8.91
540	0.1973	0.0395	119.26	13.09	9.11
570	0.2087	0.0417	121.52	13.12	9.26
600	0.2200	0.0440	122.92	13.15	9.35
630	0.2316	0.0463	123.62	13.18	9.38
660	0.2432	0.0486	123.70	13.21	9.36
690	0.2538	0.0508	123.08	13.24	9.29

Montour FGD #1**Initial Parameters**

Curing Duration	3-day
Date	8/16/2009
Diameter, in	4
Area, in²	12.57
Length, in	5
Ini mass, g	39.3
Fin mass, g	36.1
Moisture Content	8.9



Time,	Deformation,	Vertical Strain,	Load,	Corrected Area	Stress,
sec	ΔL , in	$\epsilon = \Delta L/L$	lb	$A_c = A_o/(1-\epsilon)$, in ²	σ , lb/in ²
0	0.0000	0.0000	0.00	12.57	0.00
30	0.0101	0.0020	3.82	12.60	0.30
60	0.0209	0.0042	18.95	12.62	1.50
90	0.0310	0.0062	32.13	12.65	2.54
120	0.0424	0.0085	42.82	12.68	3.38
150	0.0528	0.0106	53.90	12.70	4.24
180	0.0641	0.0128	65.13	12.73	5.11
210	0.0752	0.0150	73.73	12.76	5.78
240	0.0864	0.0173	85.48	12.79	6.68
270	0.0980	0.0196	94.22	12.82	7.35
300	0.1090	0.0218	102.10	12.85	7.95
330	0.1204	0.0241	108.65	12.88	8.44
360	0.1309	0.0262	114.34	12.91	8.86
390	0.1426	0.0285	119.02	12.94	9.20
420	0.1538	0.0308	123.16	12.97	9.50
450	0.1655	0.0331	126.67	13.00	9.74
480	0.1767	0.0353	129.16	13.03	9.91
510	0.1875	0.0375	103.72	13.06	7.94
540	0.1991	0.0398	131.58	13.09	10.05
570	0.2105	0.0421	131.89	13.12	10.05
600	0.2219	0.0444	130.88	13.15	9.95

Montour FGD #2
Initial Parameters

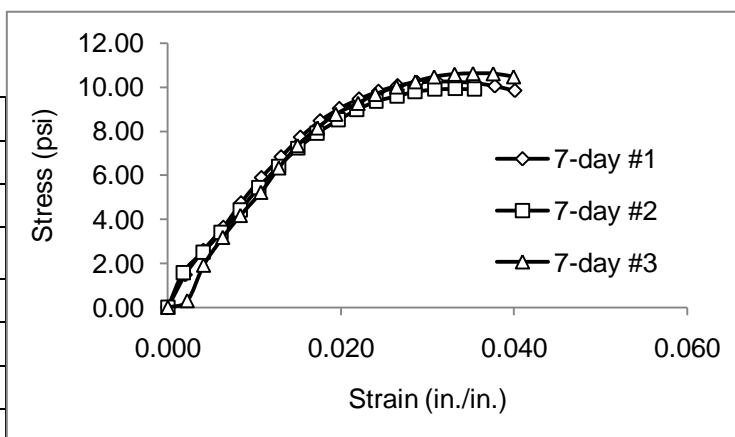
Curing Duration	3-day				
Date	8/16/2009				
Diameter, in	4				
Area, in²	12.57				
Length, in	5				
Ini mass, g	37.7				
Fin mass, g	34.8				
Moisture Content	8.3				
Time,	Deformation,	Vertical Strain,	Load,	Corrected Area	Stress,
sec	ΔL, in	$\epsilon = \Delta L/L$	lb	$A_c = A_o/(1-\epsilon)$, in²	σ, lb/in²
0	0.0000	0.0000	0.00	12.57	0.00
30	0.0107	0.0021	3.43	12.60	0.27
60	0.0206	0.0041	12.64	12.62	1.00
90	0.0306	0.0061	21.99	12.65	1.74
120	0.0415	0.0083	31.51	12.68	2.49
150	0.0527	0.0105	41.26	12.70	3.25
180	0.0636	0.0127	51.40	12.73	4.04
210	0.0747	0.0149	61.85	12.76	4.85
240	0.0859	0.0172	71.76	12.79	5.61
270	0.0973	0.0195	80.73	12.82	6.30
300	0.1087	0.0217	88.76	12.85	6.91
330	0.1198	0.0240	96.01	12.88	7.46
360	0.1314	0.0263	102.49	12.91	7.94
390	0.1423	0.0285	107.95	12.94	8.34
420	0.1535	0.0307	112.70	12.97	8.69
450	0.1652	0.0330	117.22	13.00	9.02
480	0.1762	0.0352	120.74	13.03	9.27
510	0.1881	0.0376	123.55	13.06	9.46
540	0.1994	0.0399	125.50	13.09	9.59
570	0.2102	0.0420	126.59	13.12	9.65
600	0.2221	0.0444	126.67	13.15	9.63
630	0.2325	0.0465	125.96	13.18	9.55

Montour FGD #3**Initial Parameters**

Curing Duration	3-day				
Date	8/16/2009				
Diameter, in	4				
Area, in²	12.57				
Length, in	5				
Ini mass, g	40.3				
Fin mass, g	36.9				
Moisture Content	9.2				
Time,	Deformation,	Vertical Strain,	Load,	Corrected Area	Stress,
sec	ΔL, in	ε = ΔL/L	lb	Ac = Ao/(1-ε), in²	σ, lb/in²
0	0.0000	0.0000	0.00	12.57	0.00
30	0.0094	0.0019	12.40	12.59	0.98
60	0.0204	0.0041	24.18	12.62	1.92
90	0.0320	0.0064	33.15	12.65	2.62
120	0.0426	0.0085	42.43	12.68	3.35
150	0.0534	0.0107	52.26	12.71	4.11
180	0.0648	0.0130	61.54	12.73	4.83
210	0.0760	0.0152	69.88	12.76	5.47
240	0.0874	0.0175	77.29	12.79	6.04
270	0.0981	0.0196	83.69	12.82	6.53
300	0.1098	0.0220	89.62	12.85	6.97
330	0.1212	0.0242	95.00	12.88	7.37
360	0.1318	0.0264	99.68	12.91	7.72
390	0.1433	0.0287	103.89	12.94	8.03
420	0.1547	0.0309	107.56	12.97	8.29
450	0.1659	0.0332	110.99	13.00	8.54
480	0.1775	0.0355	113.48	13.03	8.71
510	0.1885	0.0377	115.82	13.06	8.87
540	0.1995	0.0399	117.46	13.09	8.97
570	0.2114	0.0423	118.48	13.13	9.03
600	0.2224	0.0445	118.94	13.16	9.04
630	0.2341	0.0468	118.55	13.19	8.99

Montour FGD #1**Initial Parameters**

Curing Duration	7-day
Date	8/20/2009
Diameter, in	4
Area, in²	12.57
Length, in	5
Ini mass, g	38.2
Fin mass, g	35.3
Moisture Content	8.2



Time,	Deformation,	Vertical Strain,	Load,	Corrected Area	Stress,
sec	ΔL , in	$\epsilon = \Delta L/L$	lb	$A_c = A_o/(1-\epsilon)$, in ²	σ , lb/in ²
0	0.0000	0.0000	0.00	12.57	0.00
30	0.0101	0.0020	18.64	12.60	1.48
60	0.0205	0.0041	32.68	12.62	2.59
90	0.0320	0.0064	46.02	12.65	3.64
120	0.0423	0.0085	60.21	12.68	4.75
150	0.0540	0.0108	74.10	12.71	5.83
180	0.0654	0.0131	87.12	12.74	6.84
210	0.0765	0.0153	98.74	12.77	7.73
240	0.0879	0.0176	108.49	12.79	8.48
270	0.0990	0.0198	115.90	12.82	9.04
300	0.1104	0.0221	121.75	12.85	9.47
330	0.1216	0.0243	126.51	12.88	9.82
360	0.1327	0.0265	130.10	12.91	10.08
390	0.1440	0.0288	132.20	12.94	10.21
420	0.1553	0.0311	133.29	12.97	10.27
450	0.1661	0.0332	133.29	13.00	10.25
480	0.1771	0.0354	132.98	13.03	10.20
510	0.1888	0.0378	131.42	13.06	10.06
540	0.2004	0.0401	129.01	13.09	9.85

Montour FGD #2**Initial Parameters**

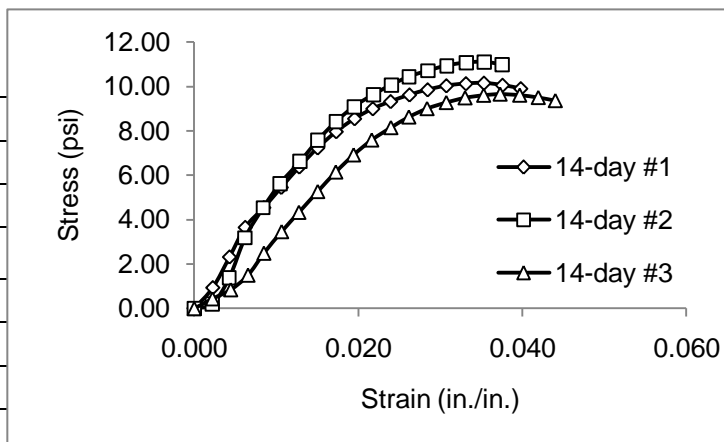
Curing Duration	7-day				
Date	8/20/2009				
Diameter, in	4				
Area, in ²	12.57				
Length, in	5				
Ini mass, g	38.2				
Fin mass, g	35.3				
Moisture Content	8.2				
Time,	Deformation,	Vertical Strain,	Load,	Corrected Area	Stress,
sec	ΔL, in	ε = ΔL/L	lb	Ac = Ao/(1-ε), in ²	σ, lb/in ²
0	0.0000	0.0000	0.00	12.57	0.00
30	0.0088	0.0018	19.89	12.59	1.58
60	0.0203	0.0041	31.74	12.62	2.51
90	0.0308	0.0062	43.05	12.65	3.40
120	0.0419	0.0084	56.16	12.68	4.43
150	0.0525	0.0105	69.26	12.70	5.45
180	0.0640	0.0128	81.66	12.73	6.41
210	0.0750	0.0150	92.27	12.76	7.23
240	0.0863	0.0173	101.39	12.79	7.93
270	0.0984	0.0197	109.19	12.82	8.52
300	0.1090	0.0218	115.43	12.85	8.98
330	0.1204	0.0241	120.74	12.88	9.37
360	0.1324	0.0265	124.09	12.91	9.61
390	0.1430	0.0286	126.90	12.94	9.81
420	0.1542	0.0308	128.54	12.97	9.91
450	0.1661	0.0332	129.16	13.00	9.93
480	0.1771	0.0354	129.24	13.03	9.92
510	0.1880	0.0376	128.54	13.06	9.84

Montour FGD #3**Initial Parameters**

Curing Duration	7-day				
Date	8/20/2009				
Diameter, in	4				
Area, in²	12.57				
Length, in	5				
Ini mass, g	35.2				
Fin mass, g	32.7				
Moisture Content	7.6				
Time,	Deformation,	Vertical Strain,	Load,	Corrected Area	Stress,
sec	ΔL, in	ε = ΔL/L	lb	Ac = Ao/(1-ε), in²	σ, lb/in²
0	0.0000	0.0000	0.00	12.57	0.00
30	0.0112	0.0022	3.82	12.60	0.30
60	0.0206	0.0041	24.18	12.62	1.92
90	0.0317	0.0063	40.25	12.65	3.18
120	0.0419	0.0084	52.96	12.68	4.18
150	0.0538	0.0108	66.45	12.71	5.23
180	0.0641	0.0128	80.73	12.73	6.34
210	0.0750	0.0150	93.83	12.76	7.35
240	0.0865	0.0173	104.36	12.79	8.16
270	0.0971	0.0194	112.55	12.82	8.78
300	0.1100	0.0220	119.26	12.85	9.28
330	0.1199	0.0240	124.72	12.88	9.68
360	0.1322	0.0264	129.40	12.91	10.02
390	0.1431	0.0286	132.75	12.94	10.26
420	0.1540	0.0308	135.95	12.97	10.48
450	0.1658	0.0332	137.82	13.00	10.60
480	0.1764	0.0353	138.52	13.03	10.63
510	0.1881	0.0376	138.75	13.06	10.62
540	0.1999	0.0400	137.27	13.09	10.48

Montour FGD #1**Initial Parameters**

Curing Duration	14-day
Date	8/27/2009
Diameter, in	4
Area, in²	12.57
Length, in	5
Ini mass, g	38.7
Fin mass, g	35.7
Moisture Content	8.4



Time,	Deformation,	Vertical Strain,	Load,	Corrected Area	Stress,
sec	ΔL, in	$\epsilon = \Delta L/L$	lb	$A_c = A_o/(1-\epsilon)$, in²	σ, lb/in²
0	0.0000	0.0000	0.00	12.57	0.00
30	0.0113	0.0023	11.86	12.60	0.94
60	0.0215	0.0043	29.33	12.62	2.32
90	0.0311	0.0062	46.25	12.65	3.66
120	0.0424	0.0085	57.64	12.68	4.55
150	0.0530	0.0106	69.34	12.70	5.46
180	0.0640	0.0128	81.19	12.73	6.38
210	0.0752	0.0150	92.35	12.76	7.24
240	0.0865	0.0173	101.94	12.79	7.97
270	0.0977	0.0195	109.66	12.82	8.55
300	0.1088	0.0218	115.67	12.85	9.00
330	0.1197	0.0239	120.11	12.88	9.33
360	0.1312	0.0262	124.25	12.91	9.63
390	0.1422	0.0284	127.52	12.94	9.86
420	0.1537	0.0307	130.17	12.97	10.04
450	0.1656	0.0331	131.73	13.00	10.13
480	0.1766	0.0353	132.36	13.03	10.16
510	0.1879	0.0376	131.42	13.06	10.06
540	0.1990	0.0398	129.71	13.09	9.91

Montour FGD #2
Initial Parameters

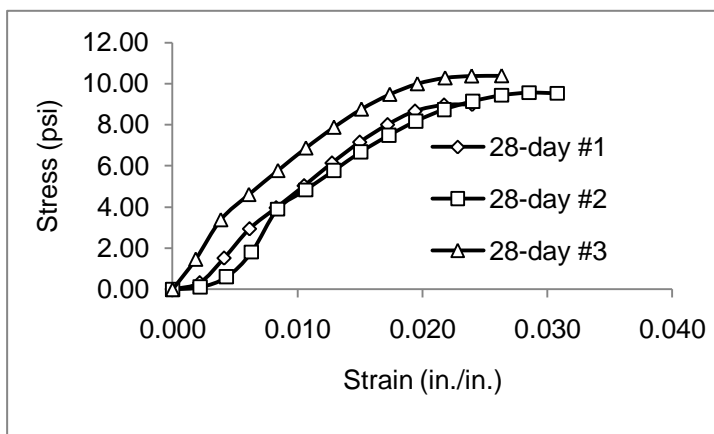
Curing Duration	14-day				
Date	8/27/2009				
Diameter, in	4				
Area, in²	12.57				
Length, in	5				
Ini mass, g	35.7				
Fin mass, g	33.2				
Moisture Content	7.5				
Time,	Deformation,	Vertical Strain,	Load,	Corrected Area	Stress,
sec	ΔL, in	$\epsilon = \Delta L/L$	lb	$A_c = A_o/(1-\epsilon)$, in²	σ, lb/in²
0	0.0000	0.0000	0.00	12.57	0.00
30	0.0111	0.0022	2.42	12.60	0.19
60	0.0214	0.0043	17.47	12.62	1.38
90	0.0310	0.0062	40.25	12.65	3.18
120	0.0421	0.0084	57.48	12.68	4.53
150	0.0523	0.0105	71.29	12.70	5.61
180	0.0646	0.0129	84.24	12.73	6.62
210	0.0756	0.0151	96.87	12.76	7.59
240	0.0865	0.0173	107.63	12.79	8.41
270	0.0975	0.0195	116.53	12.82	9.09
300	0.1092	0.0218	123.70	12.85	9.63
330	0.1201	0.0240	129.55	12.88	10.06
360	0.1310	0.0262	134.70	12.91	10.44
390	0.1426	0.0285	138.52	12.94	10.71
420	0.1540	0.0308	141.80	12.97	10.93
450	0.1658	0.0332	143.90	13.00	11.07
480	0.1768	0.0354	144.60	13.03	11.10
510	0.1878	0.0376	143.43	13.06	10.98

Montour FGD #3
Initial Parameters

Curing Duration	14-day				
Date	8/27/2009				
Diameter, in	4				
Area, in²	12.57				
Length, in	5				
Ini mass, g	31.8				
Fin mass, g	29.7				
Moisture Content	7.1				
Time,	Deformation,	Vertical Strain,	Load,	Corrected Area	Stress,
sec	ΔL, in	$\epsilon = \Delta L/L$	lb	$A_c = A_o/(1-\epsilon)$, in²	σ, lb/in²
0	0.0000	0.0000	0.00	12.57	0.00
30	0.0111	0.0022	5.54	12.60	0.44
60	0.0222	0.0044	10.69	12.63	0.85
90	0.0328	0.0066	19.03	12.65	1.50
120	0.0425	0.0085	31.59	12.68	2.49
150	0.0533	0.0107	43.99	12.71	3.46
180	0.0638	0.0128	55.14	12.73	4.33
210	0.0753	0.0151	67.23	12.76	5.27
240	0.0863	0.0173	78.62	12.79	6.15
270	0.0972	0.0194	88.68	12.82	6.92
300	0.1082	0.0216	97.49	12.85	7.59
330	0.1199	0.0240	104.90	12.88	8.15
360	0.1308	0.0262	111.30	12.91	8.62
390	0.1420	0.0284	116.45	12.94	9.00
420	0.1537	0.0307	120.27	12.97	9.27
450	0.1651	0.0330	123.31	13.00	9.49
480	0.1765	0.0353	125.11	13.03	9.60
510	0.1865	0.0373	126.04	13.06	9.65
540	0.1984	0.0397	125.73	13.09	9.61
570	0.2098	0.0420	124.64	13.12	9.50
600	0.2202	0.0440	123.08	13.15	9.36

Montour FGD #1**Initial Parameters**

Curing Duration	28-day
Date	9/11/2009
Diameter, in	4
Area, in²	12.57
Length, in	5
Ini mass, g	32
Fin mass, g	29.9
Moisture Content	7.0



Time,	Deformation,	Vertical Strain,	Load,	Corrected Area	Stress,
sec	ΔL , in	$\epsilon = \Delta L/L$	lb	$A_c = A_o/(1-\epsilon)$, in ²	σ , lb/in ²
0	0.0000	0.0000	0.00	12.57	0.00
30	0.0109	0.0022	4.13	12.60	0.33
60	0.0206	0.0041	19.26	12.62	1.53
90	0.0308	0.0062	37.28	12.65	2.95
120	0.0415	0.0083	50.31	12.68	3.97
150	0.0527	0.0105	64.03	12.70	5.04
180	0.0638	0.0128	78.23	12.73	6.14
210	0.0750	0.0150	91.33	12.76	7.16
240	0.0861	0.0172	102.41	12.79	8.01
270	0.0971	0.0194	111.07	12.82	8.66
300	0.1087	0.0217	115.12	12.85	8.96
330	0.1200	0.0240	115.75	12.88	8.99

Montour FGD #2**Initial Parameters**

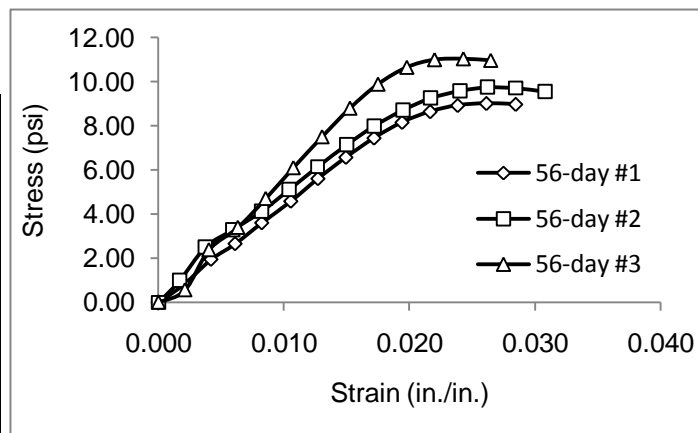
Curing Duration	28-day				
Date	9/11/2009				
Diameter, in	4				
Area, in²	12.57				
Length, in	5				
Ini mass, g	38				
Fin mass, g	34.9				
Moisture Content	8.9				
Time,	Deformation,	Vertical Strain,	Load,	Corrected Area	Stress,
sec	ΔL, in	ε = ΔL/L	lb	Ac = Ao/(1-ε), in²	σ, lb/in²
0	0.0000	0.0000	0.00	12.57	0.00
30	0.0111	0.0022	1.40	12.60	0.11
60	0.0216	0.0043	7.57	12.62	0.60
90	0.0316	0.0063	22.85	12.65	1.81
120	0.0420	0.0084	49.37	12.68	3.89
150	0.0532	0.0106	61.38	12.71	4.83
180	0.0647	0.0129	73.63	12.73	5.78
210	0.0754	0.0151	85.33	12.76	6.69
240	0.0867	0.0173	95.86	12.79	7.49
270	0.0975	0.0195	104.90	12.82	8.18
300	0.1088	0.0218	112.39	12.85	8.75
330	0.1203	0.0241	117.85	12.88	9.15
360	0.1318	0.0264	121.83	12.91	9.44
390	0.1427	0.0285	123.70	12.94	9.56
420	0.1540	0.0308	123.62	12.97	9.53

Montour FGD #3**Initial Parameters**

Curing Duration	28-day				
Date	9/11/2009				
Diameter, in	4				
Area, in²	12.57				
Length, in	5				
Ini mass, g	37.9				
Fin mass, g	34.8				
Moisture Content	8.9				
Time,	Deformation,	Vertical Strain,	Load,	Corrected Area	Stress,
sec	ΔL, in	$\epsilon = \Delta L/L$	lb	$A_c = A_o/(1-\epsilon)$, in²	σ, lb/in²
0	0.0000	0.0000	0.00	12.57	0.00
30	0.0093	0.0019	18.56	12.59	1.47
60	0.0193	0.0039	42.82	12.62	3.39
90	0.0306	0.0061	58.42	12.65	4.62
120	0.0422	0.0084	73.32	12.68	5.78
150	0.0534	0.0107	87.43	12.71	6.88
180	0.0647	0.0129	100.46	12.73	7.89
210	0.0757	0.0151	111.92	12.76	8.77
240	0.0870	0.0174	121.36	12.79	9.49
270	0.0981	0.0196	128.23	12.82	10.00
300	0.1092	0.0218	132.20	12.85	10.29
330	0.1198	0.0240	133.68	12.88	10.38
360	0.1318	0.0264	134.15	12.91	10.39

Montour FGD #1**Initial Parameters**

Curing Duration	56-day
Date	10/9/2009
Diameter, in	4
Area, in²	12.57
Length, in	5
Ini mass, g	37.3
Fin mass, g	34.4
Moisture Content	8.4



Time,	Deformation,	Vertical Strain,	Load,	Corrected Area	Stress,
sec	ΔL , in	$\epsilon = \Delta L/L$	lb	$A_c = A_o/(1-\epsilon)$, in ²	σ , lb/in ²
0	0.0000	0.0000	0.00	12.57	0.00
30	0.0101	0.0020	10.37	12.60	0.82
60	0.0209	0.0042	24.49	12.62	1.94
90	0.0305	0.0061	33.54	12.65	2.65
120	0.0412	0.0082	45.63	12.67	3.60
150	0.0527	0.0105	58.18	12.70	4.58
180	0.0636	0.0127	71.37	12.73	5.61
210	0.0747	0.0149	83.85	12.76	6.57
240	0.0859	0.0172	95.23	12.79	7.45
270	0.0971	0.0194	104.59	12.82	8.16
300	0.1083	0.0217	111.07	12.85	8.64
330	0.1193	0.0239	114.94	12.88	8.93
360	0.1307	0.0261	116.37	12.91	9.02
390	0.1424	0.0285	116.14	12.94	8.98

Montour FGD #2**Initial Parameters**

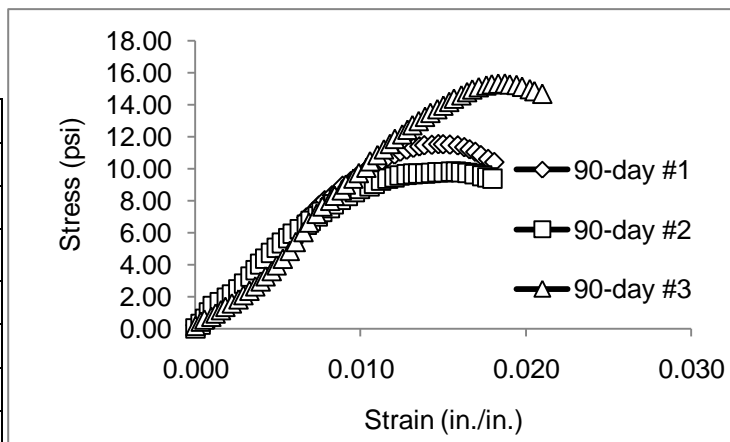
Curing Duration	56-day				
Date	10/9/2009				
Diameter, in	4				
Area, in²	12.57				
Length, in	5				
Ini mass, g	40.9				
Fin mass, g	37.5				
Moisture Content	9.1				
Time,	Deformation,	Vertical Strain,	Load,	Corrected Area	Stress,
sec	ΔL, in	ε = ΔL/L	lb	Ac = Ao/(1-ε), in²	σ, lb/in²
0	0.0000	0.0000	0.00	12.57	0.00
30	0.0084	0.0017	12.48	12.59	0.99
60	0.0187	0.0037	31.67	12.62	2.51
90	0.0295	0.0059	41.65	12.64	3.29
120	0.0411	0.0082	52.34	12.67	4.13
150	0.0521	0.0104	64.97	12.70	5.11
180	0.0634	0.0127	78.31	12.73	6.15
210	0.0750	0.0150	91.18	12.76	7.15
240	0.0860	0.0172	102.33	12.79	8.00
270	0.0974	0.0195	111.77	12.82	8.72
300	0.1084	0.0217	118.94	12.85	9.26
330	0.1201	0.0240	123.55	12.88	9.59
360	0.1310	0.0262	125.89	12.91	9.75
390	0.1424	0.0285	125.73	12.94	9.72
420	0.1541	0.0308	124.01	12.97	9.56

Montour FGD #3**Initial Parameters**

Curing Duration	56-day				
Date	10/9/2009				
Diameter, in	4				
Area, in²	12.57				
Length, in	5				
Ini mass, g	49.3				
Fin mass, g	44.1				
Moisture Content	11.8				
Time,	Deformation,	Vertical Strain,	Load,	Corrected Area	Stress,
sec	ΔL, in	$\epsilon = \Delta L/L$	lb	$A_c = A_o/(1-\epsilon)$, in²	σ, lb/in²
0	0.0000	0.0000	0.00	12.57	0.00
30	0.0105	0.0021	7.10	12.60	0.56
60	0.0201	0.0040	30.11	12.62	2.39
90	0.0316	0.0063	42.98	12.65	3.40
120	0.0427	0.0085	59.74	12.68	4.71
150	0.0538	0.0108	77.61	12.71	6.11
180	0.0652	0.0130	95.70	12.74	7.51
210	0.0763	0.0153	112.47	12.76	8.81
240	0.0875	0.0175	126.67	12.79	9.90
270	0.0990	0.0198	136.80	12.82	10.67
300	0.1101	0.0220	141.56	12.85	11.01
330	0.1216	0.0243	142.42	12.88	11.05
360	0.1325	0.0265	141.80	12.91	10.98

Montour FGD #1**Initial Parameters**

Curing Duration	90-day
Date	12/20/2009
Diameter, in	4
Area, in²	12.57
Length, in	5
Ini mass, g	67.8
Fin mass, g	54.7
Moisture Content	23.9



Time,	Deformation,	Vertical Strain,	Load,	Corrected Area	Stress,
sec	ΔL, in	$\epsilon = \Delta L/L$	lb	$A_c = A_o/(1-\epsilon)$, in²	σ, lb/in²
0	0.0000	0.0000	2.65	12.57	0.21
5	0.0015	0.0003	6.94	12.57	0.55
10	0.0035	0.0007	10.30	12.58	0.82
15	0.0052	0.0010	13.18	12.58	1.05
20	0.0069	0.0014	15.44	12.59	1.23
25	0.0089	0.0018	18.41	12.59	1.46
30	0.0108	0.0022	22.23	12.60	1.76
35	0.0123	0.0025	25.97	12.60	2.06
40	0.0142	0.0028	30.26	12.61	2.40
45	0.0157	0.0031	35.88	12.61	2.85
50	0.0174	0.0035	42.43	12.61	3.36
55	0.0194	0.0039	48.83	12.62	3.87
60	0.0210	0.0042	54.52	12.62	4.32
65	0.0232	0.0046	59.36	12.63	4.70
70	0.0247	0.0049	64.04	12.63	5.07
75	0.0265	0.0053	68.48	12.64	5.42
80	0.0290	0.0058	72.93	12.64	5.77
85	0.0303	0.0061	76.36	12.65	6.04
90	0.0322	0.0064	81.82	12.65	6.47
95	0.0335	0.0067	87.90	12.65	6.95
100	0.0358	0.0072	92.89	12.66	7.34
105	0.0373	0.0075	97.42	12.66	7.69
110	0.0391	0.0078	101.63	12.67	8.02
115	0.0413	0.0083	105.53	12.67	8.33
120	0.0433	0.0087	109.27	12.68	8.62

125	0.0445	0.0089	113.25	12.68	8.93
130	0.0470	0.0094	116.92	12.69	9.21
135	0.0488	0.0098	120.58	12.69	9.50
140	0.0511	0.0102	124.17	12.70	9.78
145	0.0524	0.0105	127.60	12.70	10.04
150	0.0548	0.0110	130.49	12.71	10.27
155	0.0565	0.0113	133.61	12.71	10.51
160	0.0581	0.0116	136.26	12.72	10.71
165	0.0603	0.0121	138.44	12.72	10.88
170	0.0620	0.0124	140.78	12.73	11.06
175	0.0639	0.0128	142.42	12.73	11.19
180	0.0659	0.0132	143.98	12.74	11.30
185	0.0678	0.0136	145.15	12.74	11.39
190	0.0693	0.0139	146.16	12.75	11.47
195	0.0715	0.0143	146.55	12.75	11.49
200	0.0735	0.0147	147.18	12.76	11.54
205	0.0749	0.0150	147.10	12.76	11.53
210	0.0770	0.0154	146.87	12.77	11.50
215	0.0794	0.0159	146.32	12.77	11.46
220	0.0814	0.0163	144.99	12.78	11.35
225	0.0830	0.0166	143.28	12.78	11.21
230	0.0847	0.0169	141.33	12.79	11.05
235	0.0864	0.0173	138.68	12.79	10.84
240	0.0886	0.0177	135.71	12.80	10.61
245	0.0905	0.0181	133.29	12.80	10.41

Montour FGD #2
Initial Parameters

Curing Duration	90-day				
Date	12/20/2009				
Diameter, in	4				
Area, in²	12.57				
Length, in	5				
Ini mass, g	68.4				
Fin mass, g	55.2				
Moisture Content	23.9				
Time,	Deformation,	Vertical Strain,	Load,	Corrected Area	Stress,
sec	ΔL, in	$\epsilon = \Delta L/L$	lb	$A_c = A_o/(1-\epsilon)$, in²	σ, lb/in²
0	0.0000	0.0000	0.16	12.57	0.01
5	0.0016	0.0003	3.43	12.57	0.27
10	0.0029	0.0006	7.80	12.58	0.62
15	0.0040	0.0008	12.95	12.58	1.03
20	0.0053	0.0011	18.02	12.58	1.43
25	0.0075	0.0015	20.75	12.59	1.65
30	0.0095	0.0019	24.57	12.59	1.95
35	0.0110	0.0022	27.07	12.60	2.15
40	0.0130	0.0026	30.65	12.60	2.43
45	0.0148	0.0030	35.57	12.61	2.82
50	0.0167	0.0033	41.10	12.61	3.26
55	0.0182	0.0036	46.17	12.62	3.66
60	0.0195	0.0039	50.93	12.62	4.04
65	0.0211	0.0042	55.30	12.62	4.38
70	0.0229	0.0046	59.75	12.63	4.73
75	0.0246	0.0049	63.96	12.63	5.06
80	0.0262	0.0052	67.70	12.64	5.36
85	0.0282	0.0056	71.29	12.64	5.64
90	0.0296	0.0059	74.88	12.64	5.92
95	0.0315	0.0063	78.62	12.65	6.22
100	0.0338	0.0068	82.05	12.66	6.48
105	0.0348	0.0070	85.41	12.66	6.75
110	0.0369	0.0074	88.99	12.66	7.03
115	0.0383	0.0077	92.35	12.67	7.29
120	0.0406	0.0081	95.47	12.67	7.53
125	0.0418	0.0084	98.67	12.68	7.78

130	0.0441	0.0088	102.25	12.68	8.06
135	0.0462	0.0092	105.29	12.69	8.30
140	0.0483	0.0097	108.41	12.69	8.54
145	0.0498	0.0100	110.83	12.70	8.73
150	0.0526	0.0105	113.25	12.70	8.91
155	0.0542	0.0108	115.36	12.71	9.08
160	0.0562	0.0112	117.54	12.71	9.25
165	0.0582	0.0116	119.10	12.72	9.36
170	0.0603	0.0121	120.58	12.72	9.48
175	0.0619	0.0124	121.91	12.73	9.58
180	0.0639	0.0128	122.69	12.73	9.64
185	0.0659	0.0132	123.23	12.74	9.67
190	0.0674	0.0135	123.47	12.74	9.69
195	0.0695	0.0139	123.70	12.75	9.70
200	0.0714	0.0143	124.09	12.75	9.73
205	0.0734	0.0147	124.64	12.76	9.77
210	0.0751	0.0150	124.95	12.76	9.79
215	0.0773	0.0155	125.26	12.77	9.81
220	0.0789	0.0158	125.26	12.77	9.81
225	0.0805	0.0161	124.95	12.78	9.78
230	0.0824	0.0165	124.33	12.78	9.73
235	0.0846	0.0169	123.31	12.79	9.64
240	0.0868	0.0174	122.22	12.79	9.55
245	0.0884	0.0177	120.82	12.80	9.44
250	0.0899	0.0180	119.80	12.80	9.36

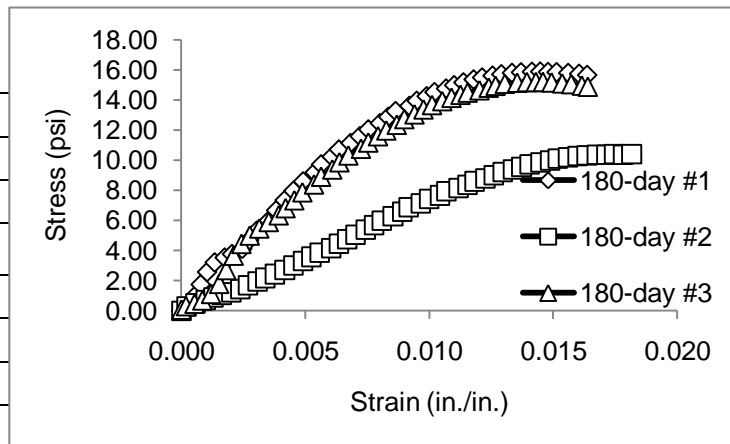
Montour FGD #3
Initial Parameters

Curing Duration	90-day				
Date	12/20/2009				
Diameter, in	4				
Area, in²	12.57				
Length, in	5				
Ini mass, g	58.1				
Fin mass, g	47.2				
Moisture Content	23.1				
Time,	Deformation,	Vertical Strain,	Load,	Corrected Area	Stress,
sec	ΔL, in	$\epsilon = \Delta L/L$	lb	$A_c = A_o/(1-\epsilon)$, in²	σ, lb/in²
0	0.0000	0.0000	2.18	12.57	0.17
5	0.0016	0.0003	5.54	12.57	0.44
10	0.0027	0.0005	7.18	12.58	0.57
15	0.0048	0.0010	9.36	12.58	0.74
20	0.0061	0.0012	11.93	12.59	0.95
25	0.0077	0.0015	14.59	12.59	1.16
30	0.0090	0.0018	17.16	12.59	1.36
35	0.0110	0.0022	19.89	12.60	1.58
40	0.0130	0.0026	23.09	12.60	1.83
45	0.0145	0.0029	26.44	12.61	2.10
50	0.0163	0.0033	29.87	12.61	2.37
55	0.0181	0.0036	33.38	12.62	2.65
60	0.0197	0.0039	37.28	12.62	2.95
65	0.0212	0.0042	41.34	12.62	3.27
70	0.0231	0.0046	45.47	12.63	3.60
75	0.0246	0.0049	50.00	12.63	3.96
80	0.0264	0.0053	55.22	12.64	4.37
85	0.0285	0.0057	61.46	12.64	4.86
90	0.0303	0.0061	68.56	12.65	5.42
95	0.0327	0.0065	76.44	12.65	6.04
100	0.0344	0.0069	84.00	12.66	6.64
105	0.0367	0.0073	90.94	12.66	7.18
110	0.0384	0.0077	96.79	12.67	7.64
115	0.0408	0.0082	101.32	12.67	7.99
120	0.0421	0.0084	105.37	12.68	8.31
125	0.0443	0.0089	109.66	12.68	8.65

130	0.0455	0.0091	114.34	12.69	9.01
135	0.0478	0.0096	119.10	12.69	9.38
140	0.0494	0.0099	123.55	12.70	9.73
145	0.0517	0.0103	127.84	12.70	10.07
150	0.0528	0.0106	132.98	12.70	10.47
155	0.0551	0.0110	137.97	12.71	10.86
160	0.0570	0.0114	142.58	12.72	11.21
165	0.0589	0.0118	146.94	12.72	11.55
170	0.0603	0.0121	151.00	12.72	11.87
175	0.0626	0.0125	154.67	12.73	12.15
180	0.0642	0.0128	158.41	12.73	12.44
185	0.0657	0.0131	162.08	12.74	12.72
190	0.0676	0.0135	165.43	12.74	12.98
195	0.0695	0.0139	168.86	12.75	13.25
200	0.0711	0.0142	172.06	12.75	13.49
205	0.0732	0.0146	175.10	12.76	13.73
210	0.0750	0.0150	177.99	12.76	13.95
215	0.0768	0.0154	181.03	12.77	14.18
220	0.0782	0.0156	183.68	12.77	14.38
225	0.0805	0.0161	186.41	12.78	14.59
230	0.0822	0.0164	189.06	12.78	14.79
235	0.0838	0.0168	191.25	12.78	14.96
240	0.0858	0.0172	193.12	12.79	15.10
245	0.0881	0.0176	194.60	12.80	15.21
250	0.0897	0.0179	195.61	12.80	15.28
255	0.0916	0.0183	196.24	12.80	15.33
260	0.0937	0.0187	196.47	12.81	15.34
265	0.0951	0.0190	195.69	12.81	15.27
270	0.0972	0.0194	195.38	12.82	15.24
275	0.0989	0.0198	193.98	12.82	15.13
280	0.1012	0.0202	192.18	12.83	14.98
285	0.1026	0.0205	190.62	12.83	14.85
290	0.1050	0.0210	188.59	12.84	14.69

Montour FGD #1**Initial Parameters**

Curing Duration	180-day
Date	3/22/2010
Diameter, in	4
Area, in²	12.57
Length, in	5
Ini mass, g	55.6
Fin mass, g	46.2
Moisture Content	20.3



Time,	Deformation,	Vertical Strain,	Load,	Corrected Area	Stress,
sec	ΔL , in	$\epsilon = \Delta L/L$	lb	$A_c = A_o/(1-\epsilon)$, in ²	σ , lb/in ²
0	0.0000	0.0000	0.16	12.57	0.01
5	0.0015	0.0003	5.30	12.57	0.42
10	0.0029	0.0006	13.34	12.58	1.06
15	0.0039	0.0008	22.15	12.58	1.76
20	0.0052	0.0010	32.60	12.58	2.59
25	0.0067	0.0013	40.56	12.59	3.22
30	0.0087	0.0017	44.61	12.59	3.54
35	0.0102	0.0020	47.58	12.60	3.78
40	0.0123	0.0025	51.95	12.60	4.12
45	0.0136	0.0027	59.20	12.60	4.70
50	0.0152	0.0030	67.08	12.61	5.32
55	0.0176	0.0035	75.66	12.61	6.00
60	0.0191	0.0038	84.24	12.62	6.68
65	0.0208	0.0042	92.74	12.62	7.35
70	0.0226	0.0045	100.61	12.63	7.97
75	0.0246	0.0049	108.57	12.63	8.59
80	0.0269	0.0054	116.14	12.64	9.19
85	0.0282	0.0056	122.92	12.64	9.72
90	0.0303	0.0061	129.47	12.65	10.24
95	0.0318	0.0064	135.48	12.65	10.71
100	0.0341	0.0068	140.94	12.66	11.14
105	0.0360	0.0072	146.71	12.66	11.59
110	0.0377	0.0075	152.48	12.67	12.04
115	0.0401	0.0080	157.79	12.67	12.45
120	0.0417	0.0083	163.17	12.68	12.87

125	0.0432	0.0086	168.08	12.68	13.26
130	0.0460	0.0092	172.53	12.69	13.60
135	0.0475	0.0095	176.89	12.69	13.94
140	0.0495	0.0099	180.79	12.70	14.24
145	0.0511	0.0102	184.30	12.70	14.51
150	0.0534	0.0107	187.42	12.71	14.75
155	0.0550	0.0110	190.31	12.71	14.97
160	0.0569	0.0114	192.73	12.71	15.16
165	0.0590	0.0118	195.30	12.72	15.35
170	0.0607	0.0121	197.02	12.72	15.48
175	0.0628	0.0126	198.66	12.73	15.61
180	0.0646	0.0129	199.90	12.73	15.70
185	0.0667	0.0133	201.15	12.74	15.79
190	0.0685	0.0137	201.70	12.74	15.83
195	0.0707	0.0141	202.24	12.75	15.86
200	0.0724	0.0145	202.48	12.75	15.87
205	0.0740	0.0148	202.17	12.76	15.85
210	0.0757	0.0151	202.09	12.76	15.83
215	0.0781	0.0156	201.54	12.77	15.78
220	0.0803	0.0161	200.92	12.78	15.73
225	0.0819	0.0164	199.98	12.78	15.65

Montour FGD #2
Initial Parameters

Curing Duration	180-day				
Date	3/22/2010				
Diameter, in	4				
Area, in²	12.57				
Length, in	5				
Ini mass, g	59.2				
Fin mass, g	48.6				
Moisture Content	21.8				
Time,	Deformation,	Vertical Strain,	Load,	Corrected Area	Stress,
sec	ΔL, in	$\epsilon = \Delta L/L$	lb	$A_c = A_o/(1-\epsilon)$, in²	σ, lb/in²
0	0.0000	0.0000	0.08	12.57	0.01
5	0.0011	0.0002	3.43	12.57	0.27
10	0.0028	0.0006	6.32	12.58	0.50
15	0.0049	0.0010	8.89	12.58	0.71
20	0.0065	0.0013	11.23	12.59	0.89
25	0.0082	0.0016	13.26	12.59	1.05
30	0.0101	0.0020	15.52	12.60	1.23
35	0.0119	0.0024	18.25	12.60	1.45
40	0.0134	0.0027	21.22	12.60	1.68
45	0.0154	0.0031	24.34	12.61	1.93
50	0.0169	0.0034	27.53	12.61	2.18
55	0.0189	0.0038	30.73	12.62	2.44
60	0.0209	0.0042	34.40	12.62	2.72
65	0.0226	0.0045	38.06	12.63	3.01
70	0.0246	0.0049	41.65	12.63	3.30
75	0.0263	0.0053	45.24	12.64	3.58
80	0.0279	0.0056	48.90	12.64	3.87
85	0.0302	0.0060	52.65	12.65	4.16
90	0.0318	0.0064	56.47	12.65	4.46
95	0.0335	0.0067	60.29	12.65	4.76
100	0.0351	0.0070	64.04	12.66	5.06
105	0.0372	0.0074	68.17	12.66	5.38
110	0.0389	0.0078	71.83	12.67	5.67
115	0.0404	0.0081	75.81	12.67	5.98

120	0.0427	0.0085	79.71	12.68	6.29
125	0.0446	0.0089	83.30	12.68	6.57
130	0.0458	0.0092	87.12	12.69	6.87
135	0.0483	0.0097	90.71	12.69	7.15
140	0.0500	0.0100	94.22	12.70	7.42
145	0.0522	0.0104	97.34	12.70	7.66
150	0.0535	0.0107	100.69	12.71	7.92
155	0.0559	0.0112	103.50	12.71	8.14
160	0.0577	0.0115	106.46	12.72	8.37
165	0.0591	0.0118	109.43	12.72	8.60
170	0.0613	0.0123	112.08	12.73	8.81
175	0.0630	0.0126	114.81	12.73	9.02
180	0.0648	0.0130	117.31	12.74	9.21
185	0.0670	0.0134	119.72	12.74	9.40
190	0.0686	0.0137	121.91	12.74	9.57
195	0.0703	0.0141	124.01	12.75	9.73
200	0.0725	0.0145	125.65	12.75	9.85
205	0.0744	0.0149	127.52	12.76	9.99
210	0.0760	0.0152	128.85	12.76	10.09
215	0.0780	0.0156	130.10	12.77	10.19
220	0.0799	0.0160	131.19	12.77	10.27
225	0.0818	0.0164	131.89	12.78	10.32
230	0.0838	0.0168	132.36	12.78	10.35
235	0.0857	0.0171	132.75	12.79	10.38
240	0.0872	0.0174	132.98	12.79	10.39
245	0.0891	0.0178	132.83	12.80	10.38
250	0.0908	0.0182	133.22	12.80	10.41
255	0.0932	0.0186	132.90	12.81	10.38
260	0.0944	0.0189	132.83	12.81	10.37
265	0.0972	0.0194	132.83	12.82	10.36
270	0.0986	0.0197	132.51	12.82	10.33
275	0.1006	0.0201	132.12	12.83	10.30
280	0.1026	0.0205	131.73	12.83	10.26
285	0.1042	0.0208	131.27	12.84	10.23
290	0.1062	0.0212	130.25	12.84	10.14

Montour FGD #3
Initial Parameters

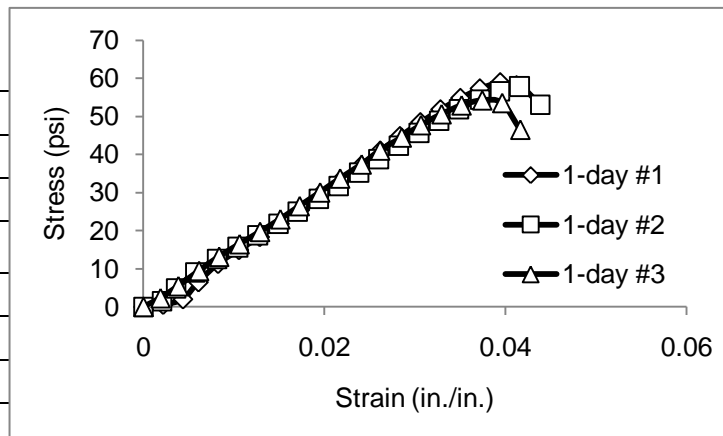
Curing Duration	180-day
Date	3/22/2010
Diameter, in	4
Area, in²	12.57
Length, in	5
Ini mass, g	56
Fin mass, g	46
Moisture Content	21.7

Time,	Deformation,	Vertical Strain,	Load,	Corrected Area	Stress,
sec	ΔL, in	$\epsilon = \Delta L/L$	lb	$A_c = A_o/(1-\epsilon)$, in²	σ, lb/in²
0	0.0000	0.0000	1.09	12.57	0.09
5	0.0009	0.0002	3.98	12.57	0.32
10	0.0026	0.0005	6.01	12.58	0.48
15	0.0042	0.0008	8.74	12.58	0.69
20	0.0060	0.0012	14.20	12.59	1.13
25	0.0076	0.0015	22.62	12.59	1.80
30	0.0090	0.0018	34.16	12.59	2.71
35	0.0105	0.0021	46.17	12.60	3.67
40	0.0121	0.0024	56.00	12.60	4.44
45	0.0138	0.0028	63.02	12.60	5.00
50	0.0157	0.0031	68.95	12.61	5.47
55	0.0176	0.0035	74.41	12.61	5.90
60	0.0196	0.0039	80.02	12.62	6.34
65	0.0210	0.0042	86.03	12.62	6.82
70	0.0228	0.0046	92.66	12.63	7.34
75	0.0244	0.0049	99.37	12.63	7.87
80	0.0268	0.0054	106.00	12.64	8.39
85	0.0282	0.0056	112.55	12.64	8.90
90	0.0304	0.0061	118.63	12.65	9.38
95	0.0319	0.0064	124.72	12.65	9.86
100	0.0337	0.0067	130.49	12.66	10.31
105	0.0362	0.0072	136.18	12.66	10.76
110	0.0377	0.0075	141.48	12.67	11.17
115	0.0397	0.0079	146.79	12.67	11.59
120	0.0414	0.0083	151.70	12.67	11.97
125	0.0435	0.0087	156.54	12.68	12.35

130	0.0450	0.0090	161.37	12.68	12.72
135	0.0470	0.0094	165.43	12.69	13.04
140	0.0489	0.0098	169.64	12.69	13.36
145	0.0506	0.0101	173.38	12.70	13.65
150	0.0526	0.0105	176.74	12.70	13.91
155	0.0545	0.0109	179.62	12.71	14.13
160	0.0563	0.0113	182.20	12.71	14.33
165	0.0578	0.0116	184.15	12.72	14.48
170	0.0602	0.0120	186.18	12.72	14.63
175	0.0620	0.0124	188.44	12.73	14.81
180	0.0634	0.0127	190.08	12.73	14.93
185	0.0653	0.0131	191.87	12.74	15.06
190	0.0678	0.0136	192.88	12.74	15.14
195	0.0697	0.0139	193.51	12.75	15.18
200	0.0715	0.0143	193.59	12.75	15.18
205	0.0730	0.0146	193.74	12.76	15.19
210	0.0747	0.0149	193.35	12.76	15.15
215	0.0769	0.0154	192.65	12.77	15.09
220	0.0787	0.0157	192.10	12.77	15.04
225	0.0808	0.0162	190.93	12.78	14.94
230	0.0820	0.0164	190.00	12.78	14.87

Seward FBC #1
Initial Parameters

Curing Duration	1-day
Date	10/20/2009
Diameter, in	4
Area, in²	12.57
Length, in	5
Ini mass, g	41.7
Fin mass, g	37.3
Moisture Content	11.8



Time,	Deformation,	Vertical Strain,	Load,	Corrected Area	Stress,
sec	ΔL , in	$\epsilon = \Delta L/L$	lb	$A_c = A_o/(1-\epsilon)$, in ²	σ , lb/in ²
0	0.0000	0.0000	0.00	12.57	0.00
30	0.0109	0.0022	7.10	12.60	0.56
60	0.0218	0.0044	25.50	12.63	2.02
90	0.0304	0.0061	81.97	12.65	6.48
120	0.0412	0.0082	143.12	12.67	11.29
150	0.0527	0.0105	189.61	12.70	14.93
180	0.0643	0.0129	233.60	12.73	18.35
210	0.0752	0.0150	278.52	12.76	21.82
240	0.0865	0.0173	325.71	12.79	25.46
270	0.0971	0.0194	374.85	12.82	29.24
300	0.1087	0.0217	425.39	12.85	33.11
330	0.1204	0.0241	477.02	12.88	37.04
360	0.1309	0.0262	528.73	12.91	40.96
390	0.1418	0.0284	579.35	12.94	44.78
420	0.1531	0.0306	628.02	12.97	48.43
450	0.1642	0.0328	673.23	13.00	51.80
480	0.1752	0.0350	713.74	13.03	54.79
510	0.1859	0.0372	748.06	13.06	57.30
540	0.1972	0.0394	770.99	13.09	58.92
570	0.2062	0.0412	761.94	13.11	58.12

Seward FBC #2
Initial Parameters

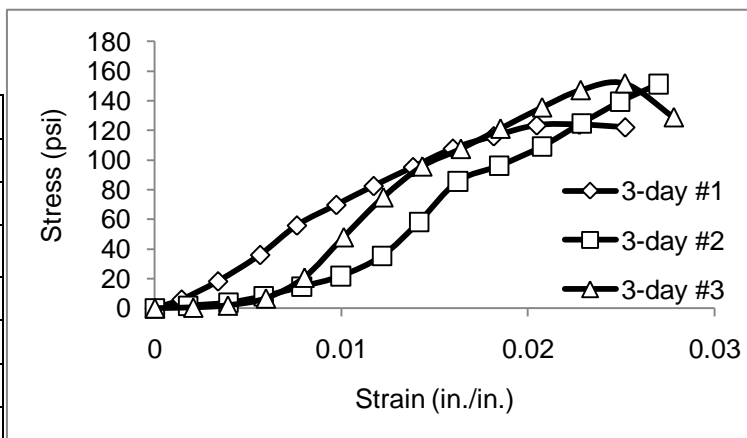
Curing Duration	1-day				
Date	10/20/2009				
Diameter, in	4				
Area, in²	12.57				
Length, in	5				
Ini mass, g	41.5				
Fin mass, g	37.1				
Moisture Content	11.9				
Time,	Deformation,	Vertical Strain,	Load,	Corrected Area	Stress,
sec	ΔL, in	ε = ΔL/L	lb	Ac = Ao/(1-ε), in²	σ, lb/in²
0	0.0000	0.0000	0.00	12.57	0.00
30	0.0103	0.0021	19.42	12.60	1.54
60	0.0182	0.0036	60.52	12.62	4.80
90	0.0286	0.0057	114.11	12.64	9.03
120	0.0406	0.0081	159.03	12.67	12.55
150	0.0523	0.0105	199.36	12.70	15.69
180	0.0632	0.0126	238.67	12.73	18.75
210	0.0746	0.0149	279.07	12.76	21.87
240	0.0854	0.0171	320.80	12.79	25.09
270	0.0970	0.0194	363.93	12.82	28.39
300	0.1080	0.0216	408.31	12.85	31.78
330	0.1193	0.0239	453.94	12.88	35.25
360	0.1300	0.0260	500.50	12.91	38.78
390	0.1410	0.0282	546.83	12.93	42.28
420	0.1523	0.0305	592.22	12.96	45.68
450	0.1633	0.0327	635.67	12.99	48.92
480	0.1744	0.0349	675.37	13.02	51.85
510	0.1861	0.0372	711.29	13.06	54.48
540	0.1969	0.0394	741.19	13.09	56.64
570	0.2078	0.0416	759.21	13.12	57.89
600	0.2192	0.0438	698.06	13.15	53.10

Seward FBC #3
Initial Parameters

Curing Duration	1-day				
Date	10/20/2009				
Diameter, in	4				
Area, in²	12.57				
Length, in	5				
Ini mass, g	41.9				
Fin mass, g	37.1				
Moisture Content	12.9				
Time,	Deformation,	Vertical Strain,	Load,	Corrected Area	Stress,
sec	ΔL, in	ε = ΔL/L	lb	Ac = Ao/(1-ε), in²	σ, lb/in²
0	0.0000	0.0000	0.00	12.57	0.00
30	0.0094	0.0019	28.86	12.59	2.29
60	0.0193	0.0039	68.71	12.62	5.45
90	0.0307	0.0061	119.33	12.65	9.43
120	0.0418	0.0084	166.76	12.68	13.16
150	0.0531	0.0106	209.08	12.70	16.46
180	0.0644	0.0129	250.60	12.73	19.68
210	0.0757	0.0151	293.50	12.76	23.00
240	0.0863	0.0173	338.27	12.79	26.45
270	0.0976	0.0195	385.07	12.82	30.04
300	0.1087	0.0217	432.88	12.85	33.69
330	0.1206	0.0241	481.39	12.88	37.37
360	0.1308	0.0262	529.59	12.91	41.03
390	0.1428	0.0286	575.06	12.94	44.44
420	0.1534	0.0307	618.35	12.97	47.68
450	0.1648	0.0330	657.04	13.00	50.55
480	0.1758	0.0352	688.78	13.03	52.87
510	0.1873	0.0375	707.66	13.06	54.19
540	0.1983	0.0397	700.09	13.09	53.49
570	0.2083	0.0417	609.62	13.12	46.48

Seward FBC #1
Initial Parameters

Curing Duration	3-day
Date	10/23/2009
Diameter, in	4
Area, in²	12.57
Length, in	5
Ini mass, g	37.5
Fin mass, g	34.1
Moisture Content	10.0



Time,	Deformation,	Vertical Strain,	Load,	Corrected Area	Stress,
sec	ΔL , in	$\epsilon = \Delta L/L$	lb	$A_c = A_o/(1-\epsilon)$, in ²	σ , lb/in ²
0	0.0000	0.0000	0.00	12.57	0.00
30	0.0072	0.0014	74.49	12.59	5.92
60	0.0169	0.0034	229.54	12.61	18.20
90	0.0282	0.0056	455.18	12.64	36.01
120	0.0381	0.0076	708.12	12.67	55.90
150	0.0487	0.0097	885.88	12.69	69.79
180	0.0587	0.0117	1050.10	12.72	82.56
210	0.0693	0.0139	1214.90	12.75	95.31
240	0.0799	0.0160	1377.00	12.77	107.80
270	0.0909	0.0182	1487.10	12.80	116.16
300	0.1024	0.0205	1585.30	12.83	123.53
330	0.1139	0.0228	1594.30	12.86	123.95
360	0.1262	0.0252	1575.00	12.90	122.14

Seward FBC #2
Initial Parameters

Curing Duration	3-day				
Date	10/23/2009				
Diameter, in	4				
Area, in²	12.57				
Length, in	5				
Ini mass, g	44.8				
Fin mass, g	39.9				
Moisture Content	12.3				
Time,	Deformation,	Vertical Strain,	Load,	Corrected Area	Stress,
sec	ΔL, in	$\epsilon = \Delta L/L$	lb	$A_c = A_o/(1-\epsilon)$, in²	σ, lb/in²
0	0.0000	0.0000	0.00	12.57	0.00
30	0.0089	0.0018	21.22	12.59	1.68
60	0.0197	0.0039	46.95	12.62	3.72
90	0.0292	0.0058	102.64	12.64	8.12
120	0.0394	0.0079	183.68	12.67	14.50
150	0.0499	0.0100	275.48	12.70	21.70
180	0.0610	0.0122	449.88	12.73	35.35
210	0.0709	0.0142	742.68	12.75	58.25
240	0.0813	0.0163	1093.70	12.78	85.59
270	0.0924	0.0185	1230.90	12.81	96.11
300	0.1039	0.0208	1402.00	12.84	109.22
330	0.1144	0.0229	1606.40	12.86	124.87
360	0.1247	0.0249	1794.70	12.89	139.22
390	0.1350	0.0270	1954.30	12.92	151.28

Seward FBC #3
Initial Parameters

Curing Duration	3-day				
Date	10/23/2009				
Diameter, in	4				
Area, in²	12.57				
Length, in	5				
Ini mass, g	46.4				
Fin mass, g	41				
Moisture Content	13.2				
Time,	Deformation,	Vertical Strain,	Load,	Corrected Area	Stress,
sec	ΔL, in	$\epsilon = \Delta L/L$	lb	$A_c = A_o/(1-\epsilon)$, in²	σ, lb/in²
0	0.0000	0.0000	0.00	12.57	0.00
30	0.0103	0.0021	6.47	12.60	0.51
60	0.0196	0.0039	24.26	12.62	1.92
90	0.0298	0.0060	84.63	12.65	6.69
120	0.0401	0.0080	262.69	12.67	20.73
150	0.0506	0.0101	609.62	12.70	48.01
180	0.0613	0.0123	953.50	12.73	74.93
210	0.0717	0.0143	1221.30	12.75	95.77
240	0.0820	0.0164	1375.00	12.78	107.59
270	0.0927	0.0185	1552.70	12.81	121.24
300	0.1038	0.0208	1740.60	12.84	135.60
330	0.1141	0.0228	1894.20	12.86	147.25
360	0.1260	0.0252	1957.80	12.89	151.83
390	0.1391	0.0278	1667.30	12.93	128.95

Seward FBC**Initial Parameters**

Curing Duration	7-day
Date	10/27/2009
Diameter, in	4
Area, in²	12.57
Length, in	5
Ini mass, g	48.9
Fin mass, g	43.5
Moisture Content	12.4

		Load, lb	Stress, σ, lb/in²
Note: loaded between 1 psi/sec and 3 psi/sec	Sample #1	15060.00	1198.09
	Sample #2	17420.00	1385.84
	Sample #3	13970.00	1111.38

Seward FBC**Initial Parameters**

Curing Duration	14-day
Date	11/2/2009
Diameter, in	4
Area, in²	12.57
Length, in	5
Ini mass, g	43.4
Fin mass, g	39
Moisture Content	11.3

		Load, lb	Stress, σ, lb/in²
Note: loaded between 1 psi/sec and 3 psi/sec	Sample #1	15370.00	1222.75
	Sample #2	18610.00	1480.51
	Sample #3	16840.00	1339.70

Seward FBC**Initial Parameters**

Curing Duration	28-day
Date	11/16/2009
Diameter, in	4
Area, in²	12.57
Length, in	5
Ini mass, g	47.5
Fin mass, g	42.3
Moisture Content	12.3

	Load, lb	Stress, σ, lb/in²
Note: loaded between 1 psi/sec and 3 psi/sec	Sample #1	19710.00 1568.02
	Sample #2	22040.00 1753.38
	Sample #3	20080.00 1597.45

Seward FBC**Initial Parameters**

Curing Duration	56-day
Date	12/14/2009
Diameter, in	4
Area, in²	12.57
Length, in	5
Ini mass, g	68.7
Fin mass, g	61.7
Moisture Content	11.3

	Load, lb	Stress, σ, lb/in²
Note: loaded between 1 psi/sec and 3 psi/sec	Sample #1	17910.00 1424.82
	Sample #2	22340.00 1777.25
	Sample #3	16610.00 1321.40

Irregular Surface

Seward FBC**Initial Parameters**

Curing Duration	90-day
Date	1/18/2010
Diameter, in	4
Area, in²	12.57
Length, in	5
Ini mass, g	59.2
Fin mass, g	52.1
Moisture Content	13.6

		Load, lb	Stress, σ, lb/in²
Note: loaded between 1 psi/sec and 3 psi/sec	Sample #1	26910.00	2140.81
	Sample #2	27820.00	2213.21
	Sample #3	28630.00	2277.65

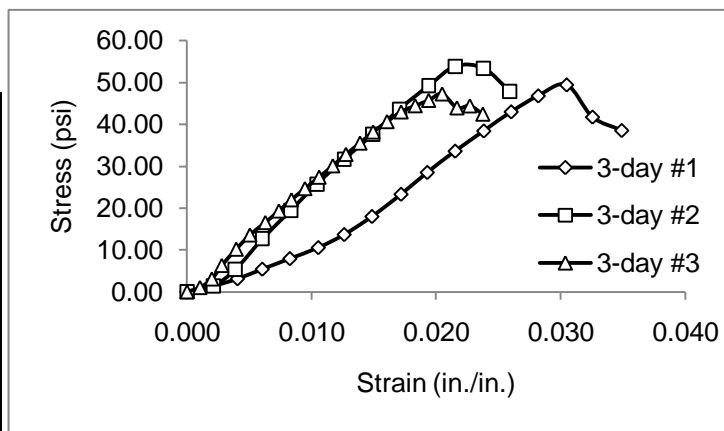
Seward FBC**Initial Parameters**

Curing Duration	180-day
Date	4/19/2010
Diameter, in	4
Area, in²	12.57
Length, in	5
Ini mass, g	56.6
Fin mass, g	52.8
Moisture Content	7.2

		Load, lb	Stress, σ, lb/in²
Note: loaded between 1 psi/sec and 3 psi/sec	Sample #1	33520.00	2666.67
	Sample #2	22430.00	1784.41
	Sample #3	28230.00	2245.82

Montour Class F #1**Initial Parameters**

Curing Duration	3-day
Date	12/4/2009
Diameter, in	4
Area, in²	12.57
Length, in	5
Ini mass, g	50.9
Fin mass, g	46.2
Moisture Content	10.2



Time,	Deformation	Vertical Strain,	Load,	Corrected Area	Stress,
sec	ΔL, in	$\epsilon = \Delta L/L$	lb	$A_c = A_o/(1-\epsilon)$, in²	σ, lb/in²
0	0.0000	0.0000	0.70	12.57	0.06
30	0.0104	0.0021	17.71	12.60	1.41
60	0.0202	0.0040	39.78	12.62	3.15
90	0.0302	0.0060	68.95	12.65	5.45
120	0.0413	0.0083	101.00	12.67	7.97
150	0.0527	0.0105	134.70	12.70	10.60
180	0.0631	0.0126	174.71	12.73	13.72
210	0.0742	0.0148	230.17	12.76	18.04
240	0.0859	0.0172	298.65	12.79	23.35
270	0.0964	0.0193	366.11	12.82	28.56
300	0.1076	0.0215	432.41	12.85	33.66
330	0.1191	0.0238	495.59	12.88	38.49
360	0.1301	0.0260	555.72	12.91	43.06
390	0.1410	0.0282	606.34	12.93	46.88
420	0.1524	0.0305	641.83	12.97	49.50
450	0.1628	0.0326	543.16	12.99	41.80
480	0.1745	0.0349	502.76	13.02	38.60

Montour Class F #2**Initial Parameters**

Curing Duration	3-day
Date	12/4/2009
Diameter, in	4
Area, in²	12.57
Length, in	5
Ini mass, g	47.6
Fin mass, g	43.5
Moisture Content	9.4

Time,	Deformation,	Vertical Strain,	Load,	Corrected Area	Stress,
sec	ΔL, in	$\epsilon = \Delta L/L$	lb	$A_c = A_o/(1-\epsilon)$, in²	σ, lb/in²
0	0.0000	0.0000	0.70	12.57	0.06
30	0.0105	0.0021	18.64	12.60	1.48
60	0.0193	0.0039	67.31	12.62	5.33
90	0.0302	0.0060	160.28	12.65	12.67
120	0.0417	0.0083	247.40	12.68	19.52
150	0.0521	0.0104	327.43	12.70	25.78
180	0.0631	0.0126	403.86	12.73	31.72
210	0.0747	0.0149	480.92	12.76	37.69
240	0.0853	0.0171	558.68	12.79	43.69
270	0.0971	0.0194	631.22	12.82	49.24
300	0.1078	0.0216	692.68	12.85	53.92
330	0.1191	0.0238	687.77	12.88	53.41
360	0.1296	0.0259	618.66	12.90	47.94

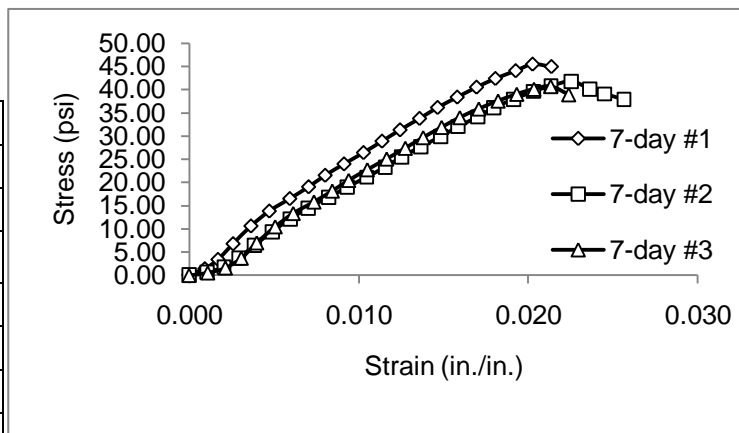
Montour Class F #3**Initial Parameters**

Curing Duration	3-day
Date	12/4/2009
Diameter, in	4
Area, in²	12.57
Length, in	5
Ini mass, g	51.9
Fin mass, g	47
Moisture Content	10.4

Time,	Deformation,	Vertical Strain,	Load,	Corrected Area	Stress,
sec	ΔL, in	$\epsilon = \Delta L/L$	lb	$A_c = A_o/(1-\epsilon)$, in²	σ, lb/in²
0	0.0000	0.0000	0.78	12.57	0.06
15	0.0052	0.0010	13.57	12.58	1.08
30	0.0100	0.0020	39.47	12.60	3.13
45	0.0139	0.0028	80.10	12.61	6.35
60	0.0197	0.0039	129.24	12.62	10.24
75	0.0252	0.0050	172.29	12.63	13.64
90	0.0314	0.0063	210.12	12.65	16.61
105	0.0369	0.0074	245.22	12.66	19.36
120	0.0419	0.0084	279.30	12.68	22.03
135	0.0473	0.0095	313.54	12.69	24.71
150	0.0530	0.0106	348.56	12.70	27.44
165	0.0585	0.0117	383.51	12.72	30.15
180	0.0637	0.0127	418.60	12.73	32.88
195	0.0694	0.0139	453.55	12.75	35.58
210	0.0747	0.0149	487.86	12.76	38.23
225	0.0803	0.0161	520.08	12.78	40.71
240	0.0859	0.0172	550.26	12.79	43.02
255	0.0916	0.0183	569.84	12.80	44.50
270	0.0970	0.0194	586.76	12.82	45.77
285	0.1024	0.0205	607.20	12.83	47.32
300	0.1083	0.0217	565.16	12.85	43.99
315	0.1135	0.0227	571.94	12.86	44.47
330	0.1187	0.0237	547.06	12.88	42.49

Montour Class F #1**Initial Parameters**

Curing Duration	7-day
Date	12/7/2009
Diameter, in	4
Area, in²	12.57
Length, in	5
Ini mass, g	54.5
Fin mass, g	49.4
Moisture Content	10.3



Time,	Deformation	Vertical Strain,	Load,	Corrected Area	Stress,
sec	ΔL, in	$\epsilon = \Delta L/L$	lb	$A_c = A_o/(1-\epsilon)$, in²	σ, lb/in²
0	0.0000	0.0000	0.86	12.57	0.07
15	0.0046	0.0009	17.32	12.58	1.38
30	0.0085	0.0017	42.51	12.59	3.38
45	0.0130	0.0026	85.33	12.60	6.77
60	0.0182	0.0036	133.76	12.62	10.60
75	0.0236	0.0047	174.55	12.63	13.82
90	0.0297	0.0059	208.64	12.65	16.50
105	0.0352	0.0070	241.16	12.66	19.05
120	0.0401	0.0080	272.75	12.67	21.52
135	0.0457	0.0091	304.26	12.69	23.98
150	0.0514	0.0103	335.62	12.70	26.43
165	0.0569	0.0114	367.36	12.71	28.89
180	0.0622	0.0124	398.79	12.73	31.33
195	0.0679	0.0136	430.54	12.74	33.79
210	0.0732	0.0146	461.19	12.76	36.15
225	0.0790	0.0158	490.28	12.77	38.39
240	0.0847	0.0169	518.28	12.79	40.53
255	0.0903	0.0181	542.77	12.80	42.40
270	0.0962	0.0192	565.00	12.82	44.08
285	0.1012	0.0202	583.80	12.83	45.50
300	0.1068	0.0214	577.64	12.84	44.97

Montour Class F #2**Initial Parameters**

Curing Duration	7-day
Date	12/7/2009
Diameter, in	4
Area, in²	12.57
Length, in	5
Ini mass, g	68.3
Fin mass, g	60.9
Moisture Content	12.2

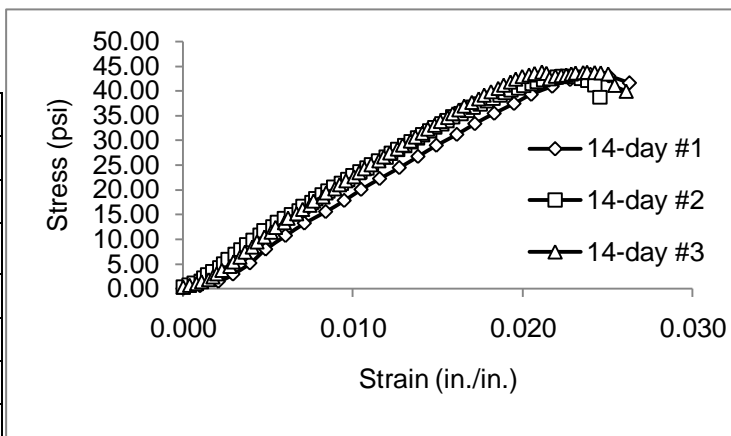
Time,	Deformation,	Vertical Strain,	Load,	Corrected Area	Stress,
sec	ΔL, in	$\varepsilon = \Delta L/L$	lb	$A_c = A_o/(1-\varepsilon)$, in²	σ, lb/in²
0	0.0000	0.0000	0.94	12.57	0.07
15	0.0053	0.0011	8.27	12.58	0.66
30	0.0102	0.0020	21.76	12.60	1.73
45	0.0146	0.0029	46.72	12.61	3.71
60	0.0192	0.0038	81.04	12.62	6.42
75	0.0246	0.0049	118.63	12.63	9.39
90	0.0297	0.0059	152.87	12.65	12.09
105	0.0351	0.0070	183.68	12.66	14.51
120	0.0412	0.0082	212.77	12.67	16.79
135	0.0466	0.0093	240.85	12.69	18.98
150	0.0524	0.0105	268.77	12.70	21.16
165	0.0578	0.0116	296.77	12.72	23.34
180	0.0627	0.0125	324.70	12.73	25.51
195	0.0683	0.0137	353.09	12.74	27.71
210	0.0742	0.0148	381.63	12.76	29.91
225	0.0793	0.0159	409.24	12.77	32.04
240	0.0850	0.0170	436.39	12.79	34.13
255	0.0898	0.0180	462.36	12.80	36.12
270	0.0957	0.0191	486.46	12.82	37.96
285	0.1015	0.0203	508.38	12.83	39.62
300	0.1067	0.0213	524.76	12.84	40.86
315	0.1127	0.0225	537.47	12.86	41.79
330	0.1182	0.0236	517.11	12.87	40.17
345	0.1226	0.0245	503.70	12.89	39.09
360	0.1283	0.0257	488.72	12.90	37.88

Montour Class F #3**Initial Parameters**

Curing Duration	7-day				
Date	12/7/2009				
Diameter, in	4				
Area, in²	12.57				
Length, in	5				
Ini mass, g	61.8				
Fin mass, g	55.3				
Moisture Content	11.8				
Time,	Deformation,	Vertical Strain,	Load,	Corrected Area	Stress,
sec	ΔL, in	$\epsilon = \Delta L/L$	lb	$A_c = A_o/(1-\epsilon)$, in²	σ, lb/in²
0	0.0000	0.0000	0.08	12.57	0.01
15	0.0055	0.0011	6.94	12.58	0.55
30	0.0107	0.0021	20.44	12.60	1.62
45	0.0154	0.0031	47.03	12.61	3.73
60	0.0200	0.0040	88.76	12.62	7.03
75	0.0254	0.0051	132.67	12.63	10.50
90	0.0307	0.0061	169.09	12.65	13.37
105	0.0369	0.0074	200.68	12.66	15.85
120	0.0423	0.0085	230.79	12.68	18.21
135	0.0471	0.0094	260.12	12.69	20.50
150	0.0526	0.0105	289.68	12.70	22.80
165	0.0583	0.0117	319.31	12.72	25.11
180	0.0638	0.0128	349.27	12.73	27.43
195	0.0691	0.0138	378.83	12.75	29.72
210	0.0745	0.0149	407.37	12.76	31.93
225	0.0799	0.0160	434.75	12.77	34.03
240	0.0855	0.0171	459.08	12.79	35.90
255	0.0912	0.0182	481.47	12.80	37.60
270	0.0967	0.0193	500.73	12.82	39.07
285	0.1018	0.0204	515.08	12.83	40.14
300	0.1067	0.0213	523.20	12.84	40.73
315	0.1120	0.0224	500.89	12.86	38.96

Montour Class F #1**Initial Parameters**

Curing Duration	14-day
Date	12/14/2009
Diameter, in	4
Area, in²	12.57
Length, in	5
Ini mass, g	65.1
Fin mass, g	58.2
Moisture Content	11.9



Time,	Deformation,	Vertical Strain,	Load,	Corrected Area	Stress,
sec	ΔL , in	$\epsilon = \Delta L/L$	lb	$A_c = A_o/(1-\epsilon)$, in ²	σ , lb/in ²
0	0.0000	0.0000	0.16	12.57	0.01
15	0.0049	0.0010	6.94	12.58	0.55
30	0.0103	0.0021	18.25	12.60	1.45
45	0.0146	0.0029	36.66	12.61	2.91
60	0.0196	0.0039	65.05	12.62	5.15
75	0.0243	0.0049	100.61	12.63	7.97
90	0.0301	0.0060	135.56	12.65	10.72
105	0.0357	0.0071	167.53	12.66	13.23
120	0.0419	0.0084	197.41	12.68	15.57
135	0.0474	0.0095	226.19	12.69	17.82
150	0.0524	0.0105	254.89	12.70	20.07
165	0.0578	0.0116	283.12	12.72	22.26
180	0.0636	0.0127	311.75	12.73	24.49
195	0.0691	0.0138	340.92	12.75	26.75
210	0.0745	0.0149	370.01	12.76	29.00
225	0.0805	0.0161	398.64	12.78	31.20
240	0.0859	0.0172	427.03	12.79	33.39
255	0.0916	0.0183	454.25	12.80	35.48
270	0.0974	0.0195	480.38	12.82	37.47
285	0.1025	0.0205	504.55	12.83	39.32
300	0.1086	0.0217	526.16	12.85	40.95
315	0.1139	0.0228	544.41	12.86	42.32
330	0.1199	0.0240	558.29	12.88	43.35
345	0.1253	0.0251	554.71	12.89	43.02
360	0.1314	0.0263	537.70	12.91	41.65

Montour Class F #2**Initial Parameters**

Curing Duration	14-day				
Date	12/14/2009				
Diameter, in	4				
Area, in²	12.57				
Length, in	5				
Ini mass, g	68.3				
Fin mass, g	60.9				
Moisture Content	12.2				
Time,	Deformation,	Vertical Strain,	Load,	Corrected Area	Stress,
sec	ΔL, in	$\epsilon = \Delta L/L$	lb	$A_c = A_o/(1-\epsilon)$, in²	σ, lb/in²
0	0.0000	0.0000	3.82	12.57	0.30
5	0.0017	0.0003	8.74	12.57	0.69
10	0.0033	0.0007	13.65	12.58	1.09
15	0.0054	0.0011	19.73	12.58	1.57
20	0.0061	0.0012	26.75	12.59	2.13
25	0.0072	0.0014	34.71	12.59	2.76
30	0.0087	0.0017	43.44	12.59	3.45
35	0.0108	0.0022	52.80	12.60	4.19
40	0.0120	0.0024	63.72	12.60	5.06
45	0.0132	0.0026	75.11	12.60	5.96
50	0.0153	0.0031	87.51	12.61	6.94
55	0.0170	0.0034	99.84	12.61	7.92
60	0.0187	0.0037	112.24	12.62	8.90
65	0.0206	0.0041	124.56	12.62	9.87
70	0.0226	0.0045	136.26	12.63	10.79
75	0.0238	0.0048	147.65	12.63	11.69
80	0.0265	0.0053	158.72	12.64	12.56
85	0.0277	0.0055	169.33	12.64	13.40
90	0.0299	0.0060	179.78	12.65	14.22
95	0.0318	0.0064	190.15	12.65	15.03
100	0.0341	0.0068	200.14	12.66	15.81
105	0.0353	0.0071	210.43	12.66	16.62
110	0.0379	0.0076	220.65	12.67	17.42
115	0.0391	0.0078	230.48	12.67	18.19
120	0.0410	0.0082	240.70	12.67	18.99
125	0.0426	0.0085	250.52	12.68	19.76

130	0.0444	0.0089	260.51	12.68	20.54
135	0.0466	0.0093	270.41	12.69	21.31
140	0.0485	0.0097	280.39	12.69	22.09
145	0.0501	0.0100	290.14	12.70	22.85
150	0.0521	0.0104	300.13	12.70	23.63
155	0.0542	0.0108	309.96	12.71	24.39
160	0.0555	0.0111	319.47	12.71	25.13
165	0.0575	0.0115	329.61	12.72	25.92
170	0.0598	0.0120	339.36	12.72	26.67
175	0.0612	0.0122	348.95	12.73	27.42
180	0.0633	0.0127	358.94	12.73	28.19
185	0.0653	0.0131	368.92	12.74	28.97
190	0.0671	0.0134	378.28	12.74	29.69
195	0.0690	0.0138	388.19	12.75	30.46
200	0.0706	0.0141	397.62	12.75	31.19
205	0.0726	0.0145	406.83	12.76	31.90
210	0.0742	0.0148	416.50	12.76	32.64
215	0.0762	0.0152	425.86	12.76	33.36
220	0.0778	0.0156	434.75	12.77	34.05
225	0.0794	0.0159	443.95	12.77	34.76
230	0.0818	0.0164	453.00	12.78	35.45
235	0.0838	0.0168	461.19	12.78	36.07
240	0.0854	0.0171	469.92	12.79	36.75
245	0.0875	0.0175	478.04	12.79	37.36
250	0.0895	0.0179	485.91	12.80	37.96
255	0.0912	0.0182	493.79	12.80	38.57
260	0.0933	0.0187	500.97	12.81	39.11
265	0.0948	0.0190	507.91	12.81	39.64
270	0.0965	0.0193	514.93	12.82	40.17
275	0.0987	0.0197	521.32	12.82	40.65
280	0.1004	0.0201	527.49	12.83	41.12
285	0.1027	0.0205	533.41	12.83	41.56
290	0.1043	0.0209	538.33	12.84	41.93
295	0.1061	0.0212	542.93	12.84	42.28
300	0.1084	0.0217	546.91	12.85	42.57
305	0.1100	0.0220	550.03	12.85	42.79
310	0.1117	0.0223	552.05	12.86	42.94
315	0.1134	0.0227	552.99	12.86	43.00
320	0.1154	0.0231	551.66	12.87	42.87

325	0.1174	0.0235	548.08	12.87	42.58
330	0.1192	0.0238	542.38	12.88	42.12
335	0.1213	0.0243	531.31	12.88	41.24
340	0.1228	0.0246	499.17	12.89	38.74

Montour Class F #3

Initial Parameters

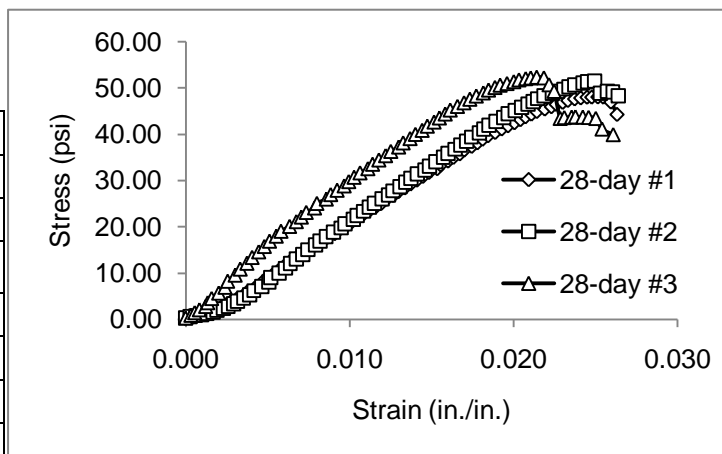
Curing Duration	14-day				
Date	12/14/2009				
Diameter, in	4				
Area, in²	12.57				
Length, in	5				
Ini mass, g	68.1				
Fin mass, g	60.7				
Moisture Content	12.2				
Time,	Deformation,	Vertical Strain,	Load,	Corrected Area	Stress,
sec	ΔL, in	$\epsilon = \Delta L/L$	lb	$A_c = A_o/(1-\epsilon)$, in²	σ, lb/in²
0	0.0000	0.0000	4.60	12.57	0.37
5	0.0019	0.0004	9.28	12.57	0.74
10	0.0039	0.0008	13.57	12.58	1.08
15	0.0054	0.0011	18.25	12.58	1.45
20	0.0075	0.0015	23.63	12.59	1.88
25	0.0088	0.0018	30.57	12.59	2.43
30	0.0099	0.0020	38.45	12.59	3.05
35	0.0114	0.0023	47.27	12.60	3.75
40	0.0137	0.0027	57.41	12.60	4.55
45	0.0148	0.0030	68.79	12.61	5.46
50	0.0167	0.0033	80.88	12.61	6.41
55	0.0182	0.0036	93.91	12.62	7.44
60	0.0203	0.0041	106.78	12.62	8.46
65	0.0217	0.0043	119.80	12.62	9.49
70	0.0239	0.0048	132.67	12.63	10.50
75	0.0259	0.0052	144.84	12.64	11.46
80	0.0272	0.0054	157.01	12.64	12.42
85	0.0298	0.0060	169.09	12.65	13.37
90	0.0309	0.0062	180.64	12.65	14.28
95	0.0334	0.0067	192.10	12.65	15.18

100	0.0352	0.0070	203.41	12.66	16.07
105	0.0373	0.0075	214.10	12.66	16.91
110	0.0384	0.0077	224.86	12.67	17.75
115	0.0412	0.0082	235.63	12.67	18.59
120	0.0421	0.0084	245.92	12.68	19.40
125	0.0447	0.0089	256.37	12.68	20.21
130	0.0460	0.0092	266.98	12.69	21.04
135	0.0479	0.0096	277.28	12.69	21.85
140	0.0503	0.0101	287.65	12.70	22.65
145	0.0518	0.0104	298.26	12.70	23.48
150	0.0534	0.0107	308.40	12.71	24.27
155	0.0553	0.0111	318.77	12.71	25.08
160	0.0576	0.0115	329.06	12.72	25.88
165	0.0591	0.0118	339.13	12.72	26.66
170	0.0608	0.0122	349.58	12.72	27.47
175	0.0631	0.0126	359.72	12.73	28.26
180	0.0646	0.0129	370.01	12.73	29.06
185	0.0669	0.0134	380.46	12.74	29.86
190	0.0684	0.0137	390.99	12.74	30.68
195	0.0704	0.0141	401.13	12.75	31.46
200	0.0720	0.0144	411.74	12.75	32.28
205	0.0740	0.0148	421.80	12.76	33.06
210	0.0758	0.0152	431.63	12.76	33.82
215	0.0779	0.0156	442.08	12.77	34.62
220	0.0793	0.0159	452.22	12.77	35.41
225	0.0812	0.0162	462.13	12.78	36.17
230	0.0827	0.0165	472.03	12.78	36.93
235	0.0850	0.0170	481.70	12.79	37.67
240	0.0870	0.0174	490.98	12.79	38.38
245	0.0886	0.0177	500.81	12.80	39.14
250	0.0906	0.0181	509.86	12.80	39.83
255	0.0928	0.0186	518.59	12.81	40.49
260	0.0944	0.0189	527.25	12.81	41.15
265	0.0964	0.0193	535.52	12.82	41.78
270	0.0979	0.0196	543.24	12.82	42.37
275	0.0998	0.0200	550.18	12.83	42.90
280	0.1018	0.0204	554.47	12.83	43.21
285	0.1035	0.0207	558.45	12.84	43.51
290	0.1056	0.0211	562.58	12.84	43.81

295	0.1070	0.0214	559.23	12.84	43.54
300	0.1079	0.0216	545.35	12.85	42.45
305	0.1096	0.0219	552.05	12.85	42.96
310	0.1113	0.0223	553.85	12.86	43.08
315	0.1128	0.0226	555.25	12.86	43.18
320	0.1143	0.0229	558.53	12.86	43.42
325	0.1155	0.0231	561.02	12.87	43.60
330	0.1178	0.0236	562.43	12.87	43.69
335	0.1189	0.0238	563.36	12.88	43.75
340	0.1212	0.0242	562.90	12.88	43.70
345	0.1230	0.0246	562.27	12.89	43.63
350	0.1252	0.0250	559.70	12.89	43.41
355	0.1271	0.0254	530.37	12.90	41.12
360	0.1305	0.0261	515.24	12.91	39.92

Montour Class F #1
Initial Parameters

Curing Duration	28-day
Date	12/28/2009
Diameter, in	4
Area, in²	12.57
Length, in	5
Ini mass, g	69.1
Fin mass, g	61.9
Moisture Content	11.6



Time,	Deformation,	Vertical Strain,	Load,	Corrected Area	Stress,
sec	ΔL, in	$\epsilon = \Delta L/L$	lb	$A_c = A_o/(1-\epsilon)$, in²	σ, lb/in²
0	0.0000	0.0000	2.34	12.57	0.19
5	0.0015	0.0003	6.40	12.57	0.51
10	0.0034	0.0007	9.83	12.58	0.78
15	0.0050	0.0010	14.04	12.58	1.12
20	0.0067	0.0013	18.64	12.59	1.48
25	0.0079	0.0016	23.79	12.59	1.89
30	0.0096	0.0019	29.25	12.59	2.32
35	0.0111	0.0022	35.18	12.60	2.79
40	0.0126	0.0025	41.49	12.60	3.29

45	0.0138	0.0028	48.20	12.60	3.82
50	0.0156	0.0031	55.53	12.61	4.40
55	0.0176	0.0035	64.35	12.61	5.10
60	0.0187	0.0037	74.25	12.62	5.88
65	0.0210	0.0042	85.09	12.62	6.74
70	0.0233	0.0047	96.56	12.63	7.65
75	0.0241	0.0048	108.41	12.63	8.58
80	0.0264	0.0053	120.58	12.64	9.54
85	0.0282	0.0056	132.83	12.64	10.51
90	0.0300	0.0060	144.99	12.65	11.47
95	0.0317	0.0063	157.16	12.65	12.42
100	0.0338	0.0068	168.86	12.66	13.34
105	0.0354	0.0071	180.40	12.66	14.25
110	0.0376	0.0075	191.71	12.67	15.14
115	0.0392	0.0078	202.71	12.67	16.00
120	0.0408	0.0082	213.55	12.67	16.85
125	0.0431	0.0086	224.39	12.68	17.70
130	0.0454	0.0091	235.00	12.69	18.53
135	0.0468	0.0094	245.69	12.69	19.36
140	0.0490	0.0098	256.29	12.69	20.19
145	0.0505	0.0101	266.75	12.70	21.01
150	0.0520	0.0104	277.51	12.70	21.85
155	0.0540	0.0108	287.96	12.71	22.66
160	0.0559	0.0112	298.57	12.71	23.49
165	0.0579	0.0116	309.10	12.72	24.31
170	0.0597	0.0119	319.86	12.72	25.14
175	0.0612	0.0122	330.16	12.73	25.94
180	0.0633	0.0127	340.92	12.73	26.78
185	0.0648	0.0130	351.53	12.74	27.60
190	0.0668	0.0134	362.06	12.74	28.42
195	0.0686	0.0137	373.05	12.74	29.27
200	0.0705	0.0141	383.74	12.75	30.10
205	0.0723	0.0145	394.19	12.75	30.91
210	0.0741	0.0148	405.11	12.76	31.75
215	0.0767	0.0153	415.95	12.77	32.58
220	0.0777	0.0155	426.17	12.77	33.38
225	0.0800	0.0160	437.17	12.77	34.22
230	0.0816	0.0163	447.46	12.78	35.02
235	0.0836	0.0167	457.45	12.78	35.78

240	0.0849	0.0170	468.05	12.79	36.60
245	0.0872	0.0174	478.43	12.79	37.40
250	0.0889	0.0178	488.41	12.80	38.16
255	0.0905	0.0181	498.55	12.80	38.94
260	0.0922	0.0184	508.53	12.81	39.71
265	0.0943	0.0189	517.74	12.81	40.41
270	0.0963	0.0193	527.64	12.82	41.17
275	0.0983	0.0197	536.69	12.82	41.86
280	0.1002	0.0200	545.42	12.83	42.52
285	0.1020	0.0204	554.08	12.83	43.18
290	0.1036	0.0207	562.04	12.84	43.79
295	0.1054	0.0211	569.84	12.84	44.38
300	0.1070	0.0214	577.25	12.84	44.94
305	0.1095	0.0219	584.42	12.85	45.48
310	0.1115	0.0223	591.13	12.86	45.98
315	0.1130	0.0226	597.84	12.86	46.49
320	0.1149	0.0230	603.61	12.87	46.92
325	0.1165	0.0233	609.15	12.87	47.33
330	0.1186	0.0237	613.83	12.88	47.68
335	0.1204	0.0241	616.71	12.88	47.88
340	0.1223	0.0245	618.97	12.89	48.04
345	0.1238	0.0248	619.36	12.89	48.05
350	0.1256	0.0251	620.14	12.89	48.10
355	0.1273	0.0255	619.75	12.90	48.05
360	0.1296	0.0259	606.34	12.90	46.99
365	0.1315	0.0263	572.02	12.91	44.31

Montour Class F #2**Initial Parameters**

Curing Duration	28-day				
Date	12/28/2009				
Diameter, in	4				
Area, in²	12.57				
Length, in	5				
Ini mass, g	91.8				
Fin mass, g	81.2				
Moisture Content	13.1				
Time,	Deformation,	Vertical Strain,	Load,	Corrected Area	Stress,
sec	ΔL, in	$\epsilon = \Delta L/L$	lb	$A_c = A_o/(1-\epsilon)$, in²	σ, lb/in²
0	0.0000	0.0000	3.59	12.57	0.29
5	0.0013	0.0003	7.41	12.57	0.59
10	0.0030	0.0006	10.22	12.58	0.81
15	0.0049	0.0010	13.42	12.58	1.07
20	0.0065	0.0013	16.61	12.59	1.32
25	0.0083	0.0017	20.20	12.59	1.60
30	0.0096	0.0019	24.41	12.59	1.94
35	0.0114	0.0023	29.33	12.60	2.33
40	0.0129	0.0026	35.33	12.60	2.80
45	0.0145	0.0029	42.04	12.61	3.33
50	0.0157	0.0031	49.29	12.61	3.91
55	0.0176	0.0035	57.72	12.61	4.58
60	0.0194	0.0039	67.31	12.62	5.33
65	0.0207	0.0041	78.15	12.62	6.19
70	0.0232	0.0046	89.85	12.63	7.11
75	0.0253	0.0051	101.86	12.63	8.06
80	0.0260	0.0052	114.34	12.64	9.05
85	0.0284	0.0057	127.13	12.64	10.06
90	0.0303	0.0061	139.61	12.65	11.04
95	0.0319	0.0064	152.64	12.65	12.07
100	0.0337	0.0067	165.59	12.66	13.08
105	0.0358	0.0072	178.14	12.66	14.07
110	0.0372	0.0074	190.78	12.66	15.06
115	0.0396	0.0079	203.18	12.67	16.04
120	0.0410	0.0082	215.19	12.67	16.98
125	0.0428	0.0086	227.20	12.68	17.92

130	0.0450	0.0090	239.29	12.68	18.87
135	0.0473	0.0095	250.68	12.69	19.75
140	0.0486	0.0097	262.30	12.69	20.66
145	0.0510	0.0102	273.92	12.70	21.57
150	0.0523	0.0105	285.23	12.70	22.45
155	0.0542	0.0108	296.85	12.71	23.36
160	0.0559	0.0112	308.32	12.71	24.25
165	0.0576	0.0115	319.70	12.72	25.14
170	0.0598	0.0120	331.09	12.72	26.02
175	0.0618	0.0124	342.71	12.73	26.93
180	0.0632	0.0126	353.79	12.73	27.79
185	0.0654	0.0131	365.49	12.74	28.70
190	0.0670	0.0134	377.19	12.74	29.61
195	0.0686	0.0137	388.34	12.74	30.47
200	0.0706	0.0141	400.35	12.75	31.40
205	0.0729	0.0146	411.82	12.76	32.28
210	0.0744	0.0149	423.21	12.76	33.17
215	0.0763	0.0153	434.98	12.76	34.08
220	0.0785	0.0157	446.92	12.77	35.00
225	0.0801	0.0160	458.07	12.77	35.86
230	0.0822	0.0164	469.92	12.78	36.77
235	0.0838	0.0168	481.23	12.78	37.64
240	0.0857	0.0171	492.23	12.79	38.49
245	0.0871	0.0174	504.01	12.79	39.40
250	0.0895	0.0179	515.40	12.80	40.27
255	0.0908	0.0182	526.32	12.80	41.11
260	0.0924	0.0185	537.47	12.81	41.97
265	0.0946	0.0189	548.39	12.81	42.80
270	0.0970	0.0194	558.61	12.82	43.58
275	0.0983	0.0197	569.37	12.82	44.41
280	0.1005	0.0201	578.96	12.83	45.13
285	0.1024	0.0205	588.24	12.83	45.84
290	0.1043	0.0209	596.90	12.84	46.50
295	0.1059	0.0212	605.09	12.84	47.12
300	0.1074	0.0215	612.89	12.85	47.71
305	0.1093	0.0219	620.92	12.85	48.32
310	0.1119	0.0224	628.18	12.86	48.86
315	0.1135	0.0227	634.65	12.86	49.34
320	0.1152	0.0230	640.42	12.87	49.77

325	0.1169	0.0234	646.66	12.87	50.24
330	0.1187	0.0237	652.98	12.88	50.71
335	0.1211	0.0242	657.50	12.88	51.04
340	0.1225	0.0245	661.79	12.89	51.36
345	0.1247	0.0249	663.43	12.89	51.46
350	0.1264	0.0253	630.67	12.90	48.90
355	0.1286	0.0257	635.59	12.90	49.26
360	0.1303	0.0261	635.04	12.91	49.20
365	0.1319	0.0264	623.73	12.91	48.31

Montour Class F #3

Initial Parameters

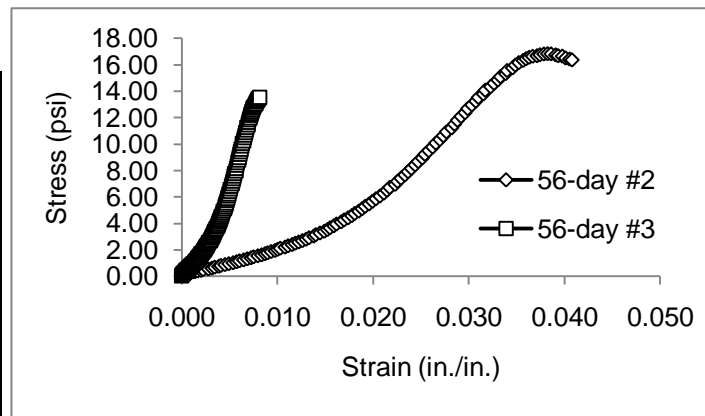
Initial Parameters					
Curing Duration	28-day				
Date	12/28/2009				
Diameter, in	4				
Area, in ²	12.57				
Length, in	5				
Ini mass, g	76.2				
Fin mass, g	67.7				
Moisture Content	12.6				
Time,	Deformation,	Vertical Strain,	Load,	Corrected Area	Stress,
sec	ΔL, in	ε = ΔL/L	lb	Ac = Ao/(1-ε), in ²	σ, lb/in ²
0	0.0000	0.0000	4.60	12.57	0.37
5	0.0016	0.0003	11.93	12.57	0.95
10	0.0028	0.0006	19.03	12.58	1.51
15	0.0042	0.0008	26.83	12.58	2.13
20	0.0061	0.0012	35.88	12.59	2.85
25	0.0067	0.0013	46.02	12.59	3.66
30	0.0079	0.0016	57.48	12.59	4.57
35	0.0101	0.0020	72.22	12.60	5.73
40	0.0120	0.0024	88.14	12.60	6.99
45	0.0128	0.0026	104.51	12.60	8.29
50	0.0151	0.0030	121.13	12.61	9.61
55	0.0167	0.0033	137.58	12.61	10.91
60	0.0187	0.0037	153.57	12.62	12.17
65	0.0203	0.0041	169.48	12.62	13.43
70	0.0223	0.0045	184.77	12.63	14.63

75	0.0240	0.0048	199.51	12.63	15.80
80	0.0256	0.0051	213.94	12.63	16.93
85	0.0277	0.0055	227.75	12.64	18.02
90	0.0291	0.0058	241.16	12.64	19.07
95	0.0317	0.0063	254.58	12.65	20.12
100	0.0338	0.0068	267.68	12.66	21.15
105	0.0353	0.0071	280.24	12.66	22.14
110	0.0368	0.0074	292.95	12.66	23.13
115	0.0393	0.0079	305.28	12.67	24.10
120	0.0401	0.0080	317.83	12.67	25.08
125	0.0429	0.0086	329.92	12.68	26.02
130	0.0443	0.0089	342.25	12.68	26.99
135	0.0462	0.0092	354.26	12.69	27.92
140	0.0484	0.0097	366.35	12.69	28.86
145	0.0498	0.0100	378.20	12.70	29.79
150	0.0514	0.0103	390.21	12.70	30.72
155	0.0532	0.0106	402.46	12.71	31.68
160	0.0556	0.0111	414.08	12.71	32.58
165	0.0570	0.0114	426.33	12.72	33.53
170	0.0590	0.0118	438.26	12.72	34.45
175	0.0610	0.0122	450.19	12.73	35.38
180	0.0626	0.0125	462.05	12.73	36.30
185	0.0650	0.0130	474.37	12.74	37.25
190	0.0664	0.0133	485.91	12.74	38.14
195	0.0685	0.0137	497.93	12.74	39.07
200	0.0701	0.0140	509.62	12.75	39.97
205	0.0722	0.0144	520.93	12.75	40.84
210	0.0738	0.0148	532.63	12.76	41.75
215	0.0758	0.0152	544.25	12.76	42.64
220	0.0774	0.0155	555.64	12.77	43.52
225	0.0792	0.0158	566.72	12.77	44.37
230	0.0807	0.0161	577.87	12.78	45.23
235	0.0829	0.0166	588.01	12.78	46.00
240	0.0849	0.0170	598.38	12.79	46.80
245	0.0867	0.0173	608.37	12.79	47.56
250	0.0887	0.0177	617.41	12.80	48.25
255	0.0908	0.0182	626.31	12.80	48.92
260	0.0924	0.0185	634.42	12.81	49.54
265	0.0944	0.0189	641.83	12.81	50.10

270	0.0960	0.0192	648.38	12.82	50.59
275	0.0981	0.0196	653.21	12.82	50.95
280	0.1001	0.0200	658.60	12.83	51.35
285	0.1017	0.0203	663.74	12.83	51.73
290	0.1038	0.0208	667.41	12.84	51.99
295	0.1053	0.0211	669.59	12.84	52.15
300	0.1071	0.0214	671.78	12.85	52.30
305	0.1093	0.0219	670.37	12.85	52.17
310	0.1109	0.0222	651.50	12.86	50.68
315	0.1124	0.0225	633.48	12.86	49.26

Montour Class F #2**Initial Parameters**

Curing Duration	56-day
Date	1/25/2010
Diameter, in	4
Area, in²	12.57
Length, in	5
Ini mass, g	56.7
Fin mass, g	51.3
Moisture Content	10.5



Time,	Deformation,	Vertical Strain,	Load,	Corrected Area	Stress,
sec	ΔL , in	$\epsilon = \Delta L/L$	lb	$A_c = A_o/(1-\epsilon)$, in ²	σ , lb/in ²
0	0.0000	0.0000	1.09	12.57	0.09
5	0.0017	0.0003	2.65	12.57	0.21
10	0.0034	0.0007	3.20	12.58	0.25
15	0.0048	0.0010	3.67	12.58	0.29
20	0.0067	0.0013	4.29	12.59	0.34
25	0.0083	0.0017	4.99	12.59	0.40
30	0.0101	0.0020	5.62	12.60	0.45
35	0.0112	0.0022	6.40	12.60	0.51
40	0.0140	0.0028	7.10	12.61	0.56
45	0.0159	0.0032	7.88	12.61	0.62
50	0.0173	0.0035	8.74	12.61	0.69
55	0.0194	0.0039	9.52	12.62	0.75
60	0.0205	0.0041	10.37	12.62	0.82

65	0.0226	0.0045	11.23	12.63	0.89
70	0.0247	0.0049	12.09	12.63	0.96
75	0.0269	0.0054	13.03	12.64	1.03
80	0.0287	0.0057	13.96	12.64	1.10
85	0.0302	0.0060	14.82	12.65	1.17
90	0.0324	0.0065	15.76	12.65	1.25
95	0.0343	0.0069	16.85	12.66	1.33
100	0.0363	0.0073	17.78	12.66	1.40
105	0.0376	0.0075	18.72	12.67	1.48
110	0.0398	0.0080	19.73	12.67	1.56
115	0.0418	0.0084	20.59	12.68	1.62
120	0.0436	0.0087	21.68	12.68	1.71
125	0.0449	0.0090	22.62	12.68	1.78
130	0.0468	0.0094	23.79	12.69	1.87
135	0.0488	0.0098	24.80	12.69	1.95
140	0.0501	0.0100	25.90	12.70	2.04
145	0.0515	0.0103	26.99	12.70	2.12
150	0.0540	0.0108	28.08	12.71	2.21
155	0.0556	0.0111	29.40	12.71	2.31
160	0.0577	0.0115	30.57	12.72	2.40
165	0.0593	0.0119	31.82	12.72	2.50
170	0.0611	0.0122	32.99	12.73	2.59
175	0.0631	0.0126	34.40	12.73	2.70
180	0.0650	0.0130	35.72	12.74	2.80
185	0.0665	0.0133	37.20	12.74	2.92
190	0.0690	0.0138	38.76	12.75	3.04
195	0.0701	0.0140	40.17	12.75	3.15
200	0.0722	0.0144	41.81	12.75	3.28
205	0.0745	0.0149	43.44	12.76	3.40
210	0.0761	0.0152	45.16	12.76	3.54
215	0.0775	0.0155	46.88	12.77	3.67
220	0.0795	0.0159	48.83	12.77	3.82
225	0.0808	0.0162	50.54	12.78	3.96
230	0.0833	0.0167	52.65	12.78	4.12
235	0.0849	0.0170	54.60	12.79	4.27
240	0.0869	0.0174	56.55	12.79	4.42
245	0.0888	0.0178	58.73	12.80	4.59
250	0.0904	0.0181	60.92	12.80	4.76
255	0.0925	0.0185	63.10	12.81	4.93

260	0.0942	0.0188	65.52	12.81	5.11
265	0.0958	0.0192	67.86	12.82	5.29
270	0.0979	0.0196	70.20	12.82	5.48
275	0.0996	0.0199	72.77	12.83	5.67
280	0.1014	0.0203	75.27	12.83	5.87
285	0.1035	0.0207	77.92	12.84	6.07
290	0.1056	0.0211	80.80	12.84	6.29
295	0.1073	0.0215	83.61	12.85	6.51
300	0.1086	0.0217	86.42	12.85	6.73
305	0.1115	0.0223	89.38	12.86	6.95
310	0.1127	0.0225	92.43	12.86	7.19
315	0.1145	0.0229	95.47	12.86	7.42
320	0.1166	0.0233	98.74	12.87	7.67
325	0.1182	0.0236	101.94	12.87	7.92
330	0.1200	0.0240	105.14	12.88	8.16
335	0.1219	0.0244	108.57	12.88	8.43
340	0.1235	0.0247	112.00	12.89	8.69
345	0.1257	0.0251	115.43	12.89	8.95
350	0.1270	0.0254	119.02	12.90	9.23
355	0.1290	0.0258	122.69	12.90	9.51
360	0.1310	0.0262	126.20	12.91	9.78
365	0.1327	0.0265	130.10	12.91	10.08
370	0.1348	0.0270	133.68	12.92	10.35
375	0.1366	0.0273	137.43	12.92	10.63
380	0.1383	0.0277	141.25	12.93	10.93
385	0.1409	0.0282	145.07	12.93	11.22
390	0.1425	0.0285	148.89	12.94	11.51
395	0.1440	0.0288	152.72	12.94	11.80
400	0.1459	0.0292	156.62	12.95	12.10
405	0.1480	0.0296	160.36	12.95	12.38
410	0.1494	0.0299	164.34	12.96	12.68
415	0.1516	0.0303	168.00	12.96	12.96
420	0.1536	0.0307	171.82	12.97	13.25
425	0.1549	0.0310	175.49	12.97	13.53
430	0.1576	0.0315	179.00	12.98	13.79
435	0.1585	0.0317	182.67	12.98	14.07
440	0.1613	0.0323	186.25	12.99	14.34
445	0.1631	0.0326	189.69	12.99	14.60
450	0.1652	0.0330	193.04	13.00	14.85

455	0.1665	0.0333	196.32	13.00	15.10
460	0.1692	0.0338	199.44	13.01	15.33
465	0.1699	0.0340	202.48	13.01	15.56
470	0.1728	0.0346	205.21	13.02	15.76
475	0.1742	0.0348	208.01	13.02	15.97
480	0.1760	0.0352	210.51	13.03	16.16
485	0.1783	0.0357	212.77	13.03	16.32
490	0.1798	0.0360	214.49	13.04	16.45
495	0.1814	0.0363	215.97	13.04	16.56
500	0.1833	0.0367	217.06	13.05	16.64
505	0.1856	0.0371	217.76	13.05	16.68
510	0.1871	0.0374	218.78	13.06	16.75
515	0.1891	0.0378	219.64	13.06	16.81
520	0.1911	0.0382	220.03	13.07	16.84
525	0.1929	0.0386	219.95	13.07	16.82
530	0.1953	0.0391	219.01	13.08	16.74
535	0.1966	0.0393	218.31	13.08	16.68
540	0.1988	0.0398	217.92	13.09	16.65
545	0.2005	0.0401	216.13	13.10	16.50
550	0.2026	0.0405	215.19	13.10	16.43
555	0.2038	0.0408	214.49	13.10	16.37

Montour Class F #3**Initial Parameters**

Curing Duration	56-day				
Date	1/25/2010				
Diameter, in	4				
Area, in²	12.57				
Length, in	5				
Ini mass, g	61.7				
Fin mass, g	55.4				
Moisture Content	11.4				
Time,	Deformation,	Vertical Strain,	Load,	Corrected Area	Stress,
sec	ΔL, in	$\epsilon = \Delta L/L$	lb	$A_c = A_o/(1-\epsilon)$, in²	σ, lb/in²
0	0.0000	0.0000	0.39	12.57	0.03
5	0.0018	0.0004	1.79	12.57	0.14
10	0.0028	0.0006	2.42	12.58	0.19
15	0.0047	0.0009	2.96	12.58	0.24
20	0.0069	0.0014	3.67	12.59	0.29
25	0.0083	0.0017	4.37	12.59	0.35
30	0.0102	0.0020	4.99	12.60	0.40
35	0.0125	0.0025	5.77	12.60	0.46
40	0.0142	0.0028	6.32	12.61	0.50
45	0.0159	0.0032	7.10	12.61	0.56
50	0.0178	0.0036	7.72	12.61	0.61
55	0.0199	0.0040	8.35	12.62	0.66
60	0.0213	0.0043	8.89	12.62	0.70
65	0.0227	0.0045	9.59	12.63	0.76
70	0.0246	0.0049	10.22	12.63	0.81
75	0.0260	0.0052	10.92	12.64	0.86
80	0.0278	0.0056	11.54	12.64	0.91
85	0.0287	0.0057	12.32	12.64	0.97
90	0.0312	0.0062	13.03	12.65	1.03
95	0.0330	0.0066	13.73	12.65	1.08
100	0.0347	0.0069	14.51	12.66	1.15
105	0.0368	0.0074	15.29	12.66	1.21
110	0.0380	0.0076	15.99	12.67	1.26
115	0.0397	0.0079	16.85	12.67	1.33

120	0.0419	0.0084	17.71	12.68	1.40
125	0.0440	0.0088	18.41	12.68	1.45
130	0.0458	0.0092	19.34	12.69	1.52
135	0.0473	0.0095	20.20	12.69	1.59
140	0.0499	0.0100	21.14	12.70	1.66
145	0.0514	0.0103	22.00	12.70	1.73
150	0.0534	0.0107	22.93	12.71	1.80
155	0.0550	0.0110	24.02	12.71	1.89
160	0.0571	0.0114	24.96	12.72	1.96
165	0.0588	0.0118	25.97	12.72	2.04
170	0.0612	0.0122	26.99	12.73	2.12
175	0.0626	0.0125	28.08	12.73	2.21
180	0.0641	0.0128	29.09	12.73	2.28
185	0.0659	0.0132	30.11	12.74	2.36
190	0.0676	0.0135	31.28	12.74	2.45
195	0.0690	0.0138	32.37	12.75	2.54
200	0.0712	0.0142	33.54	12.75	2.63
205	0.0732	0.0146	34.71	12.76	2.72
210	0.0752	0.0150	35.96	12.76	2.82
215	0.0764	0.0153	37.20	12.77	2.91
220	0.0783	0.0157	38.37	12.77	3.01
225	0.0808	0.0162	39.70	12.78	3.11
230	0.0822	0.0164	40.95	12.78	3.20
235	0.0837	0.0167	42.35	12.78	3.31
240	0.0865	0.0173	43.60	12.79	3.41
245	0.0878	0.0176	45.00	12.79	3.52
250	0.0893	0.0179	46.49	12.80	3.63
255	0.0917	0.0183	48.05	12.80	3.75
260	0.0938	0.0188	49.68	12.81	3.88
265	0.0948	0.0190	51.24	12.81	4.00
270	0.0969	0.0194	53.04	12.82	4.14
275	0.0984	0.0197	54.60	12.82	4.26
280	0.1008	0.0202	56.47	12.83	4.40
285	0.1023	0.0205	58.11	12.83	4.53
290	0.1041	0.0208	59.90	12.84	4.67
295	0.1063	0.0213	61.70	12.84	4.80
300	0.1078	0.0216	63.65	12.85	4.95
305	0.1097	0.0219	65.52	12.85	5.10
310	0.1117	0.0223	67.54	12.86	5.25

315	0.1133	0.0227	69.49	12.86	5.40
320	0.1154	0.0231	71.52	12.87	5.56
325	0.1170	0.0234	73.71	12.87	5.73
330	0.1188	0.0238	75.81	12.88	5.89
335	0.1209	0.0242	78.15	12.88	6.07
340	0.1228	0.0246	80.49	12.89	6.25
345	0.1252	0.0250	82.83	12.89	6.42
350	0.1261	0.0252	85.09	12.90	6.60
355	0.1287	0.0257	87.75	12.90	6.80
360	0.1302	0.0260	90.09	12.91	6.98
365	0.1318	0.0264	92.66	12.91	7.18
370	0.1340	0.0268	95.23	12.92	7.37
375	0.1355	0.0271	97.81	12.92	7.57
380	0.1376	0.0275	100.46	12.93	7.77
385	0.1394	0.0279	103.11	12.93	7.97
390	0.1409	0.0282	105.76	12.93	8.18
395	0.1431	0.0286	108.49	12.94	8.38
400	0.1445	0.0289	111.22	12.94	8.59
405	0.1465	0.0293	113.87	12.95	8.79
410	0.1484	0.0297	116.68	12.95	9.01
415	0.1500	0.0300	119.57	12.96	9.23
420	0.1520	0.0304	122.22	12.96	9.43
425	0.1542	0.0308	125.03	12.97	9.64
430	0.1557	0.0311	127.84	12.97	9.85
435	0.1583	0.0317	130.49	12.98	10.05
440	0.1600	0.0320	133.14	12.99	10.25
445	0.1609	0.0322	135.95	12.99	10.47
450	0.1634	0.0327	138.52	12.99	10.66
455	0.1653	0.0331	141.33	13.00	10.87
460	0.1671	0.0334	144.06	13.00	11.08
465	0.1688	0.0338	146.55	13.01	11.27
470	0.1709	0.0342	149.05	13.01	11.45
475	0.1723	0.0345	151.70	13.02	11.65
480	0.1749	0.0350	154.12	13.03	11.83
485	0.1760	0.0352	156.46	13.03	12.01
490	0.1787	0.0357	158.80	13.04	12.18
495	0.1803	0.0361	160.75	13.04	12.33
500	0.1827	0.0365	163.01	13.05	12.49
505	0.1839	0.0368	164.88	13.05	12.63

510	0.1864	0.0373	166.52	13.06	12.75
515	0.1877	0.0375	168.08	13.06	12.87
520	0.1901	0.0380	169.56	13.07	12.98
525	0.1913	0.0383	170.89	13.07	13.07
530	0.1934	0.0387	172.29	13.08	13.18
535	0.1958	0.0392	173.62	13.08	13.27
540	0.1975	0.0395	174.55	13.09	13.34
545	0.1990	0.0398	175.72	13.09	13.42
550	0.2010	0.0402	176.50	13.10	13.48
555	0.2033	0.0407	177.21	13.10	13.52
560	0.2048	0.0410	177.75	13.11	13.56
565	0.2069	0.0414	178.06	13.11	13.58
570	0.2088	0.0418	178.38	13.12	13.60
575	0.2107	0.0421	178.38	13.12	13.59
580	0.2132	0.0426	178.22	13.13	13.57
585	0.2145	0.0429	177.91	13.13	13.55
590	0.2167	0.0433	177.60	13.14	13.52
595	0.2186	0.0437	177.05	13.14	13.47
600	0.2206	0.0441	176.11	13.15	13.39
605	0.2221	0.0444	175.10	13.15	13.31
610	0.2246	0.0449	173.85	13.16	13.21
615	0.2259	0.0452	172.68	13.16	13.12

Appendix E: PARTICLE SIZE DISTRIBUTION DATA

FGD Material

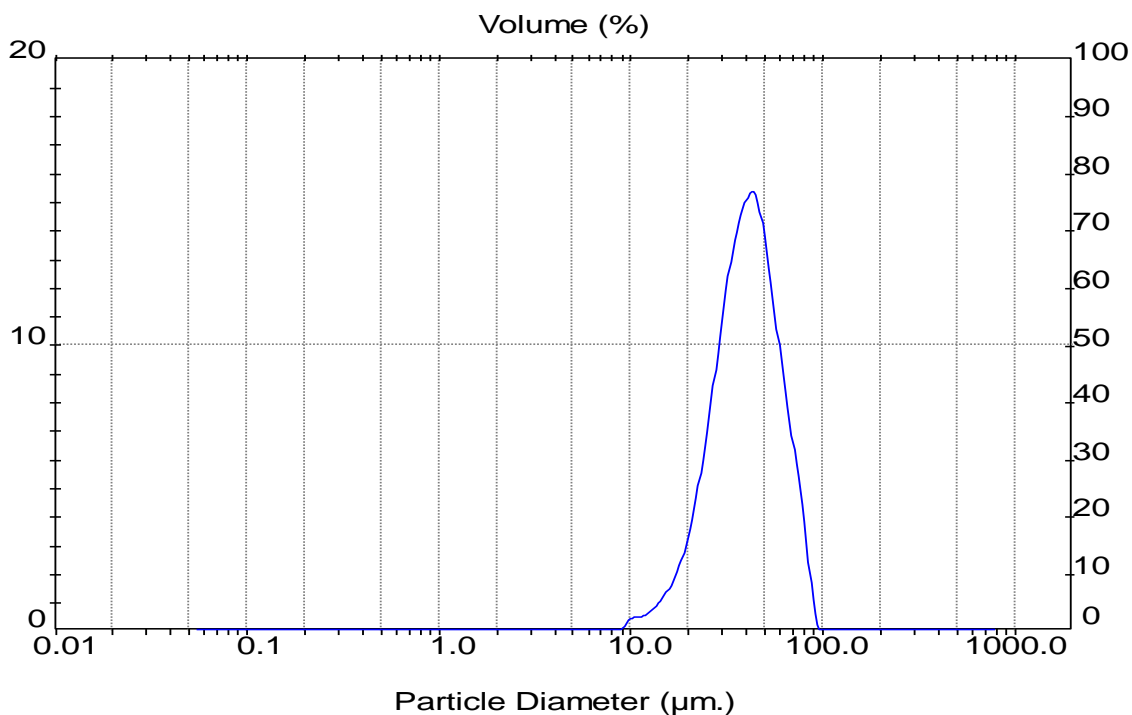
Result: Analysis Table

ID: FGD	Run No: 12	Measured: 8/5/09 11:55AM
File: ANGEL	Rec. No: 2	Analysed: 8/5/09 11:57AM
Path: C:\SIZERS\DATA\MALEK\		Source: Analysed

Range: 300RF mm	Beam: 2.40 mm	Sampler: MS1	Obs': 22.4 %
Presentation: 3_CEM2PR	Analysis: Monomodal		Residual: 1.920 %
Modifications: None			

Conc. = 0.1226 %Vol	Density = 2.600 g/cm ³	S.S.A. = 0.0647 m ² /g
Distribution: Volume	D[4, 3] = 42.16 μ m	D[3, 2] = 35.64 μ m
D(v, 0.1) = 22.94 μ m	D(v, 0.5) = 40.18 μ m	D(v, 0.9) = 65.00 μ m
Span = 1.047E+00	Uniformity = 3.218E-01	

Size (um)	Volume In %	Size (um)	Volume In %	Size (um)	Volume In %	Size (um)	Volume In %
0.05	0.00	0.58	0.00	6.63	0.00	76.32	3.16
0.06	0.00	0.67	0.00	7.72	0.00	88.91	0.08
0.07	0.00	0.78	0.00	9.00	0.38	103.58	0.00
0.08	0.00	0.91	0.00	10.48	0.52	120.67	0.00
0.09	0.00	1.06	0.00	12.21	0.84	140.58	0.00
0.11	0.00	1.24	0.00	14.22	1.36	163.77	0.00
0.13	0.00	1.44	0.00	16.57	2.29	190.80	0.00
0.15	0.00	1.68	0.00	19.31	3.92	222.28	0.00
0.17	0.00	1.95	0.00	22.49	6.45	258.95	0.00
0.20	0.00	2.28	0.00	26.20	9.70	301.68	0.00
0.23	0.00	2.65	0.00	30.53	12.86	351.46	0.00
0.27	0.00	3.09	0.00	35.56	14.74	409.45	0.00
0.31	0.00	3.60	0.00	41.43	15.21	477.01	0.00
0.36	0.00	4.19	0.00	48.27	12.70	555.71	0.00
0.42	0.00	4.88	0.00	56.23	9.44	647.41	0.00
0.49	0.00	5.69	0.00	65.51	6.35	754.23	0.00
0.58	0.00	6.63	0.00	76.32		878.67	0.00



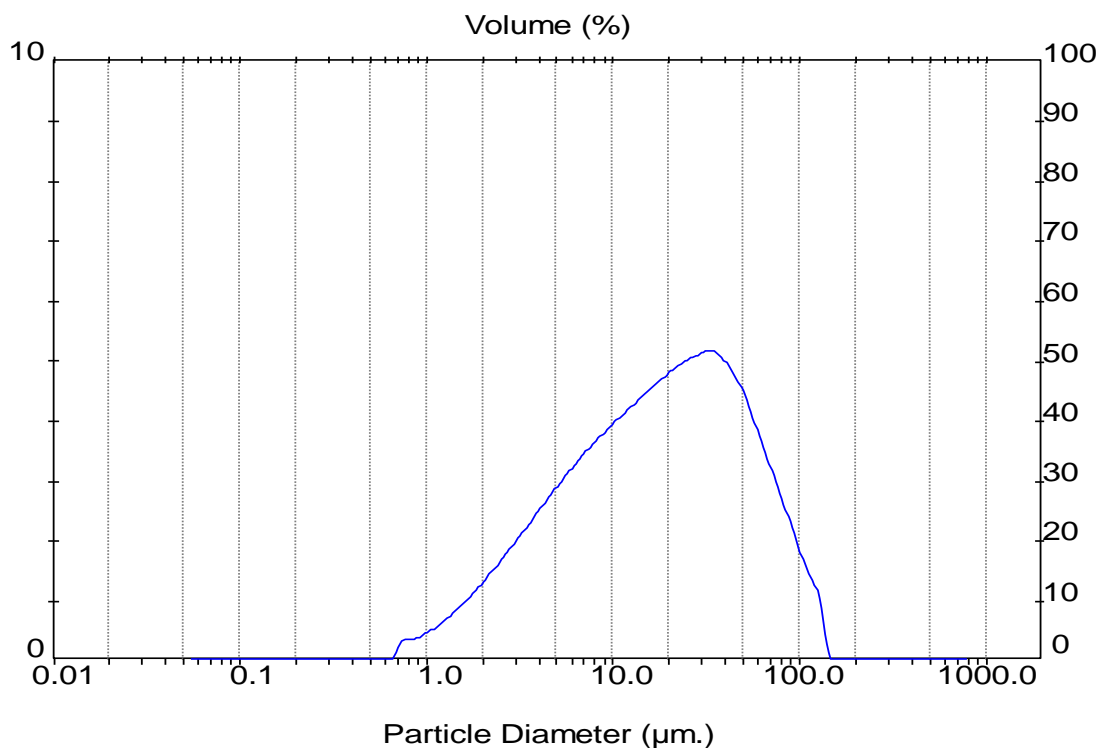
FBC Ash**Result: Analysis Table**

ID: Seward Ash	Run No: 1	Measured: 11/10/09 3:28PM
File: CEMENT	Rec. No: 8	Analysed: 11/10/09 3:28PM
Path: C:\SIZERS\DATA\MALEK\		Source: Analysed

Range: 300RF mm	Beam: 2.40 mm	Sampler: MS1	Obs': 13.6 %
Presentation: 3_CEM2PR	Analysis: Poly disperse		Residual: 1.032 %
Modifications: None			

Conc. = 0.0144 %Vol	Density = 2.600 g/cm ³	S.S.A.= 0.2881 m ² /g
Distribution: Volume	D[4, 3] = 27.42 μ m	D[3, 2] = 8.01 μ m
D(v, 0.1) = 3.19 μ m	D(v, 0.5) = 18.19 μ m	D(v, 0.9) = 65.96 μ m
Span = 3.450E+00	Uniformity = 1.068E+00	

Size (μ m)	Volume In %	Size (μ m)	Volume In %	Size (μ m)	Volume In %	Size (μ m)	Volume In %
0.05	0.00	0.58	0.00	6.63	3.49	76.32	2.61
0.06	0.00	0.67	0.28	7.72	3.71	88.91	2.03
0.07	0.00	0.78	0.37	9.00	3.91	103.58	1.46
0.08	0.00	0.91	0.46	10.48	4.11	120.67	0.88
0.09	0.00	1.06	0.59	12.21	4.30	140.58	0.00
0.11	0.00	1.24	0.76	14.22	4.49	163.77	0.00
0.13	0.00	1.44	0.95	16.57	4.68	190.80	0.00
0.15	0.00	1.68	1.16	19.31	4.85	222.28	0.00
0.17	0.00	1.95	1.40	22.49	4.99	258.95	0.00
0.20	0.00	2.28	1.65	26.20	5.09	301.68	0.00
0.23	0.00	2.65	1.91	30.53	5.17	351.46	0.00
0.27	0.00	3.09	2.18	35.56	5.04	409.45	0.00
0.31	0.00	3.60	2.45	41.43	4.77	477.01	0.00
0.36	0.00	4.19	2.73	48.27	4.33	555.71	0.00
0.42	0.00	4.88	3.00	56.23	3.76	647.41	0.00
0.49	0.00	5.69	3.25	65.51	3.18	754.23	0.00
0.58	0.00	6.63		76.32		878.67	0.00



Class F Fly Ash

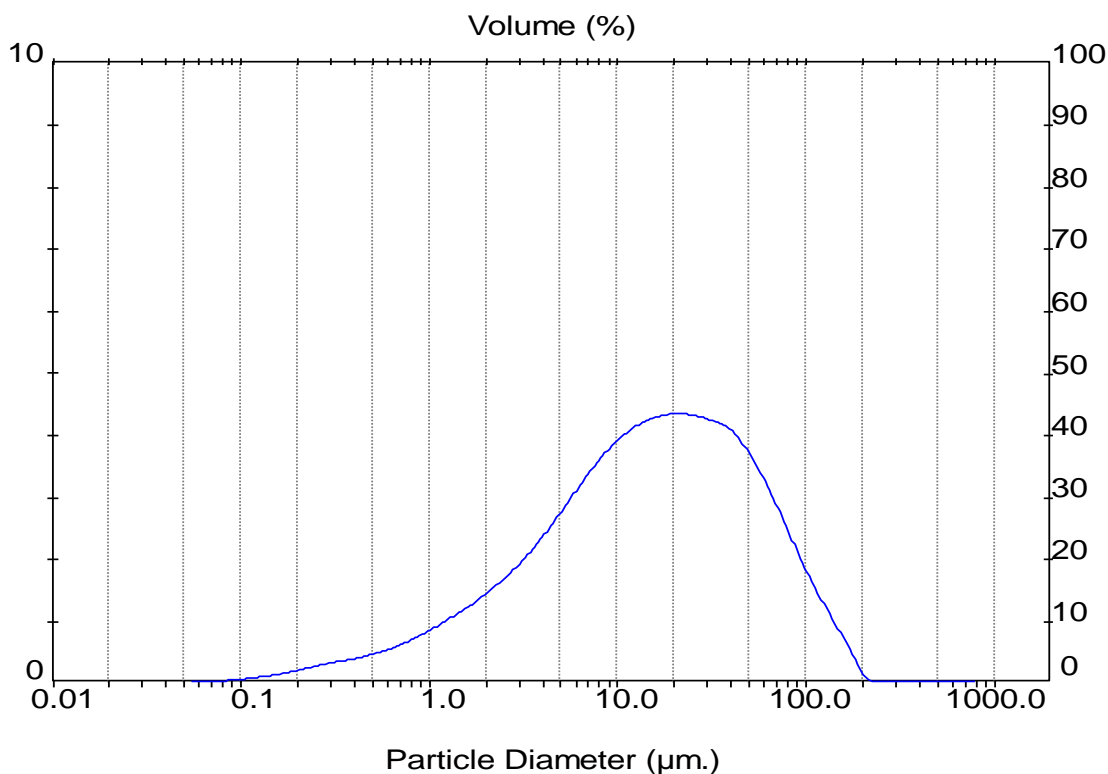
Result: Analysis Table

ID: F Ash	Run No: 1	Measured: 11/18/09 2:44PM
File: CEMENT	Rec. No: 9	Analysed: 11/18/09 2:44PM
Path: C:\SIZERS\DATA\MALEK\		Source: Analysed

Range: 300RF mm	Beam: 2.40 mm	Sampler: MS1	Obs': 26.9 %
Presentation: 3_CEM2PR	Analysis: Poly disperse		Residual: 1.059 %
Modifications: None			

Conc. = 0.0208 %Vol	Density = 2.600 g/cm ³	S.S.A.= 0.6702 m ² /g
Distribution: Volume	D[4, 3] = 27.40 μ m	D[3, 2] = 3.44 μ m
D(v, 0.1) = 1.79 μ m	D(v, 0.5) = 15.27 μ m	D(v, 0.9) = 70.07 μ m
Span = 4.471E+00	Uniformity = 1.390E+00	

Size (μ m)	Volume In %	Size (μ m)	Volume In %	Size (μ m)	Volume In %	Size (μ m)	Volume In %
0.05	0.01	0.58	0.57	6.63	3.42	76.32	2.39
0.06	0.02	0.67	0.64	7.72	3.67	88.91	1.94
0.07	0.04	0.78	0.75	9.00	3.89	103.58	1.53
0.08	0.06	0.91	0.85	10.48	4.06	120.67	1.18
0.09	0.07	1.06	0.96	12.21	4.19	140.58	0.83
0.11	0.10	1.24	1.08	14.22	4.27	163.77	0.48
0.13	0.12	1.44	1.21	16.57	4.33	190.80	0.12
0.15	0.16	1.68	1.35	19.31	4.34	222.28	0.00
0.17	0.20	1.95	1.50	22.49	4.33	258.95	0.00
0.20	0.24	2.28	1.67	26.20	4.28	301.68	0.00
0.23	0.29	2.65	1.87	30.53	4.21	351.46	0.00
0.27	0.33	3.09	2.08	35.56	4.12	409.45	0.00
0.31	0.37	3.60	2.32	41.43	3.91	477.01	0.00
0.36	0.40	4.19	2.58	48.27	3.62	555.71	0.00
0.42	0.45	4.88	2.86	56.23	3.25	647.41	0.00
0.49	0.51	5.69	3.15	65.51	2.83	754.23	0.00
0.58		6.63		76.32		878.67	0.00



Appendix F: BASELINE CHEMICAL ANALYSIS

	Major								
Analyte Symbol	SiO ₂	Al ₂ O ₃	Fe ₂ O ₃ (T)	MnO	MgO	CaO	Na ₂ O	K ₂ O	TiO ₂
Unit Symbol	%	%	%	%	%	%	%	%	%
Detection Limit	0.01	0.01	0.01	0.001	0.01	0.01	0.01	0.01	0.001
Analysis Method	FUS-ICP	FUS-ICP	FUS-ICP	FUS-ICP	FUS-ICP	FUS-ICP	FUS-ICP	FUS-ICP	FUS-ICP
FGD Material	0.71	0.21	0.17	0.002	0.05	32.26	0.03	0.04	0.006
FBC Ash	40.36	16.98	7.01	0.027	1.33	14.42	0.2	2.09	0.919
Class F Fly Ash	43.37	22.27	15.37	0.027	0.81	3.94	1.67	1.59	1.156

	Anion										
Analyte Symbol	Cl	F	SO ₃	SO ₄	P ₂ O ₅	S	Total S	LOI	Total	NO ₂ (as N)	NO ₃ (as N)
Unit Symbol	%	%	%	%	%	%	%	%	%	mg/L	mg/L
Detection Limit	0.01	0.01	0.3	0.3	0.01	0.001	0.01		0.01	0.01	0.01
Analysis Method	INAA	FUS-ISE	IR	IR	FUS-ICP	TD-ICP	IR	FUS-ICP	FUS-ICP	IC	IC
FGD Material	< 0.01	0.13	< 0.3	57.1	0.02	6.46		20.81	54.31		
FBC Ash	0.06	0.02	< 0.3	12.2	0.12	3.76	4.05	5.08	88.53	< 10	< 10
Class F Fly Ash	0.06	< 0.01	1.1	2.4	0.41	1.1	1.22	7.98	98.58	< 10	< 10

	Minor/Trace										
Analyte Symbol	Ag	As	As	Au	Ba	Be	Bi	Br	Cd	Ce	Co
Unit Symbol	ppm	ppm	ppm	ppb	ppm	ppm	ppm	ppm	ppm	ppm	ppm
Detection Limit	0.3	0.5	5	2	3	1	0.4	0.5	0.5	0.1	1
Analysis Method	TD-ICP	INAA	FUS-MS	INAA	FUS-ICP	FUS-ICP	FUS-MS	INAA	TD-ICP	FUS-MS	FUS-MS
FGD Material	< 0.3	< 0.5	< 5	< 2	6	< 1	< 0.4	< 0.5	< 0.5	1.3	< 1
FBC Ash	< 0.3	91.9	70	< 2	561	3	2.1	25.3	< 0.5	99.3	18
Class F Fly Ash	0.6	140	134	< 2	817	12	4.9	15.2	1.1	128	36

	Minor/Trace										
Analyte Symbol	Cr	Cr	Cs	Cu	Dy	Er	Eu	Ga	Gd	Ge	Hf
Unit Symbol	ppm	ppm	ppm	ppm	ppm	ppm	ppm	ppm	ppm	ppm	ppm
Detection Limit	5	20	0.5	1	0.1	0.1	0.05	1	0.1	1	0.2
Analysis Method	INAA	FUS-MS	FUS-MS	TD-ICP	FUS-MS	FUS-MS	FUS-MS	FUS-MS	FUS-MS	FUS-MS	FUS-MS
FGD Material	< 5	< 20	< 0.5	1	0.1	0.1	< 0.05	< 1	0.1	< 1	3
FBC Ash	117	110	7.6	60	5.8	3.3	1.58	23	6.3	5	5.4
Class F Fly Ash	166	140	8	87	9.9	5.5	2.45	46	10.2	33	5.9

	Minor/Trace										
Analyte Symbol	Ho	In	Ir	La	Lu	Mo	Nb	Nd	Ni	Pb	Pr
Unit Symbol	ppm	ppm	ppb	ppm	ppm	ppm	ppm	ppm	ppm	ppm	ppm
Detection Limit	0.1	0.2	5	0.1	0.04	2	1	0.1	1	5	0.05
Analysis Method	FUS-MS	FUS-MS	INAA	FUS-MS	FUS-MS	FUS-MS	FUS-MS	FUS-MS	TD-ICP	TD-ICP	FUS-MS
FGD Material	< 0.1	< 0.2	< 5	0.7	0.05	< 2	< 1	0.6	1	< 5	0.15
FBC Ash	1.1	< 0.2	< 5	49.3	0.49	6	18	39.3	47	38	11.3
Class F Fly Ash	1.8	< 0.2	< 5	68	0.77	17	25	57	101	54	15.5

	Minor/Trace										
Analyte Symbol	Rb	Sb	Sb	Sc	Sc	Se	Sm	Sn	Sr	Ta	Tb
Unit Symbol	ppm	ppm	ppm	ppm	ppm	ppm	ppm	ppm	ppm	ppm	ppm
Detection Limit	2	0.5	0.2	0.1	1	3	0.1	1	2	0.1	0.1
Analysis Method	FUS-MS	FUS-MS	INAA	INAA	FUS-ICP	INAA	FUS-MS	FUS-MS	FUS-ICP	FUS-MS	FUS-MS
FGD Material	< 2	< 0.5	< 0.2	0.2	< 1	< 3	0.1	< 1	241	< 0.1	< 0.1
FBC Ash	99	1.4	2.9	16.9	17	15	7.8	3	532	1.5	1
Class F Fly Ash	82	6.7	6.8	27.3	29	< 3	11.8	8	1083	1.8	1.8

	Minor/Trace									
Analyte Symbol	Th	Tl	Tm	U	V	W	Y	Yb	Zn	Zr
Unit Symbol	ppm	ppm	ppm	ppm	ppm	ppm	ppm	ppm	ppm	ppm
Detection Limit	0.1	0.1	0.05	0.1	5	1	2	0.1	1	4
Analysis Method	FUS-MS	FUS-MS	FUS-MS	FUS-MS	FUS-ICP	FUS-MS	FUS-ICP	FUS-MS	TD-ICP	FUS-ICP
FGD Material	0.3	< 0.1	< 0.05	0.2	< 5	< 1	< 2	0.2	3	130
FBC Ash	14.2	2.3	0.52	4.8	138	2	31	3.4	78	181
Class F Fly Ash	19.4	5.1	0.84	9.3	250	4	59	5.4	129	218

Appendix G: EFFLUENT CHEMICAL ANALYSIS

Analyte Symbol	Na	Li	Be	Mg	Al	Si	K	Ca	Sc	Ti	V	Cr	Mn	Fe	Co	Ni	Cu	Zn
Unit Symbol	µg/L	µg/L	µg/L	µg/L	µg/L	µg/L	µg/L	µg/L	µg/L	µg/L	µg/L	µg/L	µg/L	µg/L	µg/L	µg/L	µg/L	µg/L
Detection Limit	5	1	0.1	1	2	200	30	700	1	0.1	0.1	0.5	0.1	10	0.005	0.3	0.2	0.5
Analysis Method	ICP-MS	ICP-MS	ICP-MS	ICP-MS	ICP-MS	ICP-MS	ICP-MS	ICP-MS	ICP-MS	ICP-MS	ICP-MS	ICP-MS	ICP-MS	ICP-MS	ICP-MS	ICP-MS	ICP-MS	ICP-MS
FBC 1-day	332	31	< 1	15	< 20	< 2000	1430	> 200000	< 10	< 1	3.4	8.4	< 1	< 100	< 0.05	< 3	< 2	8
FBC 3-day	3540	145	< 1	22	< 20	< 2000	9140	> 200000	< 10	< 1	< 1	11.1	< 1	< 100	< 0.05	< 3	< 2	27
FBC 7-day	21000	1540	< 1	40	95	< 2000	156000	> 200000	< 10	2.3	1.6	65	< 1	< 100	0.09	< 3	4	26.7
FBC 14-day	7480	421	< 1	64	758	2000	46700	109000	< 10	< 1	11.2	5.8	< 1	< 100	< 0.05	< 3	< 2	24.2
FBC 28-day	45300	2600	< 1	173	411	10800	> 200000	> 200000	< 10	3.1	40.3	28.7	< 1	< 100	< 0.05	< 3	< 2	13.1
FBC 56-day	2790	174	< 1	148	2040	4100	17900	> 200000	< 10	< 1	27.8	< 5	< 1	< 100	< 0.05	< 3	50.2	34.4
FBC 90-day	1410	79	< 0.1	214	1780	2300	6960	> 20000	< 1	0.4	19	1.3	< 0.1	< 10	< 0.005	< 0.3	0.6	23.3
FBC 180-day		> 400	< 0.1	938	609	10900	> 20000	> 20000	3	3.3	42.5	30.8	< 0.1	310	0.141	1.1	3.2	11.8
cf 1-day	3430	80	< 1	851	2700	< 2000	1240	> 200000	< 10	< 1	18.5	< 5	< 1	< 100	< 0.05	< 3	< 2	< 5
cf 3-day	2020	231	< 1	199	790	< 2000	650	130000	< 10	< 1	32.3	< 5	< 1	< 100	< 0.05	< 3	< 2	< 5
cf 7-day	935	180	< 1	162	293	< 2000	340	19100	< 10	< 1	61.6	< 5	< 1	< 100	< 0.05	< 3	< 2	< 5
cf 14-day	1690	302	< 1	144	555	< 2000	490	36100	< 10	< 1	31.7	< 5	< 1	< 100	< 0.05	< 3	< 2	< 5
cf 28-day	2390	337	< 1	179	2550	< 2000	720	131000	< 10	< 1	54.9	< 5	< 1	< 100	< 0.05	< 3	< 2	< 5
cf 56-day	1480	134	< 1	183	176	< 2000	440	23900	< 10	< 1	60	< 5	< 1	< 100	< 0.05	< 3	< 2	< 5
cf 90-day	2390	260	< 0.1	182	> 2000	700	490	> 20000	< 1	0.4	> 50.0	< 0.5	< 0.1	< 10	< 0.005	< 0.3	0.4	8.8
fgd 1-day	145	< 10	< 1	47	28	< 2000	< 300	> 200000	< 10	< 1	< 1	< 5	3.8	< 100	0.09	< 3	2	89
fgd 3-day	128	< 10	< 1	39	< 20	< 2000	< 300	> 200000	< 10	< 1	< 1	< 5	2.6	110	0.13	< 3	2.2	83.2
fgc 7-day	87	< 10	< 1	44	26	< 2000	< 300	> 200000	< 10	< 1	< 1	< 5	1.6	180	0.1	< 3	< 2	63
fgd 14-day	95	< 10	< 1	41	28	< 2000	< 300	> 200000	< 10	< 1	< 1	< 5	1.9	150	0.14	< 3	3	73.1
fgd 28-day	102	< 10	< 1	41	< 20	< 2000	< 300	> 200000	< 10	< 1	< 1	< 5	3.2	180	0.2	< 3	4.4	88.5
fgd 56-day	115	< 10	< 1	47	22	< 2000	< 300	> 200000	< 10	< 1	< 1	< 5	2.4	170	0.23	< 3	< 2	80.2
fgd 90-day	199	< 1	< 0.1	120	13	300	80	> 20000	< 1	0.1	0.3	< 0.5	3.9	< 10	0.02	1.4	1.5	78.8

Analyte Symbol	Ga	Ge	As	Se	Br	Rb	Sr	Y	Zr	Nb	Mo	Ru	Pd	Ag	Cd	In	Sn	Sb
Unit Symbol	µg/L	µg/L	µg/L	µg/L	µg/L	µg/L	µg/L	µg/L	µg/L	µg/L	µg/L	µg/L	µg/L	µg/L	µg/L	µg/L	µg/L	µg/L
Detection Limit	0.01	0.01	0.03	0.2	3	0.005	0.04	0.003	0.01	0.005	0.1	0.01	0.01	0.2	0.01	0.001	0.1	0.01
Analysis Method	ICP-MS	ICP-MS	ICP-MS	ICP-MS	ICP-MS	ICP-MS	ICP-MS	ICP-MS	ICP-MS	ICP-MS	ICP-MS	ICP-MS	ICP-MS	ICP-MS	ICP-MS	ICP-MS	ICP-MS	ICP-MS
FBC 1-day	0.2	0.1	0.46	17.1	36	5.37	> 2000	< 0.03	0.1	< 0.05	36.7	< 0.1	0.4	< 2	< 0.1	< 0.01	< 1	< 0.1
FBC 3-day	0.1	0.1	< 0.3	7.2	438	37.2	> 2000	< 0.03	0.1	< 0.05	87.7	< 0.1	0.2	< 2	0.24	< 0.01	< 1	< 0.1
FBC 7-day	0.1	0.1	106	12.3	1410	585	> 2000	0.08	0.1	< 0.05	224	< 0.1	0.1	< 2	0.63	< 0.01	< 1	< 0.1
FBC 14-day	0.6	0.2	4.81	< 2	117	160	1850	< 0.03	0.1	< 0.05	5.6	< 0.1	0.2	< 2	< 0.1	< 0.01	< 1	< 0.1
FBC 28-day	1.3	0.1	< 0.3	8.7	784	897	> 2000	0.04	< 0.1	< 0.05	29.3	< 0.1	0.3	< 2	0.1	< 0.01	< 1	< 0.1
FBC 56-day	1.1	< 0.1	12.1	2.7	56	60.2	> 2000	< 0.03	< 0.1	< 0.05	4	< 0.1	< 0.1	< 2	< 0.1	< 0.01	< 1	< 0.1
FBC 90-day	0.69	0.03	15.7	2.1	28	29.1	> 200	0.008	0.01	< 0.005	2	< 0.01	< 0.01	< 0.2	0.02	< 0.001	< 0.1	0.24
FBC 180-day	2.08	0.49	3.6	9	413	307	> 200	0.035	0.02	0.007	42	0.01	0.09	< 0.2	0.13	< 0.001	0.1	0.27
cf 1-day	52	1	162	97.4	< 30	5.01	> 2000	< 0.03	< 0.1	< 0.05	33.3	< 0.1	< 0.1	< 2	0.1	< 0.01	< 1	6.6
cf 3-day	9.3	17	7.63	50.9	< 30	2.44	1320	< 0.03	< 0.1	< 0.05	13.7	< 0.1	< 0.1	< 2	< 0.1	< 0.01	< 1	5.4
cf 7-day	5.35	2	8.73	37.1	< 30	1.29	213	< 0.03	< 0.1	< 0.05	3.9	< 0.1	< 0.1	< 2	< 0.1	< 0.01	< 1	3.4
cf 14-day	4.9	1.6	7.59	22.1	< 30	1.71	422	< 0.03	< 0.1	< 0.05	3.9	< 0.1	< 0.1	< 2	< 0.1	< 0.01	< 1	4.5
cf 28-day	12.8	1.4	3.95	19.6	< 30	2.43	1260	< 0.03	< 0.1	< 0.05	4.2	< 0.1	< 0.1	< 2	< 0.1	< 0.01	< 1	3.7
cf 56-day	7.6	1.7	7.65	19.8	< 30	1.51	285	< 0.03	0.2	< 0.05	2.5	< 0.1	< 0.1	< 2	< 0.1	< 0.01	< 1	3.1
cf 90-day	10.2	3.12	36	17.6	< 3	1.66	> 200	< 0.003	< 0.01	< 0.005	3.4	< 0.01	< 0.01	< 0.2	0.01	< 0.001	< 0.1	4.31
fgd 1-day	< 0.1	0.1	0.43	25.7	< 30	0.539	661	0.05	< 0.1	< 0.05	< 1	< 0.1	< 0.1	< 2	0.47	< 0.01	< 1	< 0.1
fgd 3-day	< 0.1	0.1	0.41	19.4	< 30	0.35	689	< 0.03	< 0.1	< 0.05	< 1	< 0.1	< 0.1	< 2	0.28	< 0.01	< 1	< 0.1
fgc 7-day	< 0.1	0.1	0.51	11.7	< 30	0.288	723	< 0.03	0.4	< 0.05	< 1	< 0.1	< 0.1	< 2	0.15	< 0.01	1	< 0.1
fgd 14-day	< 0.1	0.1	0.5	11.1	< 30	0.408	687	< 0.03	< 0.1	< 0.05	< 1	< 0.1	< 0.1	< 2	0.27	< 0.01	< 1	< 0.1
fgd 28-day	< 0.1	0.2	< 0.3	24.8	< 30	0.368	640	0.07	< 0.1	< 0.05	< 1	< 0.1	< 0.1	< 2	0.46	1.57	< 1	< 0.1
fgd 56-day	< 0.1	0.2	0.56	11.5	< 30	0.391	689	< 0.03	< 0.1	< 0.05	< 1	< 0.1	< 0.1	< 2	0.38	< 0.01	< 1	< 0.1
fgd 90-day	0.02	0.12	0.85	20.3	< 3	0.466	> 200	0.021	0.07	< 0.005	0.5	0.01	< 0.01	< 0.2	0.56	< 0.001	< 0.1	0.03

Analyte Symbol	Te	I	Cs	Ba	La	Ce	Pr	Nd	Sm	Eu	Gd	Tb	Dy	Ho	Er	Tm	Yb	Lu
Unit Symbol	µg/L	µg/L	µg/L	µg/L	µg/L	µg/L	µg/L	µg/L	µg/L	µg/L	µg/L	µg/L	µg/L	µg/L	µg/L	µg/L	µg/L	µg/L
Detection Limit	0.1	1	0.001	0.1	0.001	0.001	0.001	0.001	0.001	0.001	0.001	0.001	0.001	0.001	0.001	0.001	0.001	0.001
Analysis Method	ICP-MS	ICP-MS	ICP-MS	ICP-MS	ICP-MS	ICP-MS	ICP-MS	ICP-MS	ICP-MS	ICP-MS	ICP-MS	ICP-MS	ICP-MS	ICP-MS	ICP-MS	ICP-MS	ICP-MS	ICP-MS
FBC 1-day	<1	<10	0.11	120	<0.01	<0.01	<0.01	<0.01	<0.01	<0.01	<0.01	<0.01	<0.01	<0.01	<0.01	<0.01	<0.01	<0.01
FBC 3-day	<1	10	0.5	167	<0.01	<0.01	<0.01	<0.01	<0.01	<0.01	<0.01	<0.01	<0.01	<0.01	<0.01	<0.01	<0.01	<0.01
FBC 7-day	<1	10	3.55	166	0.05	0.1	0.01	0.02	<0.01	0.01	<0.01	<0.01	<0.01	<0.01	<0.01	<0.01	<0.01	<0.01
FBC 14-day	<1	<10	124	219	<0.01	<0.01	<0.01	<0.01	<0.01	<0.01	<0.01	<0.01	<0.01	<0.01	<0.01	<0.01	<0.01	<0.01
FBC 28-day	<1	10	7.28	75.3	0.01	0.02	<0.01	<0.01	<0.01	<0.01	<0.01	<0.01	<0.01	<0.01	<0.01	<0.01	<0.01	<0.01
FBC 56-day	<1	<10	0.56	33.1	0.01	0.01	<0.01	<0.01	<0.01	<0.01	<0.01	<0.01	<0.01	<0.01	<0.01	<0.01	<0.01	<0.01
FBC 90-day	<0.1	1	0.347	20.2	<0.001	<0.001	<0.001	<0.001	<0.001	<0.001	<0.001	<0.001	<0.001	<0.001	<0.001	<0.001	<0.001	<0.001
FBC 180day	0.1	4	3.13	65.4	0.009	0.07	0.002	0.006	0.002	0.004	0.002	<0.001	0.002	<0.001	<0.001	<0.001	<0.001	<0.001
cf 1-day	<1	<10	0.51	87.5	<0.01	<0.01	<0.01	<0.01	<0.01	<0.01	<0.01	<0.01	<0.01	<0.01	<0.01	<0.01	<0.01	<0.01
cf 3-day	<1	<10	0.22	66.3	<0.01	<0.01	<0.01	<0.01	<0.01	<0.01	<0.01	<0.01	<0.01	<0.01	<0.01	<0.01	<0.01	<0.01
cf 7-day	<1	<10	0.115	39	<0.01	<0.01	<0.01	<0.01	<0.01	<0.01	<0.01	<0.01	<0.01	<0.01	<0.01	<0.01	<0.01	<0.01
cf 14-day	<1	<10	0.15	70.8	<0.01	<0.01	<0.01	<0.01	<0.01	<0.01	<0.01	<0.01	<0.01	<0.01	<0.01	<0.01	<0.01	<0.01
cf 28-day	<1	<10	0.21	66.6	0.01	0.02	<0.01	<0.01	<0.01	<0.01	<0.01	<0.01	<0.01	<0.01	<0.01	<0.01	<0.01	<0.01
cf 56-day	<1	<10	0.11	32.7	0.01	0.01	<0.01	<0.01	<0.01	<0.01	<0.01	<0.01	<0.01	<0.01	<0.01	<0.01	<0.01	<0.01
cf 90-day	<0.1	<1	0.139	45.6	0.001	<0.001	<0.001	<0.001	<0.001	<0.001	<0.001	<0.001	<0.001	<0.001	<0.001	<0.001	<0.001	<0.001
fgd 1-day	<1	<10	0.01	3.4	0.1	0.09	<0.01	0.03	<0.01	<0.01	<0.01	<0.01	<0.01	<0.01	<0.01	<0.01	<0.01	<0.01
fgd 3-day	<1	<10	<0.01	3.4	0.05	0.03	<0.01	0.01	<0.01	<0.01	<0.01	<0.01	<0.01	<0.01	<0.01	<0.01	<0.01	<0.01
fgc 7-day	<1	<10	0.01	3.1	0.04	0.03	<0.01	0.02	<0.01	<0.01	<0.01	<0.01	<0.01	<0.01	<0.01	<0.01	<0.01	<0.01
fgd 14-day	<1	<10	0.01	2.9	0.04	0.03	<0.01	0.01	<0.01	<0.01	<0.01	<0.01	<0.01	<0.01	<0.01	<0.01	<0.01	<0.01
fgd 28-day	<1	<10	<0.01	2.6	0.3	0.11	0.01	0.06	<0.01	<0.01	0.01	<0.01	<0.01	<0.01	<0.01	<0.01	<0.01	<0.01
fgd 56-day	<1	<10	<0.01	2.5	0.03	0.02	<0.01	<0.01	<0.01	<0.01	<0.01	<0.01	<0.01	<0.01	<0.01	<0.01	<0.01	<0.01
fgd 90-day	<0.1	<1	0.009	3	0.057	0.041	0.004	0.01	0.003	<0.001	0.003	<0.001	0.002	<0.001	<0.001	<0.001	<0.001	<0.001

Analyte Symbol	Hf	Ta	W	Re	Os	Pt	Au	Hg	Tl	Pb	Bi	Th	U	Hg	F	Cl	O ₂ (as N)	Br
Unit Symbol	µg/L	µg/L	µg/L	µg/L	µg/L	µg/L	µg/L	µg/L	µg/L	µg/L	µg/L	µg/L	µg/L	ng/L	mg/L	mg/L	mg/L	mg/L
Detection Limit	0.001	0.001	0.02	0.001	0.002	0.3	0.002	0.2	0.001	0.01	0.3	0.001	0.001	6	0.01	0.03	0.01	0.03
Analysis Method	ICP-MS	ICP-MS	ICP-MS	ICP-MS	ICP-MS	ICP-MS	ICP-MS	ICP-MS	ICP-MS	ICP-MS	ICP-MS	ICP-MS	ICP-MS	FIMS	IC	IC	IC	IC
FBC 1-day	<0.01	<0.01	5	0.01	<0.02	<3	<0.02	2	<0.01	1	<3	<0.01	<0.01	83	<0.3	<0.7	<0.3	<0.7
FBC 3-day	<0.01	<0.01	1	0.05	<0.02	<3	<0.02	<2	<0.01	2.51	<3	<0.01	<0.01	8	<0.3	4.1	0.97	<0.7
FBC 7-day	<0.01	<0.01	0.3	0.53	<0.02	<3	<0.02	<2	0.07	2.29	<3	<0.01	<0.01	18	<0.3	69.8	<0.3	<0.7
FBC 14-day	<0.01	<0.01	0.4	0.16	<0.02	<3	<0.02	<2	0.01	<0.1	<3	<0.01	<0.01	<6	<0.02	18.3	<0.02	<0.06
FBC 28-day	<0.01	<0.01	1	0.96	<0.02	<3	0.02	<2	0.25	<0.1	<3	<0.01	<0.01	<6	<0.1	119	<0.1	<0.4
FBC 56-day	<0.01	<0.01	0.6	0.04	<0.02	<3	<0.02	<2	<0.01	0.31	<3	<0.01	<0.01	<6	0.23	6.89	<0.05	7.5
FBC 90-day	<0.001	<0.001	0.58	0.025	<0.002	<0.3	<0.002	<0.2	0.017	0.27	<0.3	<0.001	0.002	<6	0.2	3.51	<0.04	<0.1
FBC 180-day	<0.001	<0.001	6.9	0.447	<0.002	<0.3	0.023	<0.2	0.165	0.03	<0.3	0.001	0.004	<6	0.72	55.9	<0.1	<0.3
cf 1-day	<0.01	<0.01	15.7	0.03	<0.02	<3	<0.02	<2	0.16	<0.1	<3	<0.01	<0.01	<6	0.93	<0.3	<0.1	4.64
cf 3-day	<0.01	<0.01	5.9	<0.01	<0.02	<3	<0.02	<2	0.07	<0.1	<3	<0.01	<0.01	<6	0.47	0.16	<0.03	<0.09
cf 7-day	<0.01	<0.01	2.65	<0.01	<0.02	<3	<0.02	<2	0.025	<0.1	<3	<0.01	<0.01	<6	<0.01	0.07	<0.01	<0.03
cf 14-day	<0.01	<0.01	2.7	<0.01	<0.02	<3	<0.02	<2	0.04	<0.1	<3	<0.01	<0.01	<6	<0.01	0.09	<0.01	<0.03
cf 28-day	<0.01	<0.01	4	<0.01	<0.02	<3	<0.02	<2	0.05	<0.1	<3	<0.01	<0.01	<6	0.42	0.12	<0.03	<0.09
cf 56-day	<0.01	<0.01	3.1	<0.01	<0.02	<3	<0.02	<2	0.01	<0.1	<3	<0.01	<0.01	<6	<0.01	0.08	<0.01	<0.03
cf 90-day	<0.001	<0.001	4.28	0.003	<0.002	<0.3	<0.002	<0.2	0.066	0.04	<0.3	<0.001	0.013	<6	0.43	0.12	<0.01	<0.03
fgd 1-day	<0.01	<0.01	<0.2	<0.01	<0.02	<3	<0.02	<2	<0.01	0.36	<3	<0.01	<0.01	<6	143	<0.3	<0.1	<0.3
fgd 3-day	<0.01	<0.01	<0.2	<0.01	<0.02	<3	<0.02	<2	<0.01	0.32	<3	<0.01	<0.01	<6	142	<0.3	<0.1	<0.3
fgc 7-day	<0.01	<0.01	<0.2	<0.01	<0.02	<3	<0.02	<2	<0.01	<0.1	<3	<0.01	<0.01	<6	108	<0.3	<0.1	<0.3
fgd 14-day	<0.01	<0.01	<0.2	<0.01	<0.02	<3	<0.02	<2	<0.01	0.23	<3	<0.01	<0.01	<6	131	<0.3	<0.1	<0.3
fgd 28-day	<0.01	<0.01	<0.2	<0.01	<0.02	<3	<0.02	<2	<0.01	103	<3	<0.01	<0.01	<6	122	<0.3	<0.1	<0.3
fgd 56-day	<0.01	<0.01	<0.2	<0.01	<0.02	<3	<0.02	<2	<0.01	0.27	<3	<0.01	<0.01	<6	<0.1	<0.3	<0.1	<0.3
fgd 90-day	<0.001	<0.001	0.07	<0.001	<0.002	<0.3	<0.002	<0.2	0.014	0.08	<0.3	0.002	0.017	<6	128	<0.3	<0.1	<0.3

Analyte Symbol	NO3 (as N)	PO4 (as P)	SO4	B
Unit Symbol	mg/L	mg/L	mg/L	µg/L
Detection Limit	0.01	0.02	0.03	3
Analysis Method	IC	IC	IC	ICP-MS
FBC 1-day	< 0.3	0.63	1070	< 30
FBC 3-day	< 0.3	< 0.5	1290	35
FBC 7-day	< 0.3	< 0.5	938	39
FBC 14-day	< 0.02	< 0.04	268	< 30
FBC 28-day	< 0.1	0.86	1610	< 30
FBC 56-day	< 0.05	< 0.1	617	< 30
FBC 90-day	< 0.04	< 0.08	481	7
FBC 180-day	< 0.1	< 0.2	1550	78
cf 1-day	< 0.1	0.23	867	2370
cf 3-day	< 0.03	0.08	301	1120
cf 7-day	0.02	< 0.02	28.5	506
cf 14-day	0.02	< 0.02	70.6	758
cf 28-day	< 0.03	< 0.06	300	931
cf 56-day	< 0.01	< 0.02	38.6	646
cf 90-day	0.02	< 0.02	70.1	992
fgd 1-day	< 0.1	0.38	1440	< 30
fgd 3-day	< 0.1	0.39	1380	< 30
fgc 7-day	< 0.1	0.66	1420	< 30
fgd 14-day	< 0.1	0.59	1450	< 30
fgd 28-day	< 0.1	0.5	1440	< 30
fgd 56-day	< 0.1	< 0.2	1270	< 30
fgd 90-day	< 0.1	< 0.2	1460	8